

**TRANSIENT ANALYSIS OF
ERRONEOUS TRIPPING AT
GRASSRIDGE STATIC VAR
COMPENSATOR**

M.W.TABERER

2013



**TRANSIENT ANALYSIS OF ERRONEOUS TRIPPING
AT GRASSRIDGE STATIC VAR COMPENSATOR**

By

Marcel Wayne Taberer
ENGINEERING: ELECTRICAL

Submitted in fulfilment of the requirements for the degree of
Masters in Technology: Engineering: Electrical

in the Faculty of Engineering, the Built Environment and
Information Technology at the
Nelson Mandela Metropolitan University

December 2013

Supervisor: Mr. A. G Roberts

Co-Supervisor: Dr. R. T Harris

Industrial Supervisor: Mr. A. Craib

DECLARATION

I Marcel Wayne Taberer, student number 20420808, in accordance with rule G4.6.3 of the prospectus hereby declare that the dissertation for the degree of Masters in Technology: Engineering: Electrical is my own work and that it has not previously been submitted for assessment or completion for any postgraduate qualification to another university or for another qualification.

Marcel Wayne Taberer

Name

30 December 2013

Date

A handwritten signature in black ink, appearing to read 'M. Taberer', is written over a light blue horizontal line.

Signature

ACKNOWLEDGEMENTS

The following persons and companies are acknowledged for their valued participation that contributed to the successful completion of this project:

I would first like to emphasise my deepest of gratitude to my Saviour Jesus Christ for enabling me to be blessed with an opportunity and the intellect to be able to reach a point in my career that challenges me as an individual and be able to be blessed with an opportunity for furthering my study and working career.

I would like to express my deepest gratitude and appreciation to my supervisor, Mr Alan Roberts, for his advice and support during this project. I also want to thank my co-supervisor, Dr Raymond Harris, for his professional advice and for encouraging me throughout this project.

I would also like to thank Mr A.Craib for his willingness to help and valued technical input. I express my appreciation to the staff at Eskom Transmission for allowing me the opportunity to solve a “real life network problem” that has been an issue to system security as a whole within the Eastern Cape, South Africa. Special thanks to Mr Ishaam Uithalder at Eskom for his help with various problems arising during this project and his willingness to assist with any outage related issues that occurred during this research.

Finally, I would like to thank my wife for her support and encouragement during the period of this project.

SYNOPSIS

The research work conducted and presented forward in this document is the evaluation of real time values obtained using three recording devices at two independent locations and implementing them as recorder devices in Eskom's power system. The research work conducted was presented at an IEEE International Conference (ICIT2013) and *Appendix A* shows the accepted paper presented. A derived model within a simulation software package known as DIgSILENT PowerFactory is created and Electromagnetic Transient (EMT) studies are performed and then compared to the real time values obtained using the OMICRON CMC 356's.

Transformers are normally energised via a circuit breaker which is controlled by an auxiliary closing contact. By applying system voltage at a random instant in time on the transformer windings may result in a large transient magnetizing inrush current which causes high orders of 2nd harmonic currents to flow under no load conditions. A philosophy known to mitigate these currents is to energise the transformer by controlling each individual phase 120 degrees apart with the first pole closing at the peak on the voltage waveform.

Transients produced due to 500MVA transformers been introduced into the power system at a certain space in time can cause nuisance tripping's at the particular location where the respective transformer is energised. OMICRON EnerLyzer is the software tool used for the Comtrade recordings at both locations.

Four independent case studies are generated within EnerLyzer software and the relevant Comtrade files are extracted for the four independent case studies relative to Transformer1 and Transformer2 switching's. TOP software, which is a mathematical tool used to analyse Comtrade files, is then used to analyse and investigate the four case studies.

Results from DIgSILENT PowerFactory are then generated according to the derived model. The results extracted depict three scenarios, indicating a power system that is weak, strong and specifically a power system that correlates to the actual tripping of a Static VAr Compensator (SVC).

The results are all formulated and then evaluated in order to produce a conclusion and bring forward recommendations to Eskom in order to effectively ensure the Dedisa/Grassridge power system is reliable once again.

TABLE OF CONTENTS

DECLARATION	i
ACKNOWLEDGEMENTS	ii
SYNOPSIS.....	iii
TABLE OF CONTENTS.....	iv
LIST OF FIGURES	vi
LIST OF TABLES AND CHARTS	viii
LIST OF SYMBOLS	ix
CHAPTER 1 - INTRODUCTION.....	1
1.1 BACKGROUND.....	1
1.2 PROBLEM STATEMENT	1
1.3 SUB-PROBLEMS.....	2
1.3.1 Data Collection	2
1.3.2 Existing Network Analysis	2
1.3.3 System Outage	2
1.3.4 Development Methods for Relay Settings and Calculations	2
1.3.5 Fault Analysis	2
1.3.6 Alternative Solutions and Costing	3
1.3.7 Real Time Implementation	3
1.3.8 Simulation Software Setbacks	3
1.4 HYPOTHESIS	4
1.5 DELIMITATION OF THE PROJECT	5
1.6 OBJECTIVES OF THE STUDY	6
1.7 OUTLINE OF THE STUDY	7
1.8 METHODOLOGY.....	8
1.8.1 Literature Review.....	8
1.8.2 Site Survey and Data Collection	9
1.8.3 Analysis of Existing AEG System.....	9
1.8.4 Harmonic and Fault Analysis.....	9
1.8.5 Manual Calculations and Studies.....	10
1.8.6 DIgSILENT Electromagnetic Transient (EMT) Studies	10
1.8.7 Testing of the AEG Relays	10
1.8.8 Implementation of Alternative Solutions.....	11
1.8.9 Documentation Method	11
1.9 DEFINITION OF CONCEPTS.....	12
CHAPTER 2 – LITERATURE REVIEW	15
2.1 INTRODUCTION.....	15
2.2 ROOT CAUSE OF HARMONIC IMPACT.....	15
2.2.1 Transformer Inrush Currents.....	16
2.3 PROTECTION FUNCTIONALITY AND OPERATIONAL SEQUENCE	20
2.3.1 Details of Grassridge SVC.....	20
2.3.2 Protection Functionality	21
2.4 STATIC VAR COMPENSATOR PROTECTION.....	22
2.5 TRANSIENT/PERMANENT FAULTS AND MAL-OPERATION	23

2.6	CALCULATION AND SHORT CIRCUIT CURRENT	23
2.7	CONCLUSION	25
CHAPTER 3 - DESIGN		26
3.1	INTRODUCTION.....	26
3.1.1	Network Layout	27
3.2	ABB F236 POINT ONTO WAVE CONTROLLER	27
3.2.1	Introduction to the ABB F236 Controller.....	27
3.2.2	ABB F236 Application	29
3.3	OMICRON CMC 356 SETUP AND CASE STUDIES.....	29
3.3.1	EnerLyzer Software Setup	30
3.3.2	Case Study 1 - Transformer 1 Energising, NO SVC Trip	32
3.3.3	Case Study 2 - Transformer 1 Energising, SVC Trip	33
3.3.4	Case Study 3 - Transformer 2 Energising, NO SVC Trip	34
3.3.5	Case Study 4 - Transformer 2 Energising, NO SVC Trip	36
3.4	DIgSILENT POWERFACTORY DERIVED MODEL	36
3.4.1	DIgSILENT PowerFactory Tools	36
3.4.2	SVC Controller Model in Detail	41
3.4.3	SVC Composite Model in Detail	42
3.4.4	RMS and Harmonic Calculations	44
3.5	HARMONIC IMPACT TEST ON THE SIT 852 RELAY.....	44
3.5.1	AEG SIT 852 Earth Fault Test.....	46
3.6	CONCLUSION	47
CHAPTER 4 - DATA COLLECTION, ANALYSIS AND INTERPRETATION		48
4.1	INTRODUCTION.....	48
4.2	OMICRON CASE STUDY RESULTS	50
4.2.1	Case Study 1 - Transformer 1 Energising, NO SVC Trip	50
4.2.2	Case Study 2 - Transformer 1 Energising, SVC Trip	53
4.2.3	Case Study 3 - Transformer 2 Energising, NO SVC Trip	55
4.2.4	Case Study 4 - Transformer 2 Energising, NO SVC Trip	57
4.2.5	Fast Fourier Transform Plots of the 4 Case Studies	58
4.3	DIgSILENT RESULTS.....	63
4.3.1	Poseidon as a weak source	63
4.3.2	Poseidon as a strong source	66
4.3.3	Poseidon replicating Case Study 2 - SVC Trip.....	69
4.4	WORKED CALCULATIONS.....	72
4.4.1	Peak current calculation	72
4.4.2	Total Harmonic Distortion Calculation for Case Study 2.....	74
4.5	DATA ANALYSIS AND INTERPRETATION	77
4.6	CONCLUSION	81
CHAPTER 5 - CONCLUSIONS AND RECOMMENDATIONS.....		82
5.1	SUMMARY	82
5.2	CONCLUSIONS	82
5.3	RECOMMENDATIONS	83
CHAPTER 6 - LIST OF REFERENCES		85
APPENDICES		87
Appendix A – IEEE Conference ICIT 2013		87
Appendix B – OMICRON CMC 356 Calibration Certification		93

LIST OF FIGURES

Figure 1: OMICRON CMC 356 Test Equipment.....	3
Figure 2: Block diagram relating to the Problem Statement.....	7
Figure 3: Magnetizing curve and hysteresis loop of a transformer core.....	17
Figure 4: Transformer inrush current, the flux in the core and the supply voltage	17
Figure 5: Single line diagram of the 132kV SVC [12]	20
Figure 6: Block diagram of protection operation.....	21
Figure 7: Simplified single line diagram (SLD) of the network under investigation.....	27
Figure 8: ABB F236 wired into the closing circuit of Transformer 1 at Dedisa substation	29
Figure 9: OMICRON CMC 356 test equipment setup	29
Figure 10: Clamp on CT setup within OMICRON EnerLyzer.....	30
Figure 11: Channel setup within OMICRON EnerLyzer	31
Figure 12: Trigger setup and conditions in OMICRON EnerLyzer	32
Figure 13: Case study 1 recorder setup and breaker operation	33
Figure 14: Case study 2 recorder setup and breaker operation.....	34
Figure 15: Case study 3 recorder setup and breaker operation.....	35
Figure 16: Case study 3 red phase voltage energising point.....	35
Figure 17: Case study 4 white phase voltage energising point.....	36
Figure 18: The derived models external grid setup in DIgSILENT	37
Figure 19: DIgSILENT symbol for a 3 winding transformer	38
Figure 20: Three winding transformer basic data dialog box	39
Figure 21: General load operating parameters on Grassridge 132kV bar	40
Figure 22: SVC Controller within DIgSILENT.....	41
Figure 23: SVC composite frame in DIgSILENT	43
Figure 24: SVC Controller within DIgSILENT.....	43
Figure 25: AEG SIT 852 relay under test in the laboratory.....	46
Figure 26: Overview of the analysis approach	48
Figure 27: formatting and evaluation methodology for deriving comparison results	49
Figure 28: High level indication for identical network process.....	50
Figure 29: Case study 1 (inrush current and applied voltage)	51
Figure 30: Case study 1 thyristor current during and after switching.....	52
Figure 31: Case study 2 thyristor current during and after switching.....	54
Figure 32: Case study 2 LV current before, during and after switching.....	54
Figure 33: Case study 3 (inrush current and applied voltage)	56
Figure 34: Case study 3 thyristor current during and after switching.....	57
Figure 35: Case study 4 (inrush current and applied voltage)	57
Figure 36: Case study 4 thyristor current during and after switching.....	58
Figure 37: Case study 1 FFT plot representing the inrush current for transformer 1.....	59
Figure 38: Case study 3 FFT plot representing the inrush current for transformer 2.....	59
Figure 39: Case study 4 FFT plot representing the inrush current for transformer 2.....	60
Figure 40: Case study 1 FFT plot representing the HV current on the SVC for transformer 1 switching	60

Figure 41: Case study 2 FFT plot representing the HV current on the SVC for transformer 1 switching	61
Figure 42: Case study 3 FFT plot representing the HV current on the SVC for transformer 2 switching	61
Figure 43: Case study 4 FFT plot representing the HV current on the SVC for transformer 2 switching	61
Figure 44: Case study 1 FFT plot representing the LV current on the SVC for transformer 1 switching	62
Figure 45: Case study 2 FFT plot representing the LV current on the SVC for transformer 1 switching	62
Figure 46: Case study 3 FFT plot representing the LV current on the SVC for transformer 2 switching	63
Figure 47: Case study 4 FFT plot representing the LV current on the SVC for transformer 2 switching	63
Figure 48: DIgSILENT (weak source) results for transformer inrush current and 400kV busbar voltage	64
Figure 49: DIgSILENT (weak source) results for Grassridge 132kV voltage relative to the SVC LV current	65
Figure 50: DIgSILENT (weak source) results for the thyristors firing angle during the switching transient	65
Figure 51: DIgSILENT (weak source) FFT plots for transformer 1 HV and the 132kV and 5.1kV side of the SVC.....	66
Figure 52: DIgSILENT (strong source) results for transformer inrush current and 400kV busbar voltage	67
Figure 53: DIgSILENT (strong source) results for Grassridge 132kV voltage relative to the SVC LV current	68
Figure 54: DIgSILENT (strong source) results for the thyristors firing angle during the switching transient.....	68
Figure 55: DIgSILENT (strong source) FFT plots for transformer 1 HV and the 132kV and 5.1kV side of the SVC.....	69
Figure 56: DIgSILENT (case study 2 replication) results for transformer inrush current and 400kV busbar voltage	70
Figure 57: DIgSILENT (case study 2 replication) results for Grassridge 132kV voltage relative to the SVC LV current	71
Figure 58: DIgSILENT (case study 2 replication) results for the thyristors firing angle during the switching transient	71
Figure 59: DIgSILENT (case study 2 replication) FFT plots for transformer 1 HV and the 132kV and 5.1kV side of the SVC.....	72
Figure 60: Case study 2 LV O/C current comparison relative to a voltage dip, OMICRON vs. DIgSILENT	79

LIST OF TABLES AND CHARTS

Table 1: Line parameters for the derived software model	38
Table 2: Three winding transformer parameters relative to the derived model.....	38
Table 3: Fundamental injected current and trip times	46
Table 4: Harmonic current injection and trip times	47
Table 5: Case study 1 voltage magnitudes for the 400kV and 132kV busbar respectively	51
Table 6: Case study 2 voltage magnitudes for the 400kV and 132kV busbar respectively	53
Table 7: Case study 3 voltage magnitudes for the 400kV and 132kV busbar respectively	56
Table 8: Case study 4 voltage magnitudes for the 400kV and 132kV busbar respectively	58
Table 9: Voltage magnitudes and peak currents relevant to all four case studies during the switching transient together with DIgSILENT results	77
Table 10: Case Study 2 voltage magnitudes OMICRON vs. DIgSILENT.....	78
Table 11: IEEE Std.1459 calculation results for case study 2	81
Chart 1: FFT Plot evaluation on the HV side of the SVC for case study 2, OMICRON vs. DIgSILENT	80
Chart 2: FFT Plot evaluation on the 5.1kV side of the SVC for case study 2, OMICRON vs. DIgSILENT	80

LIST OF SYMBOLS

B_m	Maximum Value of the Flux Density of the Transformer Core
B_N	Normal Rated Flux Density of the Transformer Core
B_r	Residual Value of the Flux Density left within the Transformer Core
E_{max}	Peak Value of the busbar Magnitude
h	Harmonic order
I_e	IEE Std.1459 Equivalent Three-Phase Current
I_{e1}	IEE Std.1459 Equivalent Three-Phase Fundamental Current
I_{eh}	IEE Std.1459 Equivalent three-phase current
I_{kA}	Short Circuit Current
$I_{rms(i)}$	Root Mean Square Phase Value for “i” Particular Phase Current
I_{R1}	Fundamental Current for Phase R
I_{W1}	Fundamental Current for Phase W
I_{B1}	Fundamental Current for Phase B
I_{Rh}	Harmonic order “h” Current for Phase R
I_{Wh}	Harmonic order “h” Current for Phase W
I_{Bh}	Harmonic order “h” Current for Phase B
$i(t)$	Peak Scalar time dependent current
$I_{THD(i)}$	IEE Std.1459 Total Harmonic Distortion for “i” Particular Phase
P_r	Rated Real Power within DIgSILENT PowerFactory
P_o	Operating Real Power within DIgSILENT PowerFactory
Re	Real part of a complex quantity
$Td(s)$	Operating Time of a Relay According to Curve Definition
Q_r	Rated Reactive Power within DIgSILENT PowerFactory
Q_o	Operating Reactive Power within DIgSILENT PowerFactory
V_r	Rated busbar Voltage
V_o	Operating busbar Voltage
$V_{RMS(i)}$	Root Mean Square Voltage of “i” Particular Phase

CHAPTER 1 - INTRODUCTION

1.1 BACKGROUND

As Eskom's national grid expands, the number of Transmission networks has increased tremendously since the year 2000. For an electrical Transmission network to function in a stable and reliable manner, it should be protected by unit protection or fuses such that the control functionality is reliable and secure and that the chosen device/s operate with minimal delay. One of the main objectives of a protection scheme is to keep the power system stable by isolating only the affected components or the section of the electrical network in which the fault has developed while allowing the rest of the network to continue operating. Protection philosophies and equipment do not prevent faults from occurring, but limit the damaging effect of a fault and protect other healthy equipment.

The Static VAr Compensator (SVC) located at Grassridge Transmission station within Eskom's power grid plays a vital role in ensuring the improvement of power system stability by providing voltage support. The application of an SVC in particular is to maintain voltage at a set level by compensating for varying loads and to correct fluctuating voltages caused by load rejections and outages.

Dedisa Transmission Station located in Eskom's Southern Region Network Grid System consists of two 500MVA transformers. This particular substation is one of Eskom largest and most valued installations taking into consideration the size of the transformers.

The SVC located at Grassridge has been operating effectively since 1987 with AEG phase I protection relays being more than adequate to accommodate for overcurrent (O/C) and earth fault (E/F) conditions, not to mention the harmonic blocking considered for various orders of harmonics. However, with over 20 years of operational time, inaccuracies within the relays could cause a potential threat to the systems reliability especially when taking into consideration the rapid growth of Eskom power grid. Thus steps need to be followed to ensure correct maintenance procedures have been adhered to and effective test results are obtained to indicate inaccuracies within the various models of the AEG Relays.

1.2 PROBLEM STATEMENT

The SVC at Grassridge substation is mal-operating/tripping on Low Voltage (LV) overcurrent (O/C) when one of the 500MVA Transformers at Dedisa substation is energised under no load conditions. However, when either one of the transformers at Dedisa substation are energised under loaded conditions the LV O/C relay protecting the SVC on the 5.1kV side remains stable at Grassridge substation.

Problem statement: To investigate the LV O/C tripping at Grassridge SVC when one of the 500MVA transformers at Dedisa substation is energised under no load conditions.

1.3 SUB-PROBLEMS

1.3.1 Data Collection

Protection settings and drawings for Dedisa and Grassridge transmission station will be required from Eskom's Protection department in Port Elizabeth and all necessary settings that cannot be found on record will need to be extracted from relays on site. Maintenance results of the old type AEG relays used on the SVC at Grassridge will be requested from Eskom.

1.3.2 Existing Network Analysis

Information relating to all calculation parameters will be required for analysis purposes as the system stands at Dedisa and Grassridge. The existing network behaviour on the vicinity of Grassridge substation will play a vital part for the proposed study and thus the reaction and interaction of Thyristor and Capacitor Bank behaviour at the SVC will be essential for the research. AEG type relays at Grassridge will need to be monitored and thus equipment and time could be a constraint.

1.3.3 System Outage

At least one outage will be required such that the SVC can be tripped at Grassridge substation. Thus a problem might occur with the outage schedulers, depending on system stability issues, to allow the SVC to be tripped purely for test/study purposes. Operator availability within the area could cause potential delays.

1.3.4 Development Methods for Relay Settings and Calculations

Relay settings are calculated in order to provide optimum protection for the network and that of the maintenance personnel. Time and setting of relays are made by selecting the correct secondary current requirement and adjusting the time dial to the position which corresponds to the characteristics required, this terminology is particular to phase 1 type relays. Due to high Current Transformer (CT) ratios used on the 5.1kV side of the SVC at Grassridge, an analysis is required to investigate whether CT saturation possess a potential threat to the SIT 852 proposed mal-operations.

1.3.5 Fault Analysis

Fault analysis is required to determine whether a fault is superimposed on the 5.1kV side of the SVC when an unloaded 500MVA transformer is energised at Dedisa transmission station. Thus the use of various analytical tools (i.e. OMICRON TransPlay, EnerLyzer and TransView) might introduce their own limitations that could threaten the integrity of the research.

1.3.6 Alternative Solutions and Costing

The investigation into alternative solutions could pose a potential threat to system integrity if replacement of the existing relay system is given the “go ahead”. Cost relating to new protection relays and man power to implement the replacement could defer a potential solution to the existing problem that exists.

1.3.7 Real Time Implementation

OMICRON test equipment and software is the primary tool used to investigate real time data obtained at both transmission stations. Real time analysis is extremely sensitive to the type of measurement tool used for the interconnection between the test set and the protection relay. Figure 1 indicates the OMICRON CMC 356 test set which is implemented as a recorder device for measurements purposes.



Figure 1: OMICRON CMC 356 Test Equipment

1.3.8 Simulation Software Setbacks

Manual calculations and software simulations using DIgSILENT PowerFactory Build 14.1.3 will be carried out in accordance with the international electro technical commission (IEC) standards. The real time values obtained using the OMICRON CMC 356 recorders are used to validate a derived model within software. The composite model offered within DIgSILENT requires a high degree of accuracy in terms of the block definitions and the type of controller that is used to replicate the exact AEG SVC controller setup at Grassridge substation. Convergence problems within the iterations will be encountered in terms of system initialisation if the model is not defined accurately. Result inaccuracies will also be incurred if the model is not correctly set such that it controls the correct busbar relating to voltage deviations in addition to the model been defined purely for an SVC with Thyristor Controlled Rectifiers (TCR) with fixed capacitance. These particular parameters are programmable in the model; however they need to be defined correctly in order to validate the real time values attained with the recorder equipment.

1.4 HYPOTHESIS

The root cause of the issue is defined in the problem statement. Real time data plays a significant part in the investigation, therefore capacitor bank and thyristor currents including HV, MV and LV secondary voltages and currents are recorded for healthy and non-healthy conditions. Manual calculations in addition to EMT Studies, using DIgSILENT PowerFactory, will be considered as a secondary proof to the real time values obtained using OMICRON test equipment. The following are the core to the hypothesis of the study undertaken:

- A) A derived model can successfully be simulated within software that accurately depicts the real time comtrade recordings of the systems plant and the switching characteristics of the network under investigation. The EMT study should also depict the secondary feed to the relay under investigation. The comtrade recordings will indicate whether or not the derived model within software is adequate for the research undertaken. The limited size of the derived model within DIgSILENT will indicate whether the results are negatively impacted.
- B) The derived model within DIgSILENT PowerFactory will be able to prove or disprove the problem statement brought forward in the research.
- C) Eskom Transmission was informed that a Point onto Wave controller (POW) such as the ABB F236 will effectively solve the problem statement. However due to actual breaker closing times that vary due to mechanical conditions that exist, the exact point on the voltage waveform will change and not effectively be issued at the exact set-point value.
- D) Real time data attained will clearly illustrate whether there are potential harmonic issues relating to the problem statement in addition it will provide information for the instances at which the system appears to be stable and no mal-operation of the AEG SIT 852 LV O/C relay occurs and visa versa. Thus fault harmonic interference studies relating to the comtrade recordings, is required to substantiate the statement of whether or not the AEG protection relays are mal-operating or whether suggested protection upgrades are required at Grassridge SVC.

From conclusive results, detailed analysis will determine whether the existing controlling circuits of the SVC operate correctly during certain transient system conditions.

1.5 DELIMITATION OF THE PROJECT

The research in this dissertation focuses on the mal-operation of the AEG SIT 852 LV O/C relay used in the protection scheme on the SVC located at Grassridge substation. The problem arises when Dedisa transformer 1 or transformer 2 is energised under no load conditions, therefore meaning that the concerned transformer been energised is not coupled at all to the 132kV system during the actual switching.

Therefore the following points form the delimitations that exist for the study undertaken relating to the problem statement:

- 1.5.1 The size of the derived model within DIgSILENT PowerFactory is smaller than the real time actual plant that exists on Eskom power system network as a whole. The simulation is performed for the plant under investigation and an equivalent source is modelled for the rest of the system. Inaccuracies may exist due to system conditions not taken into account for the rest of the network.
- 1.5.2 The software simulation does not depict all the actual points on the voltage waveforms relevant to all phases at which the energising took place during the outages. The model only performs a close on the first zero crossing particular to the red phase and the other two particular phases follow. Results may vary slightly relative to inrush conditions however w.r.t. the SVC operation, confirmation in the results will exist for correct operation or not.
- 1.5.3 The Point onto Wave controller wired in the closing circuit of the HV of the relevant transformers was not simulated in DIgSILENT PowerFactory. However the derived model was created to verify the SVC operation and not to indicate how inrush currents are reduced.
- 1.5.4 In a perfect environment with perfect conditions, infinitive transformer energising's are ideal in order to analyse and pin point the exact problematic condition on the Dedisa/Grassridge network. However multiple energising was not possible because the transformer life span is jeopardised under multiple energising conditions. System security and interruption to customers are also eminent when working outside Eskom outage times.
- 1.5.5 The SIT 852 LV O/C relay under investigation and suspected of mal-operating by Eskom are difficult to source due to non-available spares. Thus testing within the laboratory is limited and an equivalent type will be used that involves the same circuit topology. Thus, an earth fault relay will be tested under harmonic conditions to formulate results.
- 1.5.6 The actual comtrade recordings together with the simulated results that can be exported as a comtrade file will not be played back into the relay in order to verify correct operation or not due to the reason given in 1.5.5.

- 1.5.7 According to Eskom switching procedures and standards a transformer cannot be energised when the medium or low voltage side breaker is closed. Thus constraints exist such that the research entailed depict only a no load switching scenario and not a loaded scenario.

Relevant outages were arranged such that the researcher could perform maintenance tests on the SVC protection scheme to ensure that the AEG relays used for LV O/C protection and Harmonic blocking were operating correctly and within specification limits. Specific tests were also carried out particularly on the SIT 852 relay to decipher whether or not the relay is susceptible to harmonic currents during certain fault conditions thus influencing the actual value of the pick-up values.

The SVC protection scheme settings are verified and compared by means of calculations to real time data attained, thus analysing whether the relays have “drifted” over time therefore compromising the reliability and sensitivity of the particular protection scheme implemented by Telefunken in 1982.

1.6 OBJECTIVES OF THE STUDY

Certain research objectives are of extreme importance and are required to be highlighted in order to validate the outcome of the dissertation. Thus, theoretically and technically the research aim is to meet the following criteria:

- 1.6.1 Identify the root cause of the mal-operation of the AEG SIT 852 LV O/C Relay used on the SVC at Grassridge SVC.
- 1.6.2 Present a solution plan to Eskom Transmission in order to replace the AEG Telefunken protection scheme that was installed at Grassridge SVC in 1982 based upon the outcome of the maintenance results obtained together with the Harmonic related issue specific to the relay under test and in conjunction with the real time values attained with the recorder devices.
- 1.6.3 Identify whether there are predominant Harmonics present at Grassridge SVC when one of the transformers at Dedisa substation are energised under no load conditions.
- 1.6.4 Ensure that system stability is maintained at Grassridge substation after a solution is put together in a model setup therefore emphasizing to Eskom Transmission and ensuring them that the action taken will be implemented with confidence based upon a real time EMT study.
- 1.6.5 Create a detailed model in DIgSILENT PowerFactory build 14.1.3 replicating the actual network scenario at Dedisa and Grassridge together with system Impedances and fault levels are required in order to validate the results attained from the recording mediums. The model must reflect the actual no load energising scenarios. The model will be run as an EMT study allowing for transient inrush currents and voltage dips on the system.

1.6.6 Emphasize the accuracy of the test equipment utilized by Eskom to measure real time data.

1.7 OUTLINE OF THE STUDY

Eskom has been attempting to resolve this particular issue both partially and theoretically without success since January 2010 and have tried to prove many theories with no prevail. According to Eskom Transmission field staff when one of the transformers at Dedisa transmission station is energised such that they are coupled to the 132kV system, no tripping occurs at Grassridge and thus it seems from a high level perspective that the problem is solved.

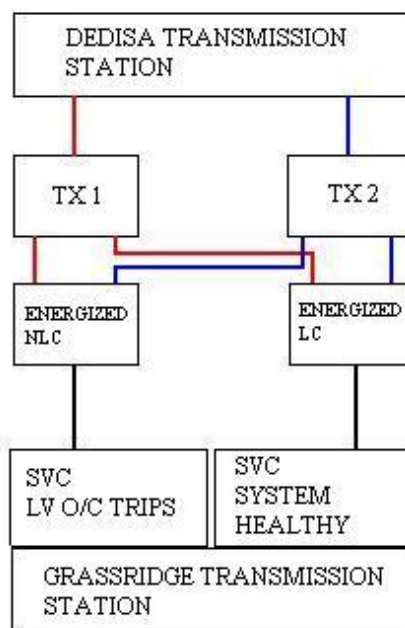


Figure 2: Block diagram relating to the Problem Statement

The research that was undertaken was planned and structured according to the following strategy.

In Chapter 2, harmonic content within a power system is emphasized. DIgSILENT PowerFactory is introduced as the main modelling software tool for the network setup under investigation. The significance of transformer inrush current is highlighted in order to emphasize the magnitudes produced under no load conditions. This relates specifically to relatively large MVA transformers. Overall Protection functionality and operations is shown and compared to the existing protection philosophy implemented at Grassridge SVC. The protection relay philosophies and the significance of the elements involved are highlighted and in particular SVC protection and the philosophies implemented on a general setup are indicated in this Chapter. Transient fault analysis and the definition of a typical scenario thereof are indicated.

In Chapter 3, the design aspect relating to the model created within DIgSILENT PowerFactory of the network topology is defined. This chapter also shows the controller setup and network modelling elements within the

simulation software. The recording medium in addition to the quantities recorded are defined in this chapter. Four case studies are introduced depicting the scenarios on how the relevant transformers are energised. The approach relative to the data capturing is well defined in each case study. The significance and potential role of the ABB F236 Point onto Wave Controller is highlighted and discussed in depth.

In Chapter 4, the analysis and interpretation of the OMICRON recording devices relative to the four case studies are tabulated and compared to the results simulated under transient switching conditions within the software model. The relevant case studies are shown and calculation quantities are formulated in TOP software in order to emphasize the root cause of the mal operation of the AEG SIT 852 LV O/C relay. This chapter also defines the process of elimination for the root cause of the mal-operation of the protection setup on Grassridge SVC.

In Chapter 5, the root cause of the mal-operation of the protection relay at Grassridge SVC is well defined and conclusions and recommendations are made. The software-based model is shown to be affective for Eskom's use at any other problematic SVC installation within the 132kV power system.

1.8 METHODOLOGY

The action plan relating to the information gathering at both Dedisa and Grassridge substation was implemented thoroughly for the investigation in the mal-operating of the LV O/C relay at Grassridge substation. Since the research aim is to solve the mal-operation of the SVC protection at Grassridge, the following are the methods that were taken to meet the objectives of the research.

1.8.1 Literature Review

The design and implementation of the AEG protection system used on Eskom's Southern Grid SVC's has clearly proven itself over the years as to be somewhat unreliable when considering the early 1980's design implemented and depreciation associated with the design. New state of the art technologies have become available and have introduced many additional features that have perfected the flaws in older type relays. Products offering reliability and user friendly interfacing are well defined in the research and equipment such as the Multilin T60 and F35 are primary examples of protection devices meeting Eskom protection philosophies. One of the key tools for the research will be Comtrade fault playback and recordings. A suitable recorder and associated software package will need to be decided on to conduct the recordings and fault playback. The tolerances for the test set will also need to be noted.

The specifications of the AEG SIT 852 LV O/C relay need to be obtained from manufactures data sheets to verify its sensitivity and response to harmonics. Methods used for harmonic transient and fault magnitude calculations need to be studied in order to perform the relevant hand calculations. All the required information will be gathered by reading related books, publications in journals and obtaining relevant papers on the IEEE website.

1.8.2 Site Survey and Data Collection

A survey will be performed in order to gather all the necessary information relating to a successful research investigation. Both primary and secondary plant drawings in addition to relay settings and specifications will be required from Eskom transmission. Insight into the spurious tripping action at Grassridge SVC will be directly related to recorded data attained at site with specialized test equipment and software (i.e. OMICRON). The gathered information will provide valuable insight relating to the operation.

1.8.3 Analysis of Existing AEG System

The interconnected power system of Eskom is equipped with reactive power compensating devices to enable the system to be utilized to its full potential. Various devices like shunt reactors, shunt capacitors, SVC's, synchronous machines, series capacitors and static shunt compensators are therefore installed in Eskom's network system. CT and VT circuits are supplied into the AEG protection system. The relevant relays then analyse the secondary values accordingly and then react in terms of either producing a protection trip or by supplying a relevant "block" function according to the type of value attained and the function required. If the design or philosophy is incorrect or if the relays are inaccurate due to various reasons they could thus produce inaccurate values during transient conditions. Inaccurate values could also be produced from transient or harmonic events which may cause saturation on either the CT or VT circuits respectively. The overall analyses will be emphasized on the AEG SIT 852 LV O/C relay which is installed in the protection scheme. The harmonic blocking relays however will need to be verified in the scheme to ensure correct operation such that the incorrect tripping is not "filtering" through from an unknown destination.

1.8.4 Harmonic and Fault Analysis

The transients that are produced at Dedisa substation and Grassridge substation respectively during switching are recorded in Comtrade format using an OMICRON CMC 356 and the OMICRON EnerLyzer software. Capacitor Bank and Thyristor currents including HV, MV and LV secondary voltages and currents are recorded for Healthy and Non-Healthy conditions during switching at the SVC. The recordings will be analysed in depth using OMICRON TransView to extract the information required for the particular hand calculations. A clip on type current transformer will be used to make the respective measurements. The following scenarios are applicable to the recorded values obtained:

- Dedisa substation, Transformer 1 closing
- Healthy normal measured values at Grassridge SVC
- Closing of the SVC after a trip
- SVC trip at Grassridge substation when Dedisa Transformer 1 is closed (unhealthy condition)

1.8.5 Manual Calculations and Studies

Mathematical analysis will be imperative when scrutinizing the recorded waveforms. The manual calculations will be in terms of transient and Harmonic analysis. Transient fault analysis together with the IEEE Std.1459 will be used to verify the following:

- The fault levels recorded
- The settings on the particular relay concerned
- The recorded Harmonic values from a high level perspective.

In depth Harmonic analysis will require the use of Fourier series interpretation. Fourier series establishes a relationship between a time-domain function and that function in the frequency domain. Analogues within a power system usually have a sinusoidal waveform which resembles the fundamental power system frequency. However in the case where switching transients are present (i.e. SVC), the magnitude of the fundamental is distorted somewhat and thus the waveform is not purely sinusoidal.

The other relevant calculations which will be performed are Transformer inrush currents indicating the 2nd Harmonic component relating to the fundamental. Calculations will be performed for the effective primary currents relating to particular settings on the relays. Simulations, if required, will be conducted in DIgSILENT to simulate the fault levels at strategic busbar locations in the vicinity of Grassridge substation and Dedisa substation. Harmonic analyses within the software will also be conducted if necessary to compare to recorded values obtained using the OMICRON CMC 356.

1.8.6 DIgSILENT Electromagnetic Transient (EMT) Studies

DIgSILENT tools support simulations with full electromagnetic transient models (EMT) thus providing instantaneous values of voltages and currents in the grid. Therefore a model will be derived in DIgSILENT for the scenario at Dedisa and Grassridge, thus enabling one to analyse and compare the OMICRON EnerLyzer results with the software model. Besides the EMT simulations, DIgSILENT provides the ability to perform RMS simulations. These simulations are also referred to as (dynamic) stability simulations, and they correspond to standard models in other power system stability simulation tools, e.g. PSS/E. The advantage of using RMS simulations is that the simulation speed can be increased significantly, but the simulations omit the fast electromagnetic transients (EMT). The RMS simulations can be done with the symmetric component only or with the asymmetric components as well. DIgSILENT also provides the ability to either simulate with a fixed time step or a variable time step for the simulations.

1.8.7 Testing of the AEG Relays

The AEG SIT 852 LV O/C will be tested using an OMICRON CMC 356 secondary injection test set. The relay will be injected with the fault recordings obtained from the initial energising recordings taken and TransPlay Software will be used to effectively “play” back the recorded fault results into the relay. The specifications of

the relay will be scrutinized according to the test results obtained and according to the desired response of the relay. These specifications are obtained from the relay manufacturer and Eskom Transmission. If the relay proves to be susceptible to harmonics generated during energising events at Dedisa substation then alternative solutions will need to be considered.

1.8.8 Implementation of Alternative Solutions

Historically, substation protection, control, and metering functions were performed with electromechanical equipment. This first generation of equipment was gradually replaced by analogue electronic equipment, most of which emulated the single function approach of their electromechanical precursors. Both of these technologies required expensive cabling and auxiliary equipment to produce functioning systems. Recently, digital electronic equipment has begun to provide protection, control, and metering functions. Initially, this equipment was either single function or had very limited multi-function capability, and did not significantly reduce the cabling and auxiliary equipment required. However, recent digital relays have become quite multi-functional, reducing cabling and auxiliaries significantly. These devices also transfer data to central control facilities and Human Machine Interfaces using electronic communications. The functions performed by these products have become so broad that many users now prefer the term IED (Intelligent Electronic Device). Users of power equipment are also interested in reducing cost by improving power quality and personnel productivity, and as always, in increasing system reliability and efficiency. These objectives are realized through software which is used to perform functions at both the station and supervisory levels. The use of these systems is growing rapidly. The new generation of equipment must also be easily incorporated into automation systems. The GE Multilin Universal Relay (UR) has been developed to meet these requirements. The Multilin T60 and F35 introduce a wealth of technology capabilities in terms of what they have to offer to the existing AEG protection system at Grassridge substation.

1.8.9 Documentation Method

The documentation will consist of the following:

- 1.8.9.1 An overlay of the topology at Grassridge substation.
- 1.8.9.2 The design of the AEG protection system currently protecting the SVC at Grassridge substation.
- 1.8.9.3 The derivation of the equivalent model for the protection circuit.
- 1.8.9.4 The transient and harmonic recorded results in terms of voltages and currents on the capacitor bank and Thyristors when one of the transformers at Dedisa substation are energised under loaded and unloaded conditions.
- 1.8.9.5 Manual calculations using mathematical derivations representing the transients and harmonics present in the recordings.
- 1.8.9.6 Maintenance test results for the AEG SIT 852 LV O/C and its response to injected recordings.

1.8.9.7 The issues relating to the existing protection system according to the problem statements and thus alternative solutions for a means forward.

1.9 DEFINITION OF CONCEPTS

Busbar - A common connection point in a distribution network substation.

Capacitor - is a device for storing electric charge. The forms of practical capacitors vary widely, but all contain at least two conductors separated by a non-conductor. Capacitors used as parts of electrical systems consist of metals foils separated by a layer of insulating film.

Critical fault clearance time - Refers to the maximum total fault clearance time that the power system can withstand without causing instability.

Current rating - The maximum current that may be permitted to flow (under defined conditions) through a distribution line or other item of equipment that forms part of a distribution network

Current transformer (CT) - A transformer for use with meters and/or protection devices in which the current in the secondary winding is, within prescribed error limits, proportional to and in phase with the current in the primary winding.

Dependability – Dependability is considered to be the most important attribute for a protection scheme as a whole. The non-operation of a relay can result in the destruction of a power system component and the collapse of the power system as a whole. Thus, the “responsibility” falls upon a specific relay to perform a specific task: “At the highest transmission voltages the level of dependability required for a rapid clearance of any protected circuit fault will still demand the use of two independent protection systems/relays” [5].

Distribution - The conveyance of electricity through a distribution network

EMT - Electromagnetic Transient

Fault clearance time - The time interval between the occurrence of a fault and the fault clearance.

Filter - due to undesirable odd-order harmonics being injected on the system by means of a reactive load, thus high power filters are usually provided to smooth the waveform. However since the filters themselves are capacitive, they also export MVARs to the power system.

Harmonic - of a wave is a component frequency of the signal that is an integer multiple of the fundamental frequency. Harmonics have the property that they are all periodic at the fundamental frequency and therefore the sum of harmonics is also periodic at that frequency.

Instrument transformer - Either a current transformer (CT) or a voltage transformer (VT)

Model -A usable knowledge based representation of the essential aspects of an existing system

Network - The apparatus, equipment, plant and buildings used to convey, and control the conveyance of, electricity to customers (whether wholesale or retail) excluding any connection assets.

Power System - A network when includes the point where the power is generated to transmission networks up to distribution. A system of high tension cables by which electrical power is distributed throughout a region.

Protection system - A system, which includes equipment, used to protect facilities from damage due to an electrical or mechanical fault or due to certain conditions of the power system.

Protective Relay - is a complex electromechanical or digital apparatus, often with more than one coil if electromechanical type. They are designed to calculate operating conditions on an electrical circuit and trip circuit breakers when a fault is detected. Protective relays have well established selectable time/current (or other operating parameters) curves.

Reliability - The possibility of a system, performing its function sufficiently for the period of time intended, under the encountered operating conditions. It is essential that protective relaying equipment is inherently reliable and that its application, installation and maintenance be such as to assure that its maximum capabilities are realized. Reliability is the assurance against incorrect operation from all extraneous causes: Incorrect operation of a relay can be attributed to incorrect design/settings, incorrect installation/testing and deterioration in service.

Security – The security of the relay system is at least as important as its dependability because an incorrect operation of a protective system reduces the overall reliability of the power system. It was found that occurrences such as rolling blackouts are related to the malfunction/mal-operation of a protective system rather than the non-operation of a system: “The application of protection to electrical power transmission schemes is biased towards security whilst ensuring dependability only for the most severe faults within the protected circuit” [5].

Selectivity – is the ability of the relay to differentiate between those conditions for which immediate action is required and those for which no action or a time-delayed operation is required. The relays must be able to recognize faults on their own protected equipment and ignore, in certain cases, all faults outside their protective area. It is the responsibility of the relay to be selective in the sense that, for a given fault condition, the minimum number of devices should operate to isolate the fault and interrupt service to the fewest customers possible: The relay must be able to select between those conditions for which prompt operation is required and those for which no operation, or time-delay operation, is required.

Sensitivity – Sensitivity applies to the ability of the relay to operate reliably under the actual condition that produces the least operating tendency: With modern digital and numerical relays the achievable sensitivity is seldom limited by the device design but by its application and CT/VT parameters.

Speed – Speed is the ability of the relay to operate in the required time period. Speed is important in clearing a fault since it has a direct bearing on the damage done by the short-circuit currents; thus, the ultimate goal of the protective equipment is to disconnect the faulty equipment as quickly as possible: “The speed of response will often depend on the severity of the fault and will generally be slower for a unit system” [5].

SVC - A Static VAR Compensator (or SVC) is an electrical device for providing fast-acting reactive power on High-Voltage electricity transmission networks. SVCs are part of the flexible AC transmission system device family, regulating voltage and stabilizing the system. The term “static” refers to the fact that the SVC has no moving parts. Prior to the invention of the SVC, power factor compensation was the preserve of large rotating machines such as synchronous condensers.

Thyristor - is a solid state semiconductor device with four layers of alternating N and P-type material. They act as bi-stable switches, conducting when their gate receives a current pulse, and continue to conduct while they are forward biased (that is whilst the voltage across the device is not reversed).

Transformer - A plant or device that reduces or increases the voltage of alternating current.

Transmission - high voltage electric transmission is the bulk transfer of electrical energy, from generating power plants to substations located near to population centres.

Unit protection - Generally, a protection scheme that compares the conditions at defined primary plant boundaries and can positively identify whether a fault is internal or external to the protected plant. Unit protection schemes can provide high speed (less than 150ms) protection for the protected primary plant.

Voltage transformer (VT) - A transformer for use with meters and/or protection devices in which the voltage across the secondary terminals is, within prescribed error limits, proportional to and in phase with the voltage across the primary terminals.

CHAPTER 2 – LITERATURE REVIEW

2.1 INTRODUCTION

Specific consideration together with ingenuity relating to various papers and books, mainly from the IEEE Xplore website, was investigated and considered in order to fulfil the essence of this chapter. The harmonic content a power system contains, due to many factors, some more “vigorous” factors than others, play a significant part in relay specification and design implementation relating to certain protection philosophies and device applications. The significance of the fundamental component relating to voltage and current and the remaining harmonic components thereof are broken down and then evaluated for transformer inrush conditions. The operations of a SVC and the controller specifically introduce harmonic orders due to thyristor applications within the controller design.

Five core protection relay attributes are empathized and the detrimental impact of not abiding by one of the protection laws therefore relate to a potential threat to the efficient and thorough operation of a well operated and protected power system.

SVC protection elements relating to the transformer itself in addition to the thyristors and capacitor banks are a fine art to set and then confidently protect with a suitable and reliable relay. Many manufactures offer various types of philosophies and techniques to perform transformer inrush blocking, earth fault protection, 2nd 3rd 5th 7th harmonic capacitor bank overcurrent protection. Therefore, when mal-operations occur, a systematic approach is required in order to produce a confident and significant hypothesis to the root cause of the problem for a complex device such as a SVC.

Transient studies are significant when investigating scenarios in a power system that relate to switching devices in particular. Thus if it is a transformer been energised or an SVC been energised, transient analysis will assist with certain investigation properties. Transient analysis is of utmost importance when capacitor banks, single or back to back, are energised and are not behaving as they ought too. For this project, significance is found within the first five cycles, 100ms, of energising the relevant transformer/s under test. Waveform analysis is crucial during this time period due to the magnetic properties of the 500MVA transformer/s.

2.2 ROOT CAUSE OF HARMONIC IMPACT

Non-active energy caused by predominant harmonics exist on a power system. SVCs use thyristors for control purposes, however there a few concerns relating to the harmonics produced: “Power electronics equipment, such as Adjustable Speed Drives, Controlled Rectifiers, Cyclo-converters, Electronically Ballasted Lamps, Arc and Induction Furnaces and clusters of Personal Computers, represent major non-linear and parametric loads proliferating among industrial and commercial customers. Such loads have the potential to create a host of

disturbances for the utility and the end-users equipment. Therefore, the main problem stems from the flow of non-active energy caused by harmonic currents and voltages” [2].

Relating to the issue of calculating the overall effective power produced or absorbed by a particular component, a few definitions are thus required in order to ensure accuracies within the calculations. The IEEE Std1459 lists definitions specifically relating to power definitions where the voltage and current waveforms are non-sinusoidal [2].

DIgSILENT PowerFactory proves to be at the leading edge when Engineers require a tool for analyzing protection relaying operations and harmonics within a power system. For this particular study where two sites (namely Dedisa and Grassridge) will be singled out for analysis, DIgSILENT proves to be more than suitable as a simulation tool if required. DIgSILENT is a computer aided engineering tool for analysis of industrial, utility and commercial electrical power systems. DIgSILENT was selected because it can perform balanced and unbalanced harmonic and protection studies. Each element has the option of balanced/unbalanced modeling where the user can model the elements as a single phase representation of the network [3].

The TCR branch of a perfectly designed SVC can cause harmonic components that are produced on the power system and thus obscuring the fundamental component [11].

If the supply voltage is purely sinusoidal it does not necessarily mean that the imposed currents are purely sinusoidal, on the contrary non-sinusoidal values are more predominant because the flux can be non-sinusoidal even when the supply voltage is sinusoidal. Certain degrees of imbalance and waveform distortion (normally with odd harmonics) are likely to be present on a power system due to the direct nature of the distribution/transmission system and the electrical loads connected [8].

2.2.1 Transformer Inrush Currents

When a part of the power system is energised by connecting it to the rest of the network by a closing operation of a breaker, the particular transformer can cause high inrush currents. The nonlinear behaviour of the transformer core is the cause of this. An air-core reactor switched on in order to compensate for cable charging currents does not cause inrush currents. When a power transformer is energised under no-load condition, the magnetizing current necessary to maintain the magnetic flux in the core is in general only a few percent of the nominal rated load current. Figure 3 shows the magnetizing curve and the hysteresis loop to explain the phenomena. [14]

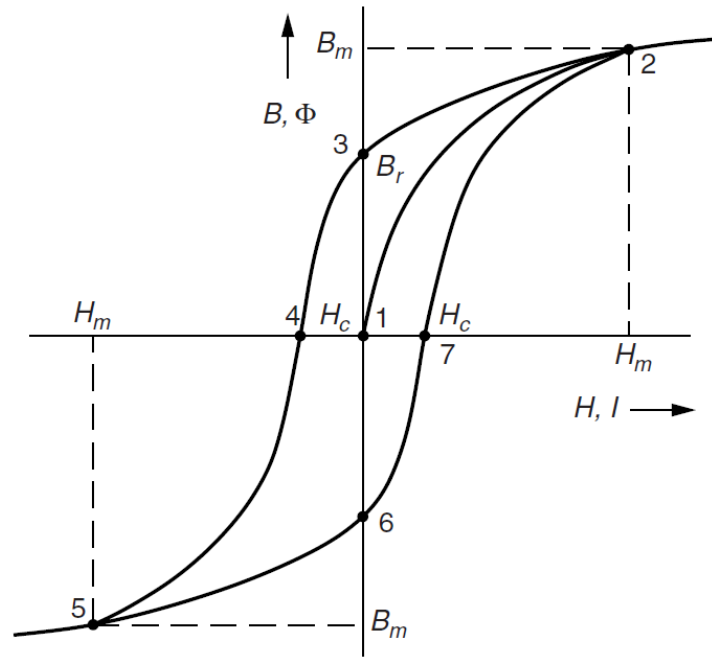


Figure 3: Magnetizing curve and hysteresis loop of a transformer core

Now, starting with an un-magnetized transformer core as seen in Figure 3, the flux density B follows the initial magnetization curve, starting at the origin (at 1). However when a power transformer has been switched off from the power system, the transformer core is left with a residual flux B_r . When the power transformer is connected to the network again at such an instant that the polarity of the system voltage is the same as the polarity of the residual flux B_r , then at maximum voltage, the total flux density in the core would have increased to $B_m + B_r$. The core is then forced into saturation and the transformer draws a magnetizing current from the supplying network. When the voltage reverses its polarity in the next half cycle, then the maximum flux in the core is less than the maximum flux density B_m in the no-load situation. The transformer inrush current is therefore asymmetrical and also contains a DC component, which takes seconds to disappear as seen in Figure 4 [14].

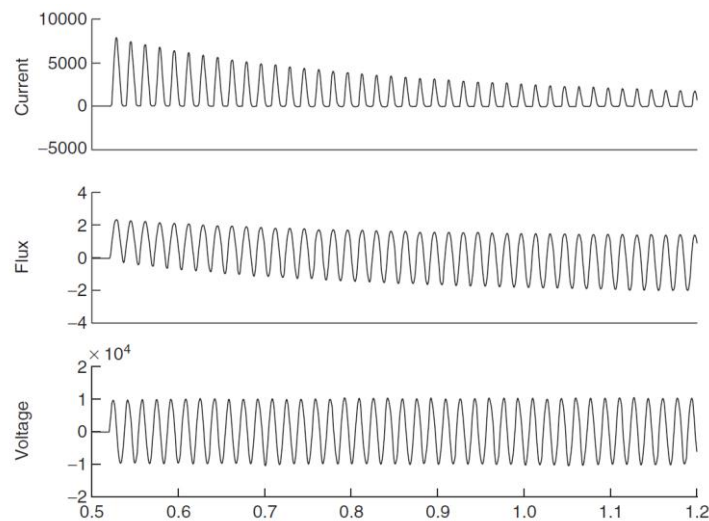


Figure 4: Transformer inrush current, the flux in the core and the supply voltage

Therefore, the peak value of transient inrush currents is an important factor when designing protection systems for a transformer and imperative for the verification of surrounding protection philosophies relating to network upgrades. A simplified set of equations can be used to calculate the peak value of the first cycle of the inrush current on the relative phase concerned. As seen in (1) the core material plays a significant part on the magnitude of the inrush component.

$$i_{peak} = \frac{\sqrt{2}V_m}{\sqrt{(\omega \cdot L)^2 + R^2}} \cdot \left(\frac{2 \cdot B_N + B_r + B_m}{B_N} \right) \quad (1)$$

where V_m is defined as the maximum applied voltage, L is defined as the air core inductance of the transformer, R is defined as the total dc resistance of the transformer, B_N is defined as the normal rated flux density of the transformer core, B_r is defined as the residual flux density of the transformer core, B_m is defined as the saturation flux density of the core material. As seen from equation (1) the value of inrush current is dependent on the parameters of the transformer in addition to the operating conditions of the power system. [5]

However if the core material components are unknown or need to be approximated then further detailed analytical equations are required in order to accommodate for the switching angle and system source impedance at the point of energising. Therefore one applies Kirchhoff's voltage law that gives us the nonhomogeneous differential equation as in (2) [14].

$$E_{max} \sin(\omega t + \theta) = Ri + L \frac{di}{dt} \quad (2)$$

Thus when the breaker closes at any time instant, the phase angle can have a value between 0 and 2π rad. In order to find the general solution of the differential equation, one has to solve the characteristic equation of the homogeneous differential equation seen in (3) [14].

$$Ri + L\lambda i = 0 \quad (3)$$

The scalar λ is the eigenvalue of the characteristic equation. We find for $\lambda = -(R/L)$, and thus the general solution for equation (2) is seen in (4).

$$i_h(t) = C_1 e^{-(R/L)t} \quad (4)$$

The particular solution is found by substituting into (2) a general expression for the current thus found in (5).

$$i_p(t) = A \sin(\omega t + \theta) + B \cos(\omega t + \theta) \quad (5)$$

Therefore, A and B can be determined and are indicated as in (6).

$$A = \frac{RE_{\max}}{R^2 + \omega^2 L^2} \quad B = -\frac{\omega LE_{\max}}{R^2 + \omega^2 L^2} \quad (6)$$

This therefore results in a particular solution for the current as seen in (7).

$$i_p(t) = \frac{E_{\max}}{\sqrt{R^2 + \omega^2 L^2}} \sin[\omega t + \theta - \tan^{-1}\left(\frac{\omega L}{R}\right)] \quad (7)$$

Thus, the complete solution which is in fact the sum of the general and particular solution is seen in (8).

$$i(t) = C_1 e^{-(R/L)t} + \frac{E_{\max}}{\sqrt{R^2 + \omega^2 L^2}} \sin[\omega t + \theta - \tan^{-1}\left(\frac{\omega L}{R}\right)] \quad (8)$$

Now, as compared to the formulation and criteria needed in (1), before the breaker is closed, the magnetic flux or the residual flux of the transformer is assumed to be zero and therefore owing to the law of conservation of flux, $t=0$ and we can find (9).

$$C_1 + \frac{E_{\max}}{\sqrt{R^2 + \omega^2 L^2}} \sin[\theta - \tan^{-1}\left(\frac{\omega L}{R}\right)] = 0 \quad (9)$$

This therefore established the complete solution for C_1 and hence the complete expression for the instantaneous value of the peak current that is vital for this particular research and will be utilised to quantify the real time values obtained. Thus the complete expression is found in (10).

$$i(t) = e^{-(R/L)t} \left\{ \frac{-E_{\max}}{\sqrt{R^2 + \omega^2 L^2}} \sin\left[\theta - \tan^{-1}\left(\frac{\omega L}{R}\right)\right] \right\} + \frac{E_{\max}}{\sqrt{R^2 + \omega^2 L^2}} \sin\left[\omega t + \theta - \tan^{-1}\left(\frac{\omega L}{R}\right)\right] \quad (10)$$

The first part of (10) contains the component responsible for the damping out effect of the ‘‘DC component’’ as it is well known [14].

Therefore, we know that when a transformer is energised under ‘‘no load conditions’’ certain harmonics are produced, therefore, from an economic point of view, a transformer is designed to operate in the saturating region of the magnetic core [4].

Thus, the magnitude of the inrush current is unpredictable without a certain degree of control switching. That inrush current could be as high as 10 to 20 times the rated current and could cause mal-operation of protection relays if a blocking function is not applied to the relay protecting the particular transformer. The magnitude of

the inrush current depends on the instant of the voltage wave at which the transformer is connected to the power system [4].

Concerning the exciting currents percentage value of the predominant harmonics superimposed onto the fundamental: “The exciting current will contain the fundamental and all odd harmonics, however the third harmonic is the predominant one and at rated voltage the exciting current can be 5% to 10% of the fundamental and at 150% of the rated voltage the third harmonic can be as high as 30% to 40% of the fundamental” [4].

2.3 PROTECTION FUNCTIONALITY AND OPERATIONAL SEQUENCE

2.3.1 Details of Grassridge SVC

The range of the 132kV SVC is 10MVar inductive to 35MVar capacitive. The SVC is connected to the 132kV busbar via a breaker and a step-down transformer. The secondary side of the transformer has a nominal voltage of 5.1kV and feeds a thyristor controlled reactor (TCR) and a fixed capacitor bank (35MVar) which is connected in parallel to the TCR, Figure 5 depicts this setup. The thyristors are used to vary the current through the reactor smoothly from zero to full rated current (0 to 45MVar). Due to the non-sinusoidal waveform of the reactor current the TCR produces harmonic currents. Thus the fixed capacitor bank is specifically tuned using series reactors to form filters to filter out the harmonic currents produced by the TCR. The filters are tuned to the 2nd, 3rd and 5th harmonic frequencies.

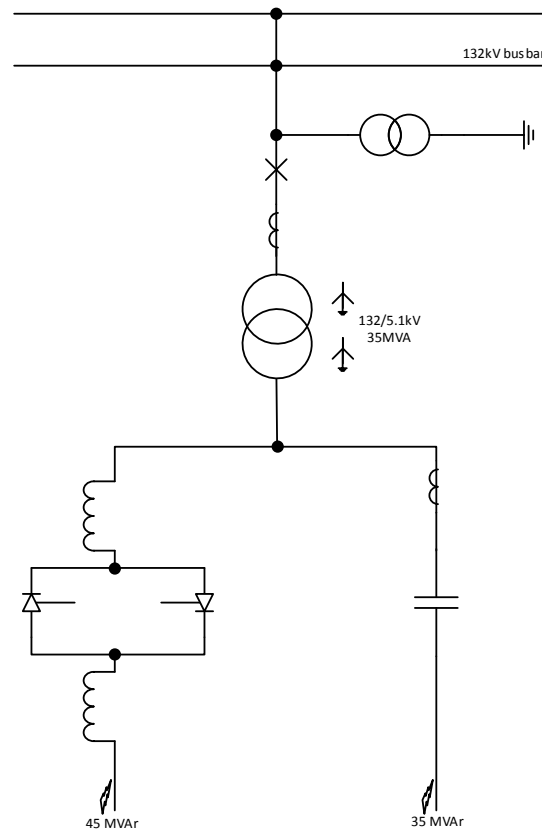


Figure 5: Single line diagram of the 132kV SVC [12]

The Reactors – are of the coreless, air insulated type (air cored reactor). The reactor of each branch is divided into two sections. The two sections are connected between two phases on both sides of the thyristor valve, this is purely due to manufacturing specifications and also to make use of the mutual inductance between the two sections. Therefore by using the mutual inductance a significant amount of material is saved. Each section is therefore designed to withstand the full branch voltage. The possibility of reactor flashovers is therefore limited. If one section is possibly short circuited due to mal-operation, the valve current control circuits will limit the current in the TCR branch to acceptable levels [12].

The Capacitor/Filter Banks – are tuned to filter out the harmonics produced by the TCR's. The nominal rating of the capacitor/filter bank is 35MVar. The filter is tuned to the 2nd, 3rd and 5th harmonic frequencies [12].

2.3.2 Protection Functionality

A protection system is required to make integrated decisions based on settings allocated to the particular relay and thus decide and quantify whether the info received justifies a trip condition with a certain time frame or whether to block a trip due to certain criteria. Thus the protection philosophy on Grassridge SVC follows just that. Electrical quantities (voltage, current, frequency, etc.) are fed into the protection relay and based on its program and internal configuration, the protection relay makes a decision on what to do and causes a circuit breaker to trip (action), see Figure 6 for the flow sequence: “It is essential to ensure that settings are chosen for protection relays and systems which take into account the parameters of the primary systems, including fault and load levels and dynamic performance requirements” [5].

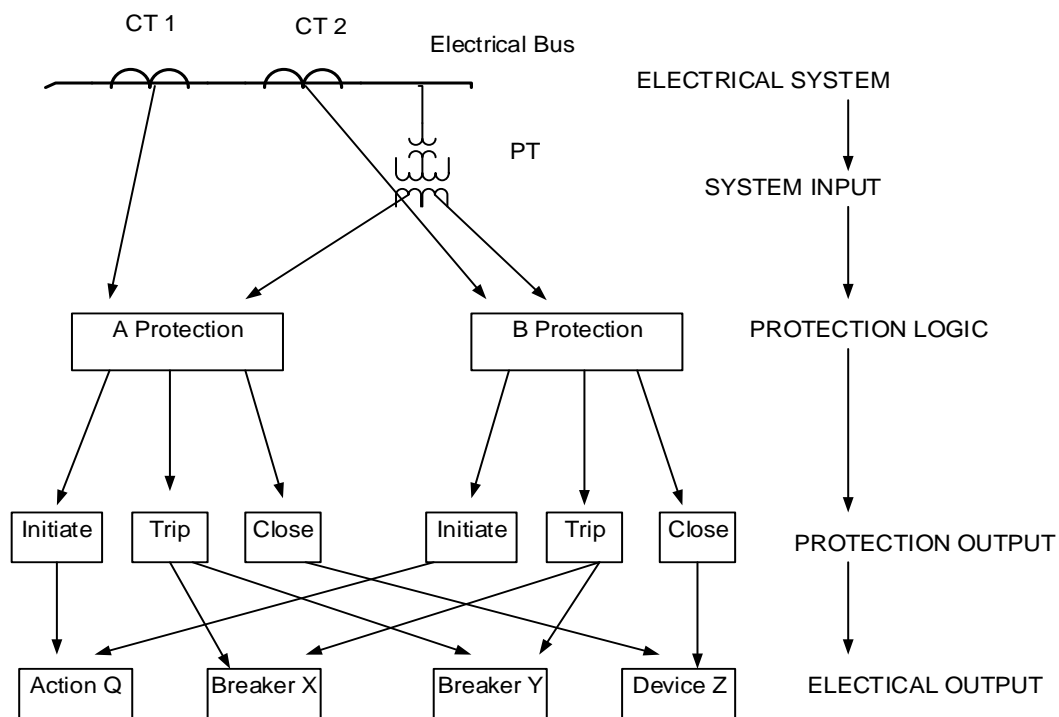


Figure 6: Block diagram of protection operation

2.4 STATIC VAR COMPENSATOR PROTECTION

Certain relays are tasked for certain protection philosophies relating to the SVC found at Grassridge substation. The protection equipment relative to the study undertaken is emphasised within this particular section.

The Thyristor Controlled Reactor (TCR) has its own protection relay to monitor certain disturbances that might occur. The reactor branch protection can be categorized into many different philosophies however emphasis is made on the overcurrent protection which is specific to Grassridge SVC. Multi-phase overcurrent protection is used and can be set for both instantaneous and time overcurrent. Back-up protection for the reactor branch may be included in the overall back-up for the SVC. Ground overcurrent protection is provided for each reactor branch [10].

The system that controls the gating of the thyristor valves incorporates checks for firing malfunctions by comparing the presence of valve current with the timing of gating signals [10]. Thus unbalance or negative sequence protection is achieved.

The relative capacitor branch protection on the SVC can be categorized into namely unbalance protection, overcurrent protection, differential protection, overvoltage protection and voltage surge protection. These are all important protection philosophies to ensure the capacitor bank of the SVC is protected effectively, however in depth analysis will not be made due to the problem at hand, however is noted for an overall dynamic picture of the system.

In terms of the nature of the study it is noted that the capacitors do not generate harmonics, but provide low impedance path for harmonics that may be generated by the TCR branch [11].

Filter Protection devices or the switching of SVC elements may produce harmonics on a power system. The magnitude of the harmonics greatly depend on the type of SVC, the SVC configuration, the system impedance and the amount of reactance switched. These harmonics are investigated in depth in order to verify and conclude whether it's the root cause of the mal-operating relay. In the SVC application, harmonic currents are mainly generated by the TCR branches. The triplen harmonics (3, 9, 15 etc) are removed by a delta (or wye ungrounded) connection only if the SVC is balanced and controlled as a three-phase unit. Even harmonics are also removed by symmetrical gating of the TCR thyristors [11].

Thyristor Protection emphasizes mainly overcurrent protection. Thyristors are gated into conduction or fired by a gate trigger pulse generated in the thyristor control system, therefore in TCRs, the thyristor firing can achieve full or partial conduction by adjusting the gate trigger pulses in relation to the power system voltage waveform. Thyristor protection is based on the maximum off-state voltage and on-state current the thyristor can withstand. Thus it is imperative for the research conducted to monitor the thyristors reaction to certain voltage deviations on the system in order to verify correct operation [11].

Overcurrent Protection is used to protect the thyristor valves and this is achieved by means of thermal protection. A model evaluates the junction temperature and hot spot effects. The thermal model may first initiate continuous firing if the valve's blocking capability is threatened, followed by a trip command. Now, in the reactor branch, a dc current can be produced. Although this component will decay, it should be measured in order to give correct feedback to the respective model. Normal operation may occur if enough time is given for cooling of the junction. In the TCR, the thyristor control equipment monitors the current in the reactors and it decreases the conduction to keep the current below the rating of the valve. This is called partial conduction. [11].

2.5 TRANSIENT/PERMANENT FAULTS AND MAL-OPERATION

Transient faults are faults that do not damage the insulation of transformers permanently and as such allow the circuit to be safely re-energised after a short period of time.

When a transformer is energised under no-load conditions, the magnetizing surge current is so great such that it could cause mal-operation of transformer differential schemes. A transformer energised under no-load conditions can cause 2nd harmonic inrush currents to flow, also known as the magnetizing currents of the particular transformer. These particular currents may be as high as 40%-50% of the fundamental component [9].

Now after a closing operation, transient currents will flow through the power system. During an opening operation, when a power-frequency current is interrupted, a transient recovery voltage (TRV) will appear across the terminals of the interrupting device. Now for comparison purposes relating to the research conducted, when capacitor banks are placed in a substation for voltage regulation or stabilization, the switching devices interrupt a mainly capacitive load when operating under normal load conditions and it is well known that the current and voltage are approximately 90° out of phase and the current is leading the voltage. However, when a large transformer such as one of the 500MVA's located at Dedisa substation are disconnected in a normal load situation, current and voltage are also approximately 90° out of phase but now the current is lagging due to the large inductance. Closing a switch or circuit breaker in a dominantly capacitive or inductive network results in inrush currents, which can cause problems for the protection system [14].

2.6 CALCULATION AND SHORT CIRCUIT CURRENT

Accurate fault current calculations are normally carried out using an analysis method called "Symmetrical Components." This method involves the use of higher mathematics and is based on the principal that any unbalanced set of vectors can be represented by a set of 3 balanced systems, namely; positive, negative and zero sequence vectors. However, for practical purposes, it is possible to attain a good approximation of three phase short circuit currents using some very simplified methods, which are discussed below. The short circuit current

close to the transformer and at the secondary side of the transformer can be quickly calculated, using the following formula:

$$\text{Short-circuit MVA} = \frac{100P}{X\%} \quad (11)$$

$$\text{Short - circuit current } I_{kA} = \frac{MVA}{kV\sqrt{3}} \quad (12)$$

Where

P = Transformer rating in MVA

X% = Internal reactance of transformer in %

I_{kA} = Short-circuit current in kA

kV = Transformer secondary voltage in kV

Normally, the % reactance value of the transformer can be obtained from the nameplate, or if not, from the transformer data sheets. If a length of cable (more than 100m) exists between the transformer and the fault, the impedance of the cable has to be taken into account to arrive at a realistic value for the worst-case fault current. This is done by calculating the source impedance and then adding the cable impedance, as follows:

$$\text{Source Impedance } Z = \frac{kV}{kA\sqrt{3}} \quad (13)$$

$$\text{Fault Current kA} = \frac{kV}{Z_{source} + Z_{cable}} \quad (14)$$

Z cable can be obtained from the manufacturer's cable data sheets. However the above calculation is another approximation, as Z source and Z cable are not necessarily in phase, and complex algebra should be used. This is accurate enough in most practical applications. The fault current found in (14) is imperative for calculating the source impedance required to effectively model an external grid system in software.

Protection IDMT curve calculations are derived from the formula that complies with the BS 142 and IEC 60255 standards. It is mathematically defined as follows:

$$T_d(s) = \frac{K}{\left(\frac{I}{I_s}\right)^\alpha - 1} \times \left(\frac{T}{\beta}\right) \quad (15)$$

Where

T_d = Operating time in s

T = Operational time at 10Is

I_s = Actual secondary pick-up value

I = Setting value in terms of secondary magnitude

α = 0.02 for a normal inverse curve

β = 2.97 for a normal inverse curve

K = 0.14 for a normal inverse curve

2.7 CONCLUSION

Transformer inrush currents are well defined in this section and are related to the research work and procedure to follow to effectively produce a solution plan to Eskom Transmission. Formulas relating to the specific types of switching are highlighted in detail and reference is made to the particular expression/s required for an effective approach to peak inrush currents. Formulas relating to the material composition of a transformer are also highlighted.

The parameters and components making up the SVC located at Grassridge substation is emphasised together with the significant protection functionalities required in order to ensure continuous reliable operation. The transient response according to voltage deviations in a power system is explained and demonstrated against transformer and capacitor bank switching respectively.

Further calculations are outlaid in order to assist with manual calculations for the software tool in terms of the external grid source. Particular emphasis on the formulas is imperative as it is shown to be a key tool when performing per unit system calculation and derivation in the studies conducted.

CHAPTER 3 - DESIGN

3.1 INTRODUCTION

For this project a certain recording medium was required such that current and voltage quantities could be measured with a high degree of accuracy. This accuracy was required to withstand measuring standards specifically during certain switching transients. The first five cycles of the system response due to a power system disturbance or switch is crucial for the study. The OMICRON CMC 356 and Enerlyzer software met all these criteria.

Thus the approach for the design aspects of the research was firstly the evaluation of real time values obtained using two OMICRON CMC 356's, at two independent locations and implementing them as recorder devices in Eskom's power system. Four case studies are evaluated to establish a working platform in order to compile results from the captured quantities. Two of the case studies are significant to transformer 1 and the angle on the voltage waveform at which the transformer is energised. Case study three and four are significant to transformer 2 energising and the method of switching thereof. One of the four case studies are of significant relevance due to an SVC trip that occurred. Transformers are normally closed via an auxiliary contact. Thus by applying system voltage at a random instant in time on the transformer windings resulted in a high transient magnetizing inrush current which resulted in high orders of 2nd harmonic currents to flow under no load conditions. A known philosophy to mitigate these inrush currents is to energise the transformer by controlling the circuit breaker closing times such that the magnetic flux produced in the windings corresponds to the prospective flux in the core. Inrush transients produced can cause nuisance tripping's at the particular location where the respective transformers are energised. Thus the ABB F236 controller is introduced and tested and the relevant implementation in the study is shown.

A derived model within DIgSILENT was then created and electromagnetic transient studies were performed and compared to the real time values obtained. Three scenarios are simulated within software in order to demonstrate the effectiveness the SVC introduces for the 132kV system. The three scenarios depict firstly a strong source at Poseidon, a weak source at Poseidon and lastly a replication of the exact system voltages that existed when the SVC tripped.

OMICRON EnerLyzer was the software tool used for the Comtrade recordings at both locations. The setup of the EnerLyzer software is shown and the accuracies within the setup is emphasised within this chapter.

3.1.1 Network Layout

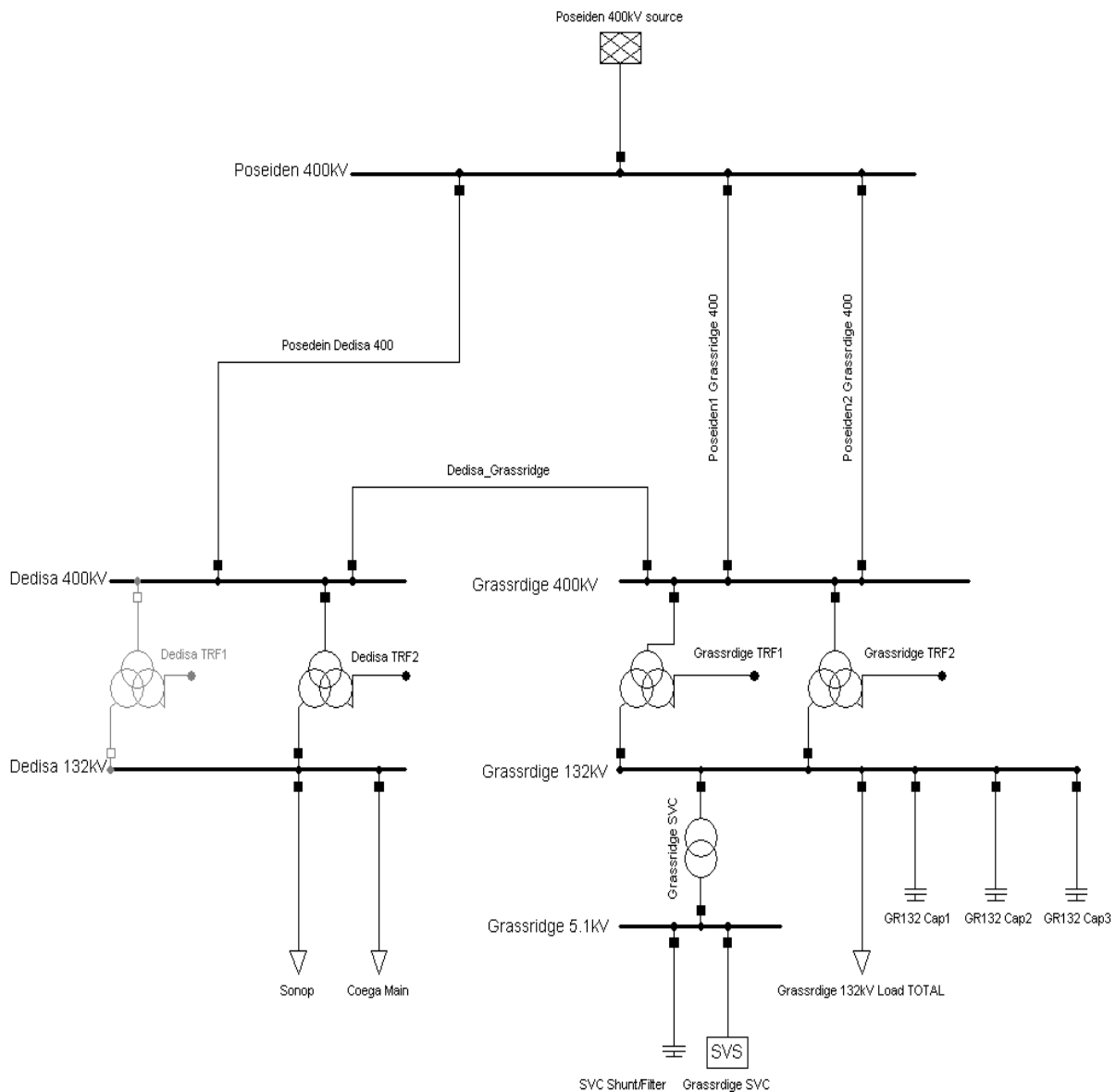


Figure 7: Simplified single line diagram (SLD) of the network under investigation

3.2 ABB F236 POINT ONTO WAVE CONTROLLER

3.2.1 Introduction to the ABB F236 Controller

The ABB F236 controller enables controlling of the switching moment so that switching always takes place in a pre-determined phase position selected. This is done in order to eliminate the switching transients or limit the transient as far as possible. The magnitude of the transients is determined by the phase position at which the energising of the primary apparatus occurs. By closing a breaker randomly due to a supervisory close or an actual close from the panel results in a closure at any point on the voltage waveform according to the operating time of the breaker and the operating time of the close coil. The ABB F236 is primarily meant for controlling of

both closing and opening of single-pole operated circuit-breakers, however it can be used with three-pole operated circuit-breakers [15].

The advantages of using an ABB F236 controller compared to applying conventional transient limiting methods are that there are reduced transients when switching the following primary plant:

- Power transformers.
- Shunt reactors
- Capacitor banks

There is an adaptive control setting within the F236 relating to the switching moment which therefore safeguards the controlled switching regardless of the aging effects on operational times of different circuit breakers. When the ABB F236 is used in adaptive mode, it notes the result of a performed switching for each respective pole and adjusts its waiting time for the next switching, taking into account any deviation from the intended target. Such deviations can, for example, be caused by variations in the operating time.

Power Transformers are energised normally under no load conditions. However energising at an unsuitable phase position with respect to the voltage waveform could result in large current surges which makes controlled closing favourable. Certain types of transformers can be energised in such a manner that the residual flux can be ignored. This is especially the case if the capacitance between the circuit-breaker and transformer is so large that the capacitive energy at the previous interruption was sufficient to demagnetize the iron core of the transformer. This can usually be seen by studying voltage variations on the load side after interruption. Now, if the closing pulse is the same at every switching occasion, then the problem can be solved by controlling both the opening and closing times, thus allowing the controlled closing time to be adjusted in such a way to fit the residual flux defined by the controlled opening [15].

With single-pole operated circuit-breakers, switching instants for the poles can be pre-set independently of each other for closing as well as opening. Since the switching sequence of a three-pole operated circuit-breaker is determined by a fixed mechanical design, the opening and closing sequences depend on each other. It may be difficult to find a compromise which yields an absolute minimum of influence of residual flux on magnetic flux symmetry at closing. It is also difficult to predict the behaviour of the circuit by calculation, partly because magnetic characteristics and stray capacitances are difficult to model exactly, and partly because the exact interruption instants of the no-load currents are difficult to predict [15].

The demand on precision at controlled energising of a transformer can be as high as for capacitors and reactors, which is why adaptation control is the desired method to use and Figure 8 indicates the implementation of the controller wired in the closing circuit of the HV controlling the energising of the relevant 500MVA transformer under test. The low magnetizing current of a no-load transformer will, however, make it impossible to use detection of current onset for adaptation. The detection delay will also be unpredictable. Instead detection of voltage onsets on the load side, connected via voltage transformers to inputs "VOLTAGE DETECTOR" can be used [15].

3.2.2 ABB F236 Application



Figure 8: ABB F236 wired into the closing circuit of Transformer 1 at Dedisa substation

3.3 OMICRON CMC 356 SETUP AND CASE STUDIES

OMICRON CMC 356 recording devices are setup at both Dedisa and Grassridge substations. OMICRON test equipment and software is the primary tool to investigate real time data obtained at both substations. Real time analysis is extremely sensitive to the type of measurement tool used for the interconnection between the test set and the protection relay. Figure 9 shows the test set used for recording purposes.

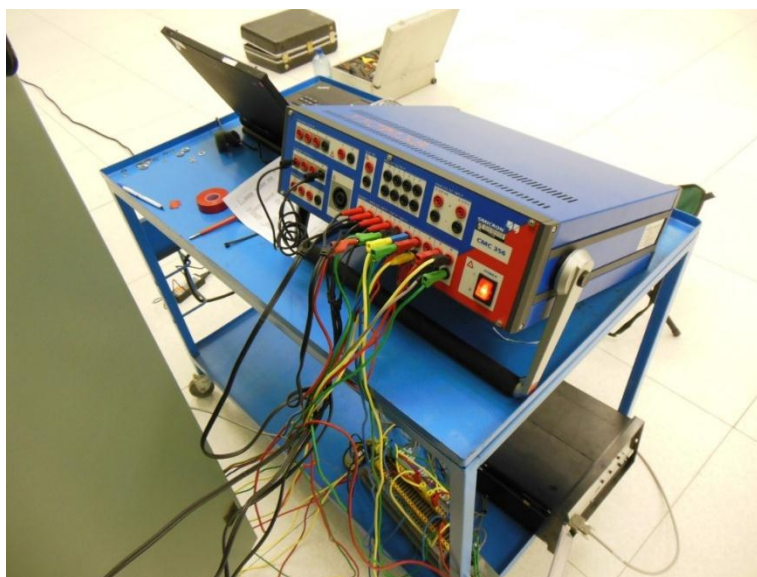


Figure 9: OMICRON CMC 356 test equipment setup

Secondary transient current and voltage waveforms are recorded for various switching scenarios according to a POW controller issuing switching commands to the relevant transformer HV breaker. These recordings are then analysed to determine whether a POW controller is significant at Dedisa for the sporadic tripping of the SVC at Grassridge substation. DIGSILENT results formulated from a derived model, mimicking the switching scenario causing the sporadic tripping of the SVC, will be compared, in terms of busbar voltage variations and current magnitudes, to the actual real time results obtained using the OMICRON CMC 356's. Analysis will confirm whether further recommendations are required for the entire protection setup at Grassridge SVC due to harmonic sensitive relays.

3.3.1 EnerLyzer Software Setup

OMICRON EnerLyzer is a recording medium specific for real time analysis. Recordings are individually captured in COMTRADE format. Sensitivity settings on the current probes are imperative when evaluating distorted waveforms. The current probes are external CT connections for measurements purposes only and are directly calibrated according to the desired sensitivity within the specific software tool. Figure 10 shows the range at which the clamp-on CT was set together with the CT ratio of the particular circuit it was recording (i.e. the thyristor circuit relating to the SVC at Grassridge substation is in the example below).



Figure 10: Clamp on CT setup within OMICRON EnerLyzer

An OMICRON CMC 356 test set allows for 10 channels to be configured as analogue or digital recording inputs. Figure 11 indicates the 10 channels that are allowed to be addressed as either voltage inputs or current inputs or merely “dry” or “wet” contacts according to the users interface specifications and recording setup.

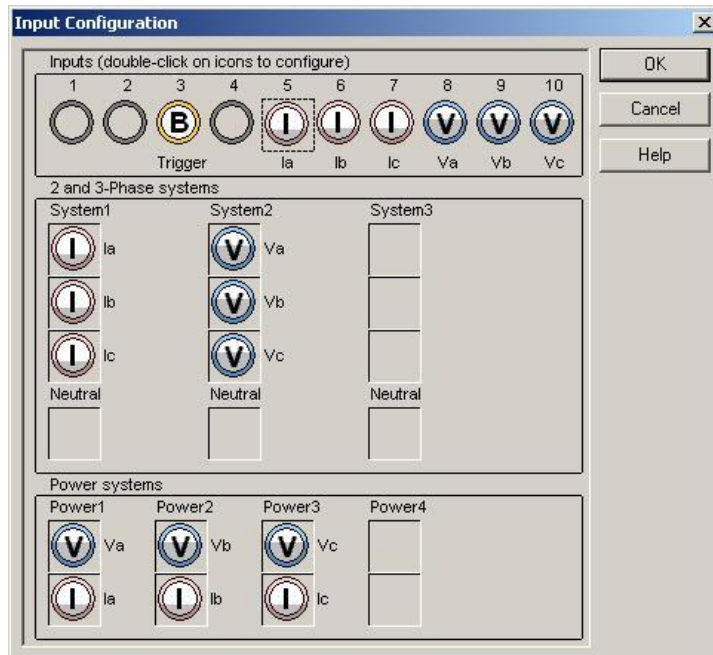


Figure 11: Channel setup within OMICRON EnerLyzer

For the recordings specific to the research carried out in this project a certain threshold current was desirable in order to trigger the recording such that it could take a snapshot of the waveforms at the instant of the disturbance on the system. This particular setup was imperative such that the recording device at Dedisa substation would commence recording at the exact same time instance as Grassridge SVC recording device starts. Therefore the current channel was selected and the desired or expected secondary current was defined for the commencement of the recording. The CT ratio of the primary plant was defined in the software such that the secondary current is relevant to the full value of the actually primary current. Thus for transformer inrush at Dedisa substation any current value would be acceptable as the transformers initial secondary value is zero. Figure 12 indicates the channel selected for the trigger condition together with the secondary current pick-up value. The sampling frequency relates to the accuracy and details at which the waveforms (voltage and current) are recorded, however the time of the recording is jeopardized with a higher sampling Frequency (i.e. higher degree of accuracy). The sampling Frequency was selected to 9 KHz for the research outlined. This provided waveforms that were more than adequate to analyse and compare.

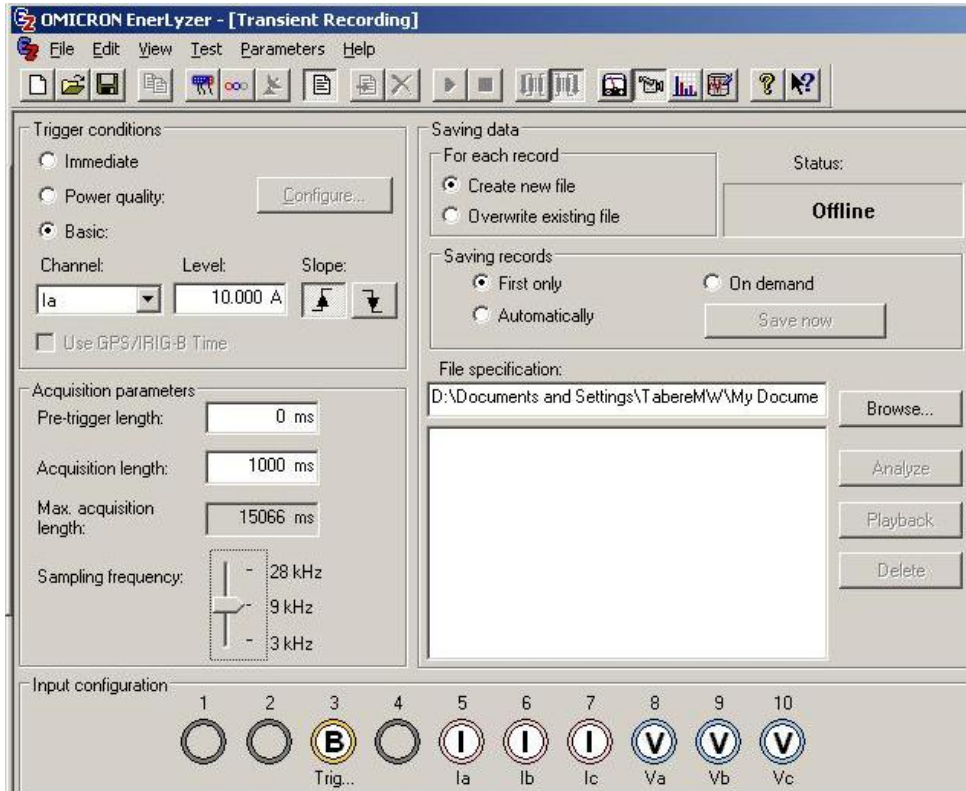


Figure 12: Trigger setup and conditions in OMICRON EnerLyzer

3.3.2 Case Study 1 - Transformer 1 Energising, NO SVC Trip

In case study 1 the Point onto Wave (POW) controller was set such that a close pulse was sent to the HV breaker poles after a pre-defined time that was adjustable within the software. Figure 13 indicates a simplified diagram of the controller that was pre-wired for test purposes. Recorder 1 was setup at Dedisa substation to measure the 400kV voltage and inrush current during the switching. There were two recorders (i.e. recorder 2 and recorder 3) setup at Grassridge SVC in order to measure the 132kV and 5.1kV analogues in terms of the voltage and current quantities of all relevant phases. A digital input was recorded for a trip contact. The reason why two recorders were used is purely due to the limitation one standalone unit presented for the number of inputs available on the OMICRON CMC 356. In this particular case study no trip occurred when Dedisa transformer 1 was energised. Waveforms were captured and are illustrated and explained in detail together with simulated results and comparisons in chapter 4.

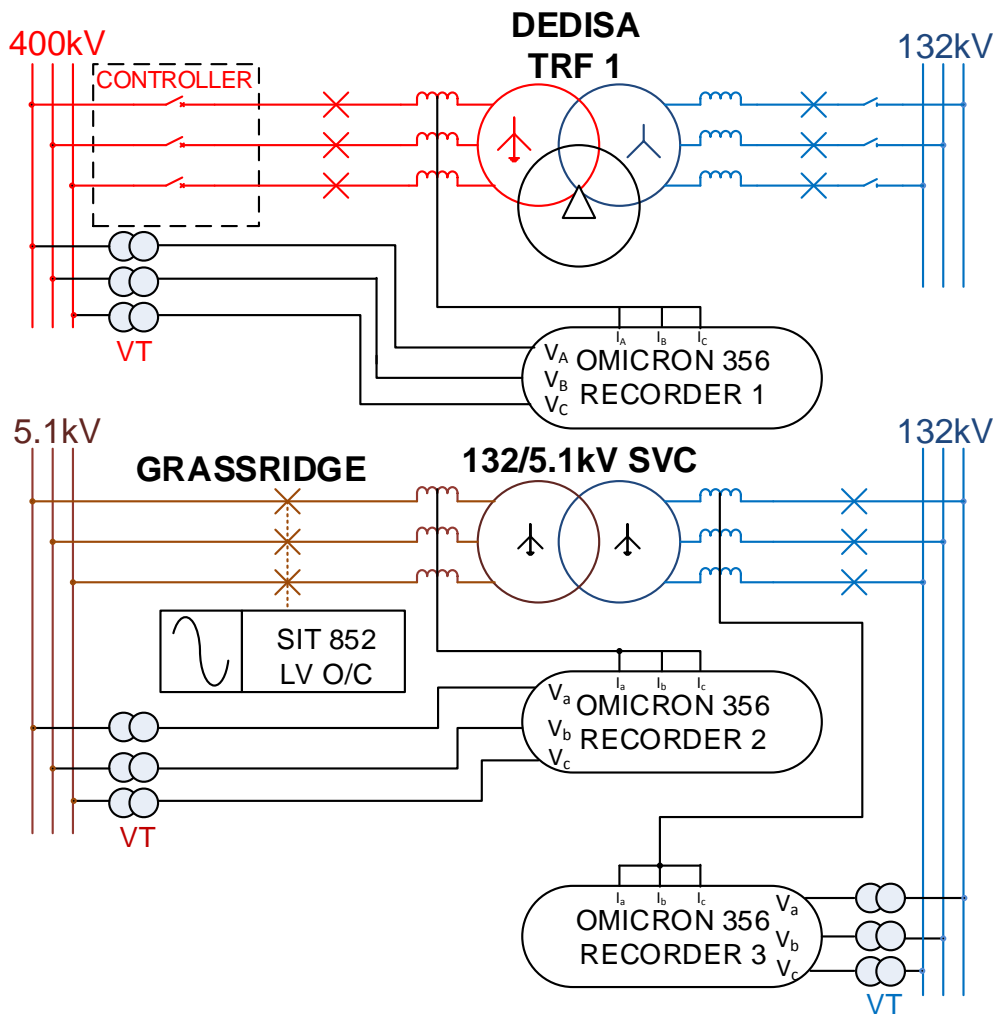


Figure 13: Case study 1 recorder setup and breaker operation

3.3.3 Case Study 2 - Transformer 1 Energising, SVC Trip

Now, as compared to case study 1 there was a recorded trip at Grassridge SVC due to the SVC's LV O/C (AEG SIT 852) relay operating. Case study 2 demonstrates the significance of a POW Controller and shows whether or not it is relevant to the root cause of the actual problem at hand. Chapter 4 illustrates the captured waveforms together with the EMT simulation results comparing what actually occurred on the system against the expected or the instantaneous values of the secondary currents relative to the 5.1kV side of the SVC. Figure 14 indicates the recording medium setup at the two substations together with a simplified indication of the relevant relay under investigation causing the actual suspected mal-operation.

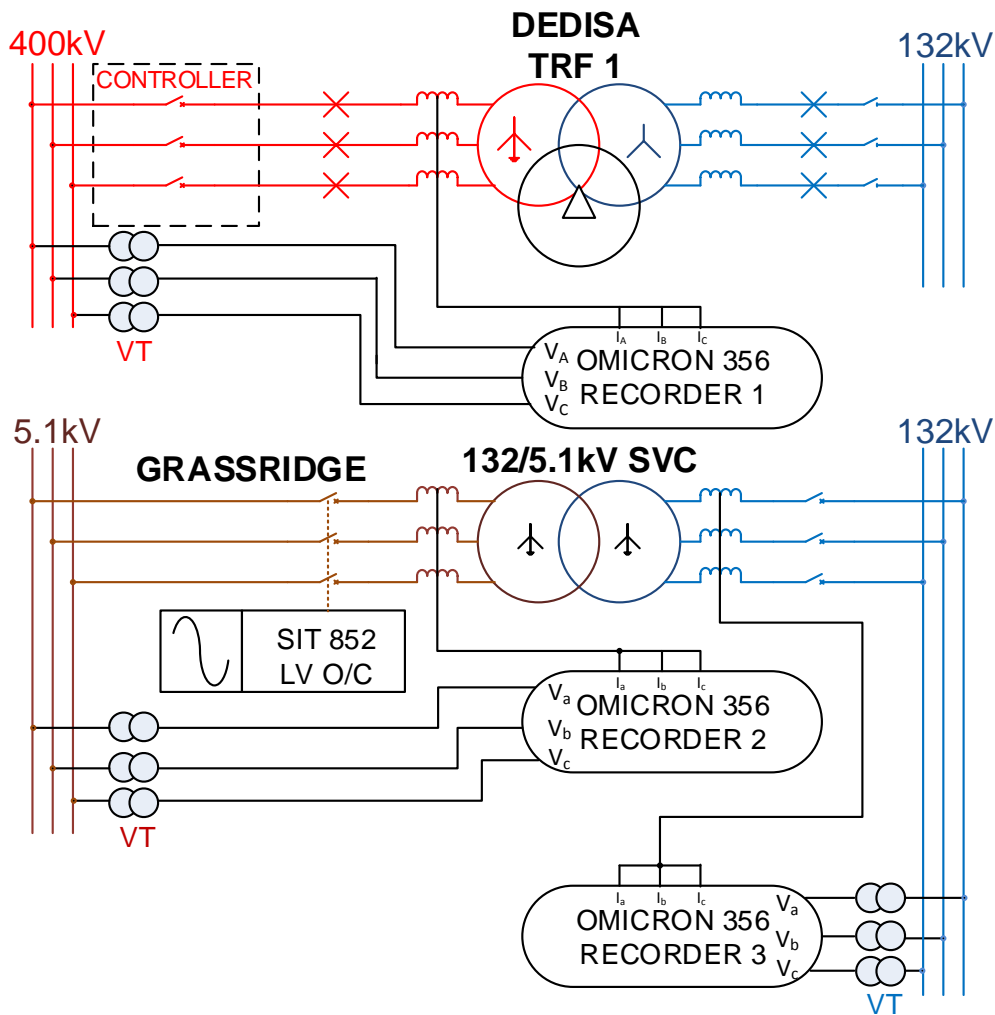


Figure 14: Case study 2 recorder setup and breaker operation

3.3.4 Case Study 3 - Transformer 2 Energising, NO SVC Trip

Case study 3 is a rather important case study that is used to demonstrate and confirm the results obtained for the previous cases. Case study 3 has the same setup regarding the recording devices as the previous case studies and is demonstrated in Figure 15, however the major difference is the relevant transformer been energised on the system. Chapter 4 will indicate the details of the recorded waveforms together with the simulated EMT results of the expected current and voltage waveforms.

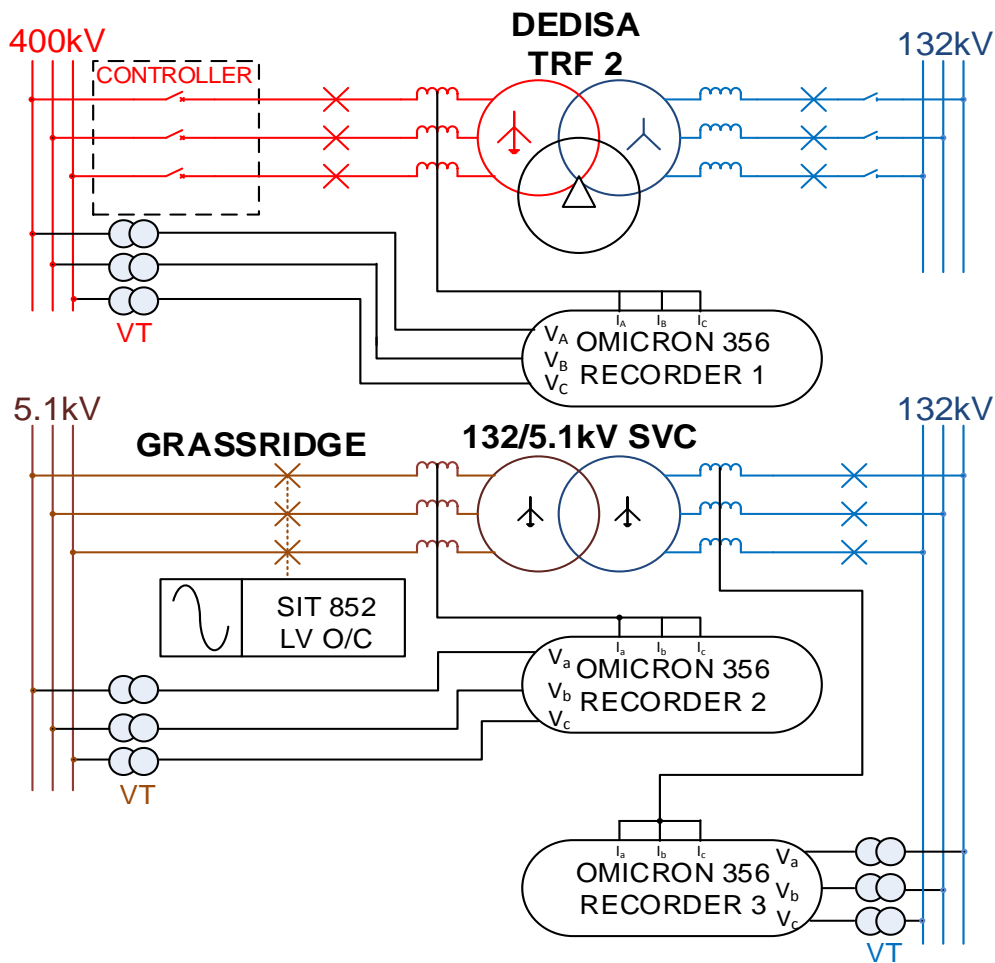


Figure 15: Case study 3 recorder setup and breaker operation

As illustrated in Figure 16, transformer 2 is energised when the red phase voltage is at a positive peak. From the literature review one recalls that in order to minimize the magnitude of the inrush current, the point at which the breaker poles make contact with the HV winding is at a peak and not a zero crossing.

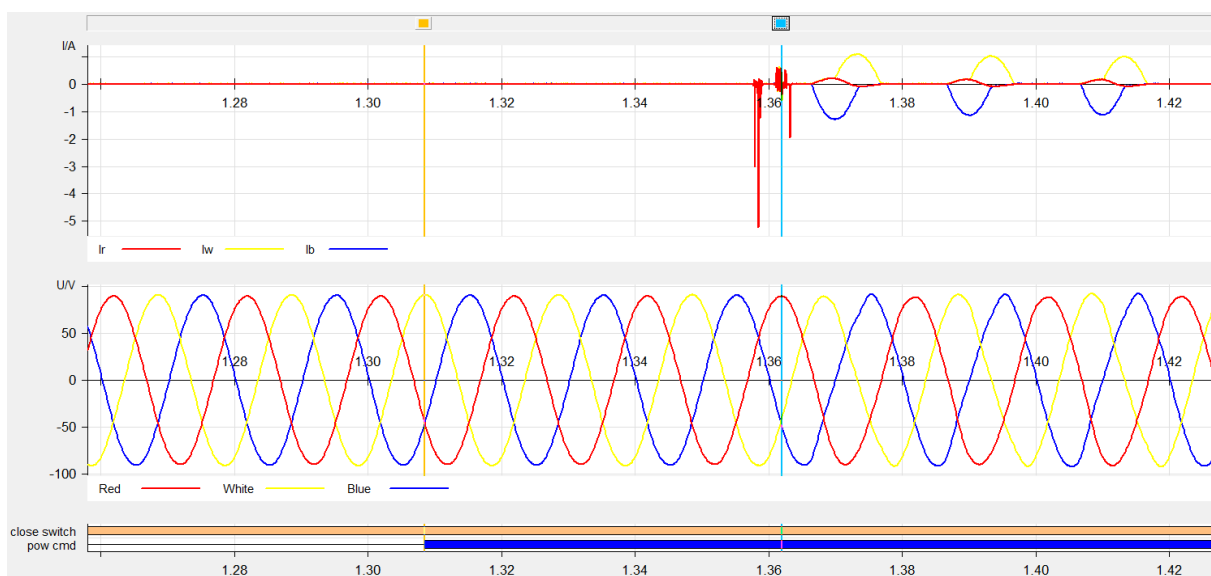


Figure 16: Case study 3 red phase voltage energising point

3.3.5 Case Study 4 - Transformer 2 Energising, NO SVC Trip

Case study 4 is the same as case study 3 however the energising point on the voltage waveform is shifted and the relevant transformer is now energised when the white phase voltage is at a negative peak value. One can see from Figure 17 the magnitude of the inrush current on the white phase relevant to the white phase voltage is noticeably low as compared to the other two phase currents.

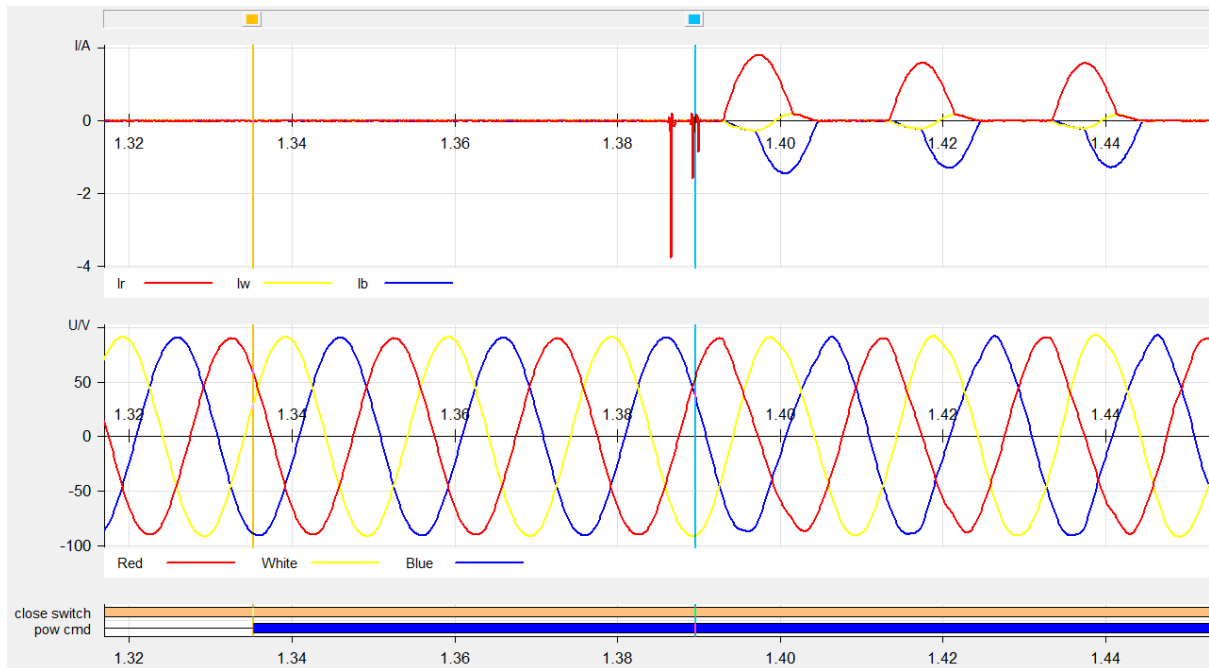


Figure 17: Case study 4 white phase voltage energising point

Case study 4 has the same setup regarding the recording devices as case study 3. Chapter 4 will indicate the details of the recorded waveforms together with the simulated EMT results of the expected current and voltage waveforms together with detailed analysis thereof.

3.4 DIGSILENT POWERFACTORY DERIVED MODEL

3.4.1 DIgSILENT PowerFactory Tools

DIgSILENT Version 7 was the world's first power system analysis software with an integrated graphical one-line representation of a three-phase network system. The interactive one-line diagram included drawing functions, editing capabilities and all relevant static and dynamic calculation features [1].

DIgSILENT power system calculation package was designed as an integrated engineering tool which provides complete diversity through available functions, rather than a collection of different software modules.

An added bonus is that DIgSILENT produces power definition results, thus forming an essential tool for power system analyses.

The following elements were used to model the network under investigation.

3.4.1.1 Busbar

The busbar object can be created directly in the single line graphic (by using the busbar button in the toolbox) and in the database manager. When creating a single line diagram, bus-bars must be placed first before any other element to ensure that other elements can be connected to them. The relevant busbar voltage level is imperative when connecting transformers and overhead lines as the simulation will not converge if the voltage levels are incorrect.

3.4.1.2 Grid voltage source

An external grid is used as the primary source voltage for the 400kV model. The voltage set point is set according to the external grid per unit value equivalence according to the “strong” source value together with the set-point voltage angle. The external grid is modelled as a “slack” bus, also known as the “reference” or “swing” bus, is selected to provide or absorb active and reactive power to and from the transmission lines in order to provide losses since these particular quantities are unknown until the final convergence occurs in the simulation. Figure 18 indicates the setup within the derived model for the external grid. As seen from Figure 18 the “slack” bus is the only bus that has the fixed per unit set-point voltage and angle according to system conditions.

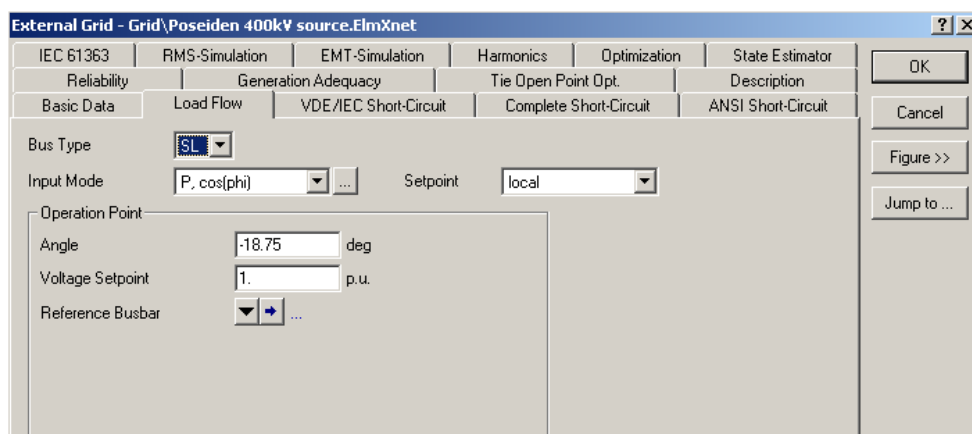


Figure 18: The derived models external grid setup in DIgSILENT

3.4.1.3 Network line impedance

The network impedances are represented as overhead lines within the software. The actual resistance and inductive reactance is required for a successful overhead line model. The line models are setup according to a distributed parameters setup and the time constant is set to be at least 1/10th the travelling time constant of the

particular line. Setting the line parameters correctly thus enables a better resolution after convergence is achieved within the simulation.

The line models used for the feeders are shown in Table 1 and are all transposed:

Table 1: Line parameters for the derived software model

	Poseidon Dedisa	Dedisa Grassridge	Poseidon Grassridge	
	400kV	400kV	400kV Line1	400kV Line2
Line length	115km	6km	116.4km	103km
Rated Current	2.44kA	2.63kA	2.44kA	1.83kA
+ Seq R1	3.48Ω	0.098Ω	5.43Ω	2.53Ω
+ Seq X1	28.24Ω	1.65Ω	32.98Ω	27.30Ω
0 Seq R0	41.72Ω	1.13Ω	46.79Ω	36.78Ω
0 Seq X0	130.28Ω	4.14Ω	123.57Ω	118.67Ω
Earth Factor Magnitude	1.28	0.54	0.99	1.19
Earth Factor Angle	-13.53deg	-19.08deg	-15.18deg	-15.25deg

3.4.1.4 Three winding transformer

The three winding transformer was simulated with the following parameters as shown in Table 2:

Table 2: Three winding transformer parameters relative to the derived model

Voltage Rating	kV	400/132/22
MVA Rating	MVA	500
Positive Sequence Impedance HV-MV	%	13.75
Positive Sequence Impedance MV-LV	%	12.36
Positive Sequence Impedance LV-HV	%	13.81
Zero Sequence Impedance HV-MV	%	12.34
Zero Sequence Impedance MV-LV	%	6.23
Zero Sequence Impedance LV-HV	%	7.87
Vector Group	NA	YN0yn0d1

Figure 19 indicates the symbolic view for a three winding transformer including the vector group representation and earthing arrangement together with the breaker status of each winding.

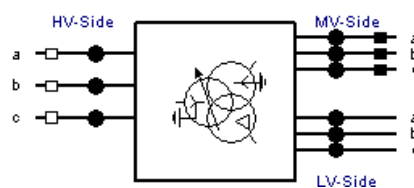


Figure 19: DIGSILENT symbol for a 3 winding transformer

Figure 20 indicates a three winding transformer dialog box which illustrates the basic data input parameters of the transformer model within DIgSILENT particular to Dedisa transformer 1.

Figure 20: Three winding transformer basic data dialog box

3.4.1.5 General load

A linear load is one which has not been specified as either a synchronous machine, asynchronous machine or as a shunt machine, but as a general active or reactive load. Figure 21 represents the rating of the balanced general load lumped on the 132kV busbar at Grassridge substation and thus is represented as one load for studies purposes. The effective reason is to simplify the model for EMT analysis at the SVC, thus the “lumped” load reduces inaccuracies within the model. Linear loads are modeled on the following two formulae [6]:

$$P_r = P_o \cdot \left(\frac{V_r}{V_o} \right)^{kpu} \quad (16)$$

$$Q_r = Q_o \cdot \left(\frac{V_r}{V_o} \right)^{kqu} \quad (17)$$

Where:

P_r : Rated real and reactive power

Q_r : Rated real and reactive power

P_o : Operating real and reactive power

Q_o : Operating real and reactive power

V_r : Rated busbar voltage

V_o : Actual operating busbar voltage

kpu : Voltage dependency index for P

kqu : Voltage dependency index for Q

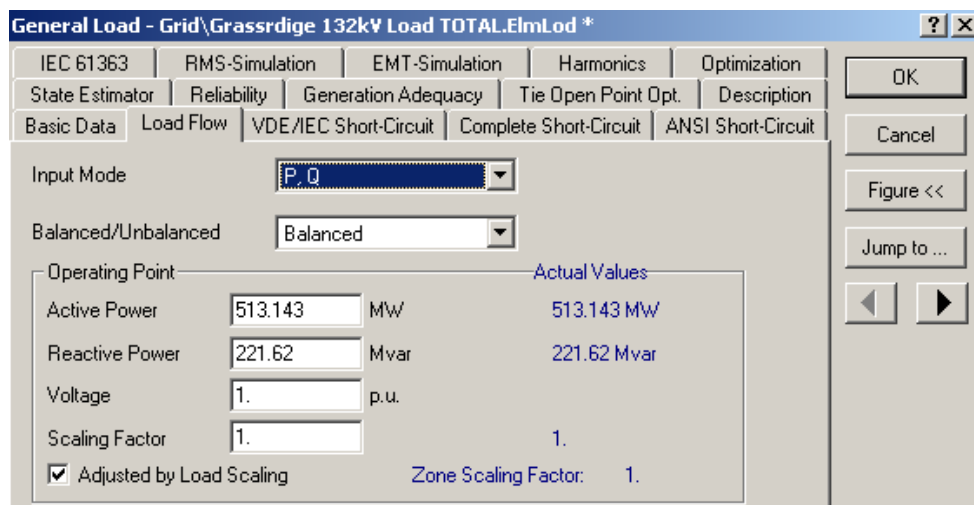


Figure 21: General load operating parameters on Grassridge 132kV bar

3.4.1.6 Capacitor Bank

The fixed shunt capacitor banks at Grassridge substation is simulated within the software as fixed capacitor banks on the 132kV busbar. The individual capacitor banks are not switchable according to a specific MVAR value (i.e. three or four switching stages making up the entire MVAR value of the bank) and are either switched in or out according to system requirements and regulations stipulating voltage depression limits. There are three capacitor banks on the 132kV busbar. Two of the banks comprise of 72MVAR each and the third bank is relatively small at 36MVAR.

3.4.1.7 SVC

The SVC model within DIGSILENT uses an approach that is rather different and more intricate than the other relevant components making up the derived network model. The composite model is defined with a fixed capacitor bank in parallel with it. This is an effective method to model the SVC as the particular SVC under investigation has a thyristor controlled reactor (TCR) and a fixed capacitor bank (35MVAR). Thus, emphasis is made in section 3.4.2 on the TCR and the controller thereof.

3.4.2 SVC Controller Model in Detail

The controller for the SVC is specific to the design aspect of the SVC used and how it is integrated into the power systems grid. Therefore, as discussed in depth in the previous chapters, the SVC located at Grassridge substation has a fixed capacitor bank with a thyristor controlled reactor. The purpose of the SVC is purely to stabilize the 132kV busbar voltage during voltage depression and surge stages. Therefore, the controller within DIgSILENT is designed specifically with block definitions that allow for certain parameter input quantities that replicate the real life installation.

Each block definition generally has one or more parameters which can be changed to define the model's behavior. The parameters that are supported are the scalar parameters, amplification factors, offsets and the set-points.

Figure 22 shows the internal program logic relating to the decision process that the SVC undergoes when deciding how to control the 132kV busbar voltage relating to the set-point the user has inputted via the *usetp* value which is the set-point voltage in pu desirable by the relevant operator/controller. The scalar quantities such as V_{max} and V_{min} are used to set the range that the SVC is allowed to adjust the busbar voltage and of course is dependent on the limit of the size of the capacitors and reactors making up the SVC. At the end of the process of decision making within the controller a value is passed on to the next stage, *ysvs*, within the composite model in order to allow the SVC to react accordingly such that the thyristors firing angles are turned on or off relating to the amount of reactive power that is required to be absorbed within the system in order to compensate for voltage surges that might be occurring on the relevant 132kv busbar. Similarly the decision process might call for the thyristors to be completely turned off such that the capacitor bank can be switched in therefore allowing for MVAR's to be “shunted” onto the 132kV busbar in order to compensate for voltage depression that might be occurring.

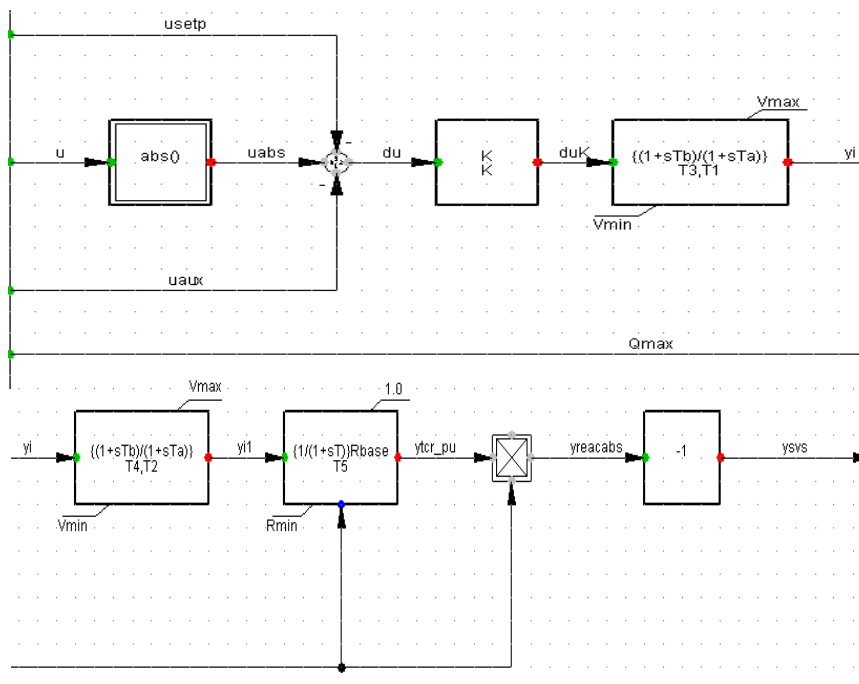


Figure 22: SVC Controller within DIgSILENT

3.4.3 SVC Composite Model in Detail

A composite model element can be created in DIgSILENT PowerFactory. A composite frame is the essential for the definitions required for creating a specific function or operation for an electrical element. The reason why one would want to create a composite model including specific controllers are for specific applications where studies are required for EMT analysis specifically. This is due to the fact that SVC's and Automatic Voltage Regulators (AVR's) for generators and wind turbines are devices that react according to system conditions. Thus, in order to model an entire system correctly to ascertain the response the specific elements are producing, one needs to create composite frames that consist of a specific composite model that then shows the list of slots in the composite frame making up the specific element. Particular controllers or models can be assigned to a slot which inherently makes up a standard composite model.

DIgSILENT PowerFactory has specific standard composite models which are available for:

- The synchronous motor and generator
- The asynchronous motor and generator
- The SVC system

When a composite frame has been created for a specific application together with all the specific models and interfaces making up that particular frame then there is now no longer any connection between the original elements and the new elements of the composite model or frame. Therefore, one can change the controller settings within the SVC without changing the network or part of the network that the SVC is attempting to control.

There is a specific function that allows the user to test the controller before it is enabled to control a specific device. Thus the step response test can be performed to ensure all parameters are correct and that the correct busbar for example are been controlled correctly according to the settings inputted. Once the user is satisfied with the results then the step response test can be deleted completely without loss of information in the original network.

Figure 23 shows the Composite frame that is used in DIgSILENT PowerFactory and was created specifically for the research carried out in this project in order to replicate the controller configuration at site for the SVC. Figure 23 indicates four models within the frame that manipulates the SVC in such a way that it knows when and how to correct the 132kV busbar voltage at Grassridge. One can see that one of the models within the frame consists of the *SVC-Controller ElmSvc* which makes up the entire controller model as discussed in the previous section.

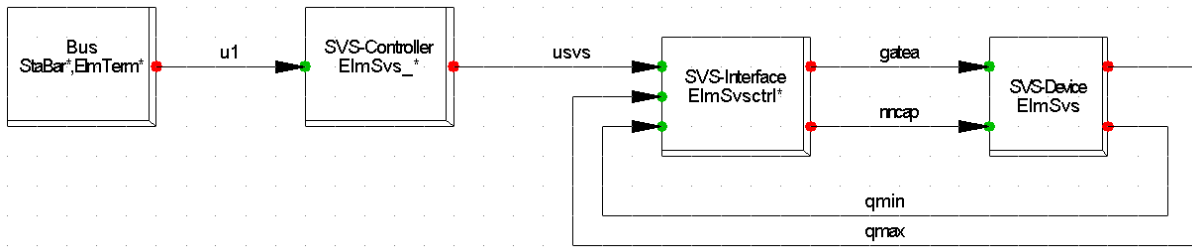


Figure 23: SVC composite frame in DIgSILENT

To ensure that the settings are correctly applied within the software before an EMT study is performed each model within the composite frame needs to be verified to ensure that it is in fact doing the job required to complete the overall model. Thus, as seen in Figure 24 each slot for the four devices are updated accordingly (linked) to the appropriate device or section within the frame. Therefore the *bus* needs to know that it is controlling the 132kV busbar at Grassridge and not another busbar that is unknown. The *SVS-Controller ElmSvs* is linked to the controller that was created in depth previously and saved on DIgSILENT's database. The actual *SVS-device* element is linked to the actual thyristor controlled reactor/capacitor bank and not to another unknown element. Figure 24 indicates all the slots together with the *step response test* that can be performed before implementation.

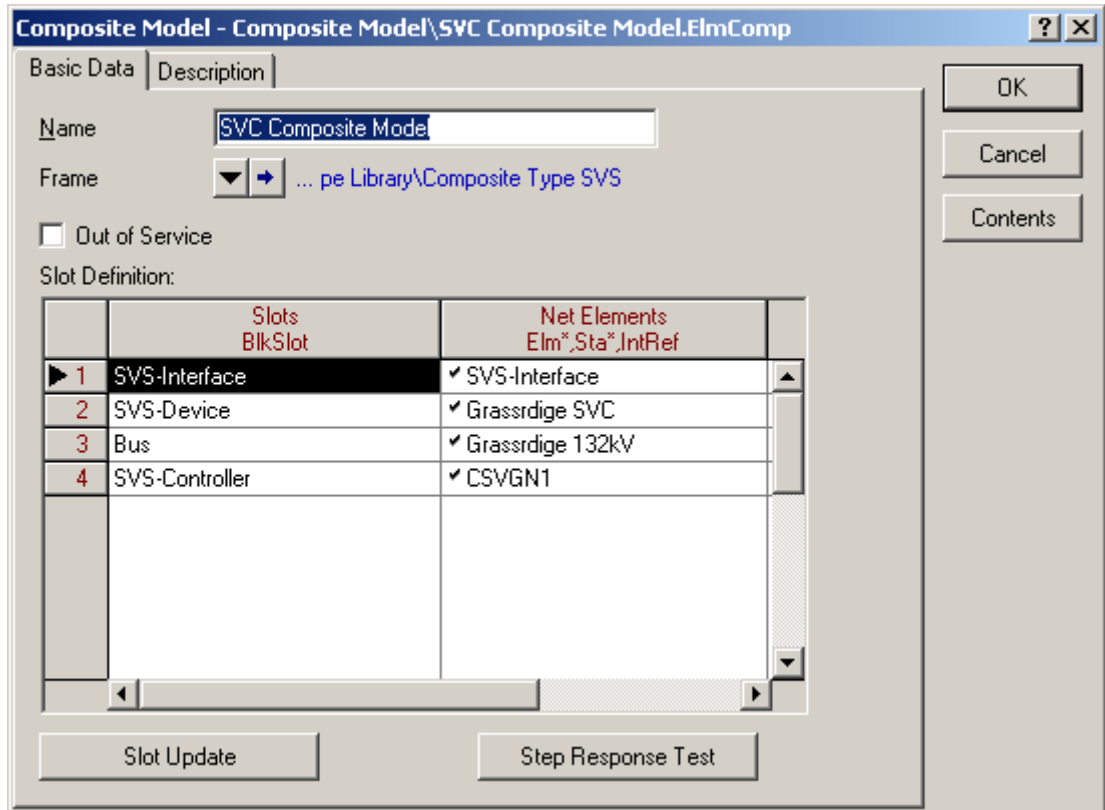


Figure 24: SVC Controller within DIgSILENT

3.4.4 RMS and Harmonic Calculations

To confirm whether or not harmonics, specifically 2nd harmonic inrush currents, play a significant role in the mal-operating of the LV O/C relay, extensive Fast Fourier Transform (FFT) analysis was required in order to validate the results obtained in Chapter 4.

Fast Fourier Transform (FFT) is far superior in terms of accuracy and content as compared to the other variations of Fourier transforms available. Discrete-Time Fourier Transform (DTFT) is a time sampling Fourier Transform and Discrete Fourier Transform (DFT) is a frequency sampling DTFT. So therefore DFT is a time sampling and frequency sampling Fourier Transform. We define a DTFT because we would want to sample the continual infinite signal whereas with a DFT one cannot calculate all the frequencies specific in a particular range. Therefore DTFT is used for harmonic analysis relating to their time domain only whereas DFT is used for the frequency domain in addition to the time domain. So therefore the reason why an FFT approach was chosen for harmonic analysis relating to this particular research is because it is simply a fast implementation of the DFT analysis approach.

Therefore, the 2nd harmonic analysis, in particular, was performed in order to verify whether the SVC is operating normally under system conditions or harmonic generating conditions. Thus, the 2nd harmonic order analysis was imperative in order to substantiate whether or not the filters at Grassridge substation, that are specifically tuned to filter out certain harmonics, inclusive is the 2nd harmonic order, is in fact operating correctly or not.

The capacitor bank associated to the SVC is specifically tuned to filter out specific harmonics produced by the TCR's (Thyristor Controlled Reactors). The nominal rating of the capacitor/filter bank relating to the 132kV SVC is 35 MVar. The filter is tuned to the 2nd, 3rd and 5th harmonic frequencies.

3.5 HARMONIC IMPACT TEST ON THE SIT 852 RELAY

It is a well-established phenomenon that a current or voltage waveform that is distorted due to certain conditions will therefore allow for the normal fundamental quantity to not hold true in RMS calculations. Thus the RMS representation of the current and voltage per phase are defined as:

$$I_{rms(i)} = \sqrt{\sum_{\substack{h=1 \\ i=R,Y,B,n}} I_{ih}^2} \quad (18)$$

$$V_{rms(i)} = \sqrt{\sum_{\substack{h=1 \\ i=R,Y,B,n}} V_{ih}^2} \quad (19)$$

Where i defines the relative phase (R, Y, B, n) and h defines the harmonic order dependant on the harmonic spectrum present within the network system.

The total current harmonic distortion expressed in percentage is defined as:

$$I_{THD(i)} = \frac{\sqrt{\sum_{\substack{h \neq 1 \\ i=R,Y,B,n}} I_{ih}^2}}{I_{i1}} \% \quad (20)$$

The IEEE Std.1459 introduced definitions that are utilised for distorted waveforms in a three-phase 3-wire network system [7]; each index is divided into a fundamental and a harmonic component.

The effective current I_e is the square root of the sum of squares of the effective fundamental current I_{e1} and the effective harmonic current I_{eH} .

$$I_e = \sqrt{I_{e1}^2 + I_{eH}^2} \quad (21)$$

The effective fundamental current is dependent on the fundamental components present in all three phases.

$$I_{e1} = \sqrt{\frac{1}{3}(I_{R_1}^2 + I_{Y_1}^2 + I_{B_1}^2)} \quad (22)$$

I_{eH} is the sum of all the harmonic currents that are present within each phase, noted with a lower case h (I_{Rh} , I_{Yh} and I_{Bh}).

$$I_{eH} = \sum_{h \neq 1} \sqrt{\frac{1}{3}(I_{R_h}^2 + I_{Y_h}^2 + I_{B_h}^2)} \quad (23)$$

Now when relating the fundamental and harmonic definitions to relays and specifically to the operational characteristic of overcurrent and earth fault relays then the following should be considered.

- The particular relay should be designed such that it can filter out harmonic orders that can alter the relay characteristic curve and ultimately cause incorrect relay trips for an RMS quantity instead of a fundamental quantity
- The relay should be designed such that it can extract the fundamental quantity from a distorted fault current waveform and trip correctly for the designed fundamental quantity element

3.5.1 AEG SIT 852 Earth Fault Test

In order to demonstrate the susceptibility the SIT 852 relay has on distorted waveforms that are originated from the thyristors controlling the reactive part of the SVC or harmonic conditions already existing on the network at Grassridge substation, harmonic current injection tests was performed on the SIT 852 relay.

A test set was set up, as in Figure 25, and on a workbench in the laboratory the OMICRON CMC 356 was selected as the suitable tool for current injection on the particular relay under test (SIT 852).

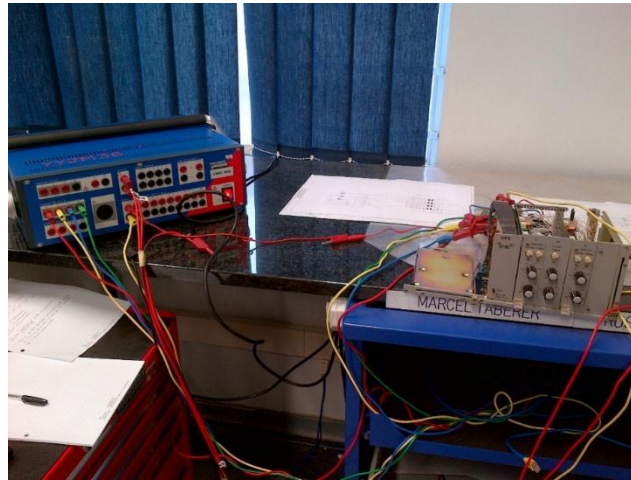


Figure 25: AEG SIT 852 relay under test in the laboratory

3.5.1.1 Current Injection – NO HARMONICS

A normal inverse curve characteristic was selected on the relay thus replicating the relay on site in the SVC control room. The settings for test purposes was the following and was primarily selected for harmonic component distortion emphasis. $I_e = 0.4A$ secondary and $K = 0.2$ (time multiplier)

The test was conducted according to Table 3 such that only a fundamental current was injected for a red phase earth fault. Table 3 shows the fundamental component injected together with the expected time of trip and the actual time of the trip. Considering the pick-up level of 0.4A, Table 3's selected values are injection values above the set pick-up level therefore allowing for a variation in test magnitudes in order to select a fundamental value suitable for harmonic distortion injection.

Table 3: Fundamental injected current and trip times

I_l Injected	Expected Trip Time	Actual Trip Time
mA	seconds	seconds
469.7	8.71	6.11
561.3	4.12	3.75
670.8	2.71	2.87

3.5.1.2 Current Injection – HARMONICS

The normal inverse characteristic curve was selected for this particular test however the test set was adjusted accordingly to accommodate for various harmonic orders to emphasise whether the relay is susceptible to harmonic content on a distorted waveform or not irrespective of the current distortion. Thus Table 4 indicates the harmonic orders that were injected in conjunction with the fundamental component together with the actual trip times. Now taking into consideration that the actual trip time for a fundamental current injection of **561.3mA** would result in an actual trip time of **3.75s** from the previous test, Table 4 indicates a peculiar phenomenon such that **561.3mA** was selected as a base fundamental component for harmonic distortion emphasis.

Table 4: Harmonic current injection and trip times

Test No	I1 Injected	I2 Injected	I3 Injected	I5 Injected	I7 Injected	Actual Trip Time
	mA	%	%	%	%	seconds
1	561.3	0	0	0	0	3.75
2	561.3	50	0	0	0	2.61
3	561.3	100	0	0	0	1.87
4	561.3	0	50	0	0	3.43
5	561.3	0	100	0	0	2.22
6	561.3	0	0	50	0	2.42
7	561.3	0	0	100	0	1.81
8	561.3	0	0	0	50	2.76
9	561.3	0	0	0	100	2.11

Thus following from Table 4 it is clearly shown that the SIT 852 LV O/C relay is susceptible to harmonics and that a large value of a superimposed harmonic content (50%-100%) on the fundamental component could cause a deviation in the set trip time.

Therefore in Chapter 4 further analysis is required in order to determine whether there are harmonic components superimposed on the fundamental component. Thus Fast Fourier Transforms (FFT) analysis is shown in detail in Chapter 4 and is used extensively and the significance is well defined in order to quantify the findings.

3.6 CONCLUSION

A DIgSILENT derived model was well defined in this chapter together with the relative modelling tools and user defined controllers. The ABB F236 POW controller and its effectiveness was highlighted and wiring techniques were emphasized for transformer energising. Four case studies evolved in this particular chapter and the wiring of the relative Analogues and Binaries were detailed. The method of recording the Comtrade captured waveforms according to the user defined technique was defined using EnerLyzer software. The software setup was shown and the calibration certificate depicting the test set used was inserted as *Appendix B*. Harmonic impact tests via secondary injection were done in a laboratory and results were tabled in order to derive conclusive information to pave the way forward.

CHAPTER 4 - DATA COLLECTION, ANALYSIS AND INTERPRETATION

4.1 INTRODUCTION

From the results portrayed in this particular chapter, emphasis is made on whether or not the suspected mal-operating relay is in fact triggering incorrectly or not under certain system conditions. Figure 26 shows a brief overview of how the results for the research are analysed and what method of analysis was undertaken in order to best indicate the conclusive evidence brought forward in chapter 5.

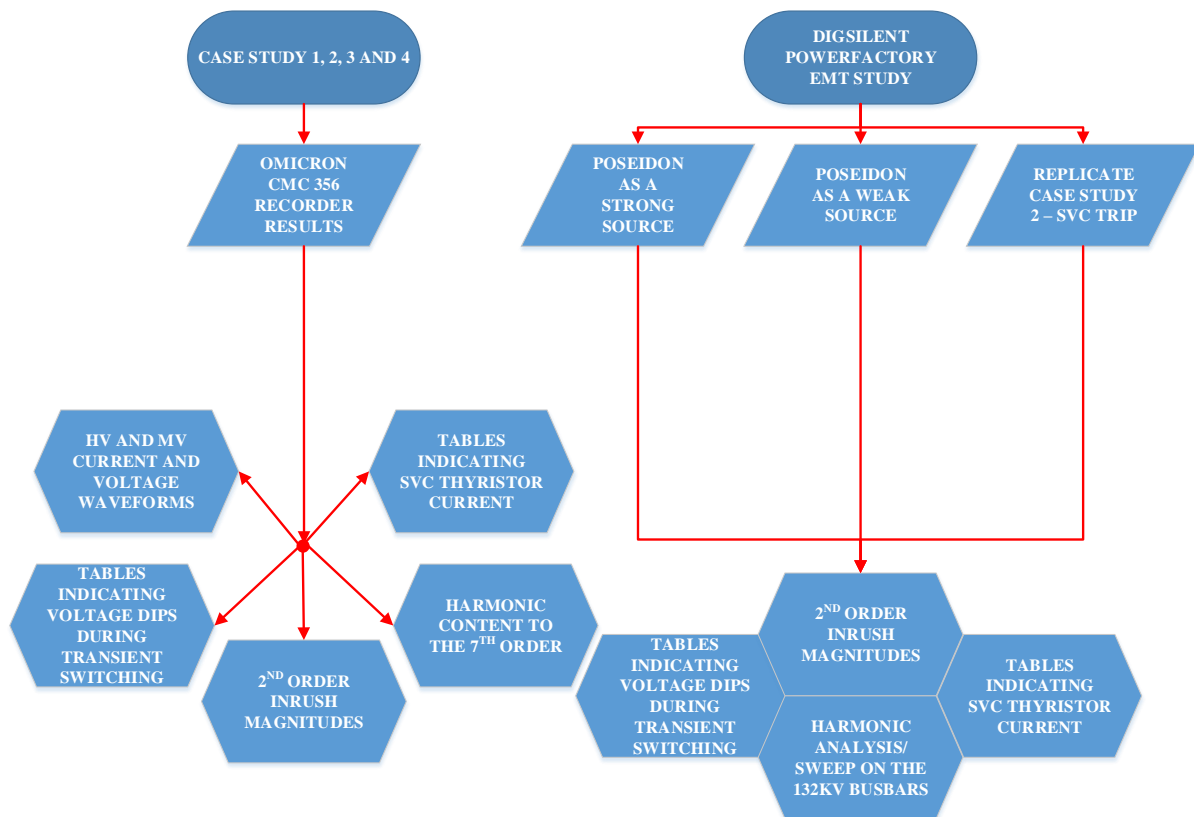


Figure 26: Overview of the analysis approach

The emphasis on Harmonics within the case studies will always pose questions, therefore extensive analysis was done in terms of FFT scans at various points within the derived power system. The simulated software results supplement the FFT scans derived in “TOP” software from the recorder results and are clearly portrayed in this particular chapter.

Therefore a derived model constructed in DiGSILENT software is used to supplement the OMICRON real time results attained. The model will be altered such that three scenarios are analysed under system outage conditions. Therefore the results drawn from the simulation will allow the researcher to provide Eskom with insight on whether future conditions of the same magnitude will cause interference or mal-operations of certain

equipment within the defined network topology identified in the model. Figure 27 indicates how each software package is related and it also indicates the process followed between stages in order to formulate or output certain results in a derived table format that can indicate magnitudes and angles for current, voltage, power etc. The type of format that the recorders capture data is clearly identified in Figure 27 and is extremely important in terms of analysis for the reasoning behind the chosen packages.

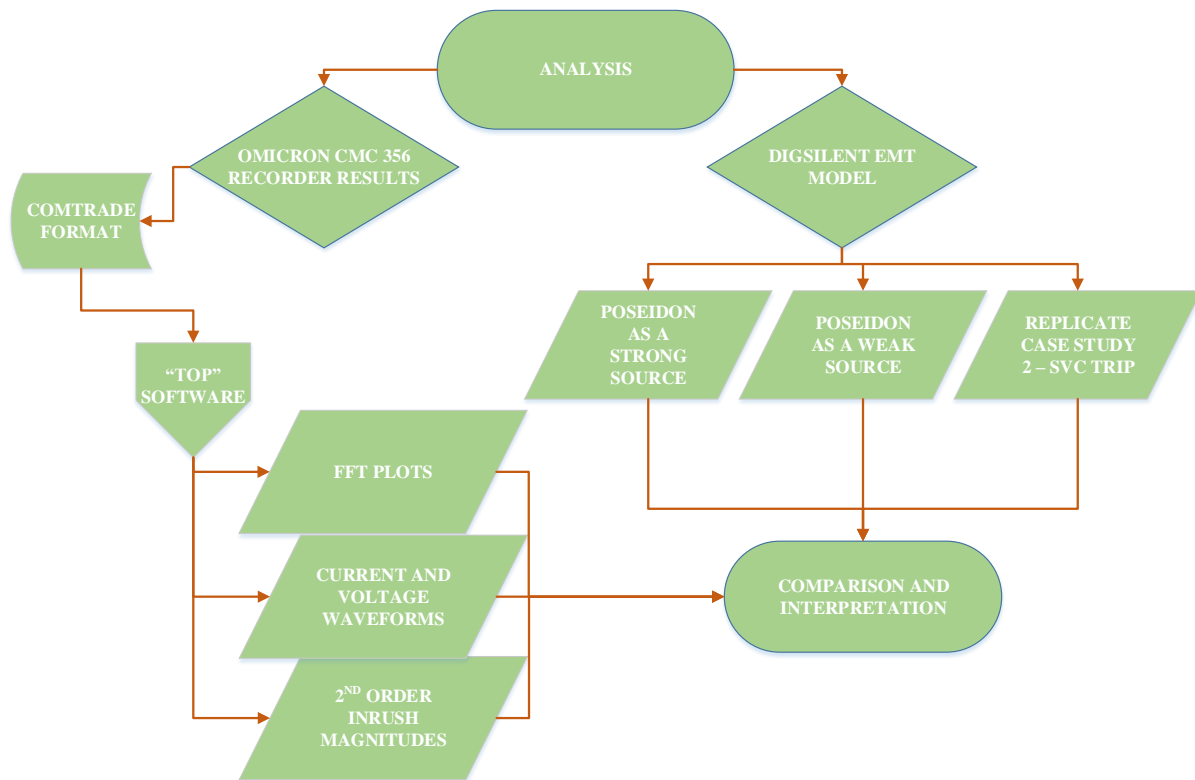


Figure 27: formatting and evaluation methodology for deriving comparison results

The EMT simulations was such that the total simulation ran for 5 seconds and the energising of transformer 1 occurred 3 seconds into the simulation. This setup was identical for the results obtained for transformer 2 energising. The design attributes of the defined model does not allow for load variations that occur during a 24 hour period and thus the EMT results will not correlate 100% with the recorders comtrade files processed with “TOP” software.

Harmonic analysis was performed in order to confirm whether or not harmonics, specifically 2nd harmonic inrush currents, play a significant role in the mal-operating of the LV O/C relay, extensive Fast Fourier Transform (FFT) plots are generated in “TOP” software using the actual recorded values during the switching transient. The 2nd harmonic analysis, in particular, was performed in order to verify whether the SVC is operating normally under system conditions or harmonic generating conditions. Therefore the 2nd harmonic order analysis was imperative in order to substantiate whether or not the filters at Grassridge substation, that are specifically tuned to filter out certain harmonics, inclusive is the 2nd harmonic order, is in fact operating correctly or not.

Finally, a comparison table of results will be derived in order to indicate the short falls, if there are any, between a recorded case study that is identically replicated in an EMT simulated model therefore allowing readers to identify whether or not the SIT 852 relay correctly operated or if in fact there is a fault at a particular point or apparatus hindering the effective integrity and operability of the protection philosophy at Grassridge or Dedisa substation as a whole. Figure 28 shows the process to be followed from a high level point of view.

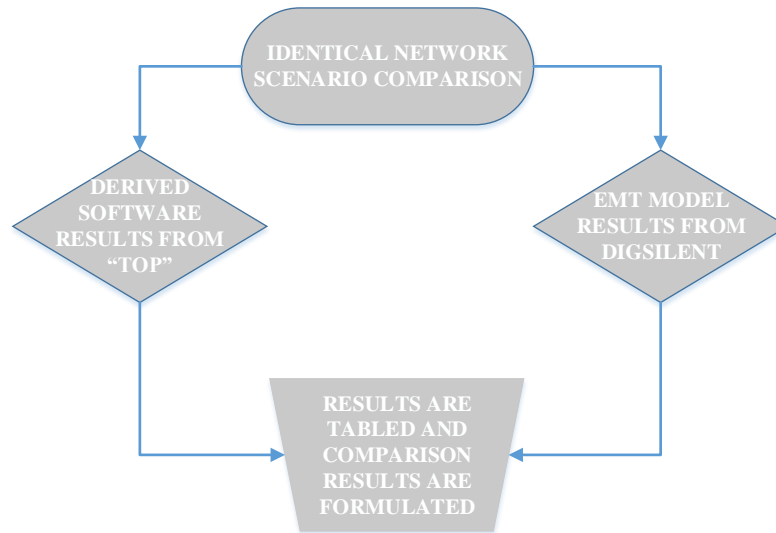


Figure 28: High level indication for identical network process

4.2 OMICRON CASE STUDY RESULTS

4.2.1 Case Study 1 - Transformer 1 Energising, NO SVC Trip

At the point at which transformer 1 is energised under no load conditions, a certain inrush current phenomenon, indicated in Figure 29, occurs due to the large impedance that is instantaneously introduced onto the power system. The close command from the POW controller is issued via the close switch on the control panel. From Figure 29 it can be seen that the close command is executed from the controller however from the current waveforms it is clearly shown that the breaker does not close at that particular instant but rather 53.4ms later due to the operational mechanical characteristics of the breaker which correlates with the settings. Thus proving it very difficult to effectively predict where exactly on the voltage waveform the transformer would be effectively energised. Therefore, as seen from Figure 29 the POW controller effectively issued a close command at a peak white phase voltage as per the settings (i.e. indicated by the orange vertical line) however the breaker poles made contact with the system voltage when the red phase voltage was at a positive peak magnitude (i.e. indicated by the blue vertical line) which resulted in a much smaller energising current on the red phase as compared to the other two phases.

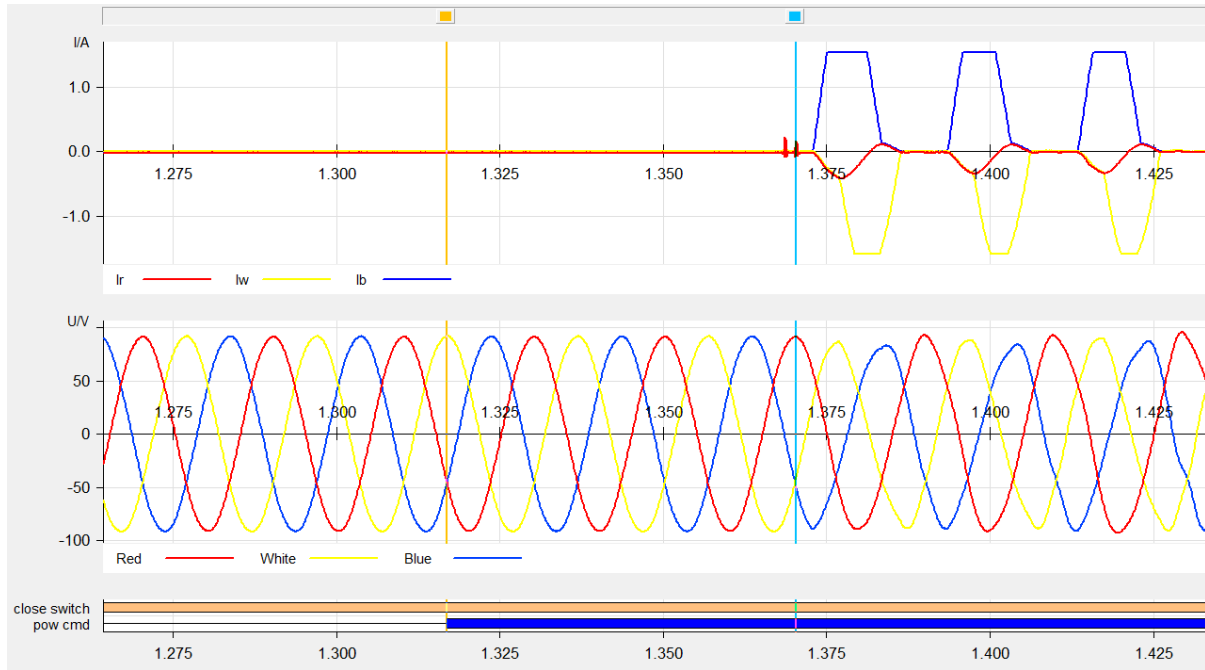


Figure 29: Case study 1 (inrush current and applied voltage)

Now, during the switching transient it is imperative to note how the voltage on the 400kV busbar at Dedisa substation reacts according to the 132kV busbar voltage at Grassridge substation at the point of energising. Table 5 indicates the voltage magnitudes in a per unit value. Table 5 is divided into three sections (i.e. before, during and after the switching transient).

Table 5: Case study 1 voltage magnitudes for the 400kV and 132kV busbar respectively

	Before switching	During the switching	After switching
Dedisa 400kV busbar			
Vr (pu)	1.014	1.003	1.021
Vw (pu)	1.023	0.946	0.992
Vb (pu)	1.021	0.935	0.962
Grassridge 132kV busbar			
Vr (pu)	1.015	1.059	1.185
Vw (pu)	1.015	0.948	1.129
Vb (pu)	1.019	0.951	1.133
DURATION OF THE TRANSIENT = +-180ms			

From Table 5 it is clearly shown that there is an average voltage dip of 5.7% across the relevant phases at Grassridge 132kV busbar during the instant at which the transformer is connected to the 400kV busbar at Dedisa substation. This voltage dip is seen throughout the network and is clearly shown at the 132kV busbar at Grassridge substation. However after the system becomes stable the voltage recovers and the system is stronger than before in terms of busbar voltage levels.

It is therefore imperative to outline the reaction the 35MVA 132:5.1kV SVC undergoes during the switching transient of transformer 1 and effectively show what the SVC control system decides to implement or put into action in order to accommodate for the sudden voltage dip on the 132kV busbar at Grassridge substation. Therefore, one needs to note that the 132kV busbar voltage is directly proportional to the 5.1kV busbar voltage at Grassridge substation due to the 132:5.1kV transformer having a fixed tap ratio.

Therefore, outlined from a high level perspective when the SVC detects a voltage instability, normally created from traction stations in close proximity to the substation, the SVC's control system will immediately start to adjust the firing angles of the thyristors accordingly such that they will turn off completely if the voltage on the 132kV busbar is below the set-point value programmed in the controller. This particular value is normally 1.02pu. In this particular case the thyristors should intermittently shut down whilst the capacitor bank takes over and is allowed to "attempt" to boost the 132kV busbar voltage during the moment of voltage depressions within the limits of the 35MVA capacitor bank. Once voltage stability is reached then the thyristors should turn on once again due to the voltage on the busbar regaining stability and strength. Figure 30 indicates the magnitude of the thyristors current for this particular case study. It indicates how the thyristors adjust within milli-seconds and begin to turn off during the voltage dip and then gradually turn on as the busbar voltage strengthens. Thus, according to designs perspective the control system is operating correctly due to the fact that as the voltage on the busbar increases then the thyristor currents must increase in order to provide more inductive reactance on the system in order to regulate the voltage and keep it within the set-point value processed on the control panel.

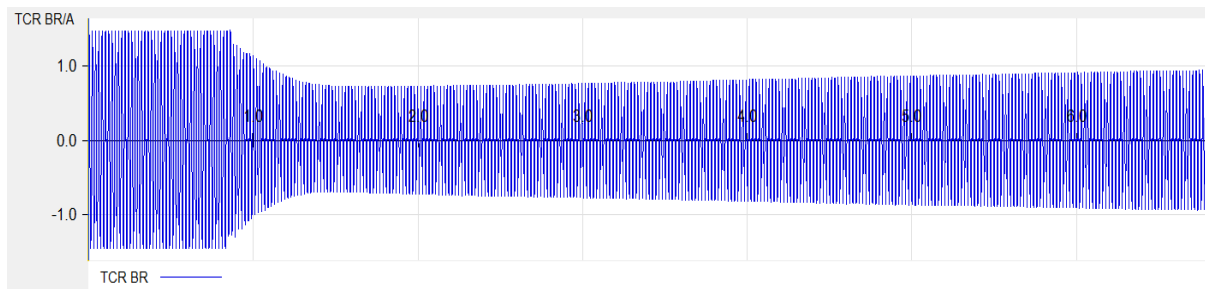


Figure 30: Case study 1 thyristor current during and after switching

Interestingly, from Figure 30 the thyristor current clearly indicates that no recorded trips have occurred during this particular switching and that system stability in terms of power demand and voltage is regained over a certain time period and one can see that for the particular recording of 7 seconds, the current has not diminished to 0A. Therefore from this particular case study it is shown that the SVC remains healthy and that the SIT 852 relay remains stable.

4.2.2 Case Study 2 - Transformer 1 Energising, SVC Trip

As compared to the previous case study, an LV O/C trip was recorded for this particular energising of transformer 1. The exact point on the voltage waveform at which the transformer HV winding is connected to the power system was not recorded due to a fault that occurred simultaneously whilst attempting to record. However all other relevant recorders triggered as they were taking snapshots at the remote site (i.e. Grassridge substation). Nevertheless, the exact energising point on the voltage waveform is irrelevant for this case study due to the fact that emphasis is made on the reaction the SVC undergoes at Grassridge substation together with certain phenomena that occurs.

Table 6 indicates the voltage magnitudes in a per unit value together with the voltage instability period (transient time). Table 6 is divided into three sections (i.e. before, during and after the switching transient).

Table 6: Case study 2 voltage magnitudes for the 400kV and 132kV busbar respectively

	Before switching	During the switching	After switching
<u>Dedisa 400kV busbar</u>			
Vr (pu)	No recorded values due to a simultaneous fault that occurred during the switching, however the 132kV busbar is a relative representation of the 400kV busbar		
Vw (pu)			
Vb (pu)			
<u>Grassridge 132kV busbar</u>			
Vr (pu)	1.069	0.961	1.083
Vw (pu)	1.065	1.024	1.117
Vb (pu)	1.065	1.019	1.131
DURATION OF THE TRANSIENT = +-150ms			

From Table 6 it is clearly shown that there is an average voltage dip of 6.1% across the relevant phases during the instant at which the transformer is connected to the 400kV busbar at Dedisa substation. Now, before the relevant disturbance/energising on the system, the 132kV busbar voltage was relatively stable and effectively equal across all three phases. A voltage dip is then seen throughout the network and is clearly shown that all three phases become unstable and unequal at the 132kV busbar at Grassridge substation. However after the power system becomes stable, thus during the transient stage, the voltage recovers and the system is stronger than before however with a relevant inequality between the relevant phase magnitudes in terms of busbar voltage levels.

It is therefore imperative to outline the reaction the 35MVA 132:5.1kV SVC undergoes during the switching transient of transformer 1 and effectively show what the SVC control system decides to implement or put into action in order to accommodate for the sudden voltage dip on the 132kV busbar at Grassridge substation.

Therefore, as outlined for the previous case study certain control conditions are required to be put into action when certain conditions occur on the power system and the SVC is required to regain or maintain system security and stability during these periods. In this particular case the thyristors should intermittently shut down

whilst the capacitor bank takes over and is allowed to “attempt” to boost the 132kV busbar voltage during the moment of voltage depressions. Once voltage stability is reached then the thyristors should turn on once again due to the voltage on the busbar regaining stability and strength.

Figure 31 indicates the magnitude of the thyristors current for this particular case study. As compared to the previous case study the thyristor current switches off completely once a voltage depression is detected on the 132kV busbar and remains off until the SVC breaker has opened. Thus interpreting Figure 31 one will notice that the SVC PLC allows the Thyristors to switch off and therefore allows the SVC to purely behave as a capacitor bank for a period of 2.998 seconds and then, due to a certain protection philosophy (LV O/C protection operation), the breaker poles open thus allowing the 132kV busbar to be uncontrollable in the sense of voltage stability.

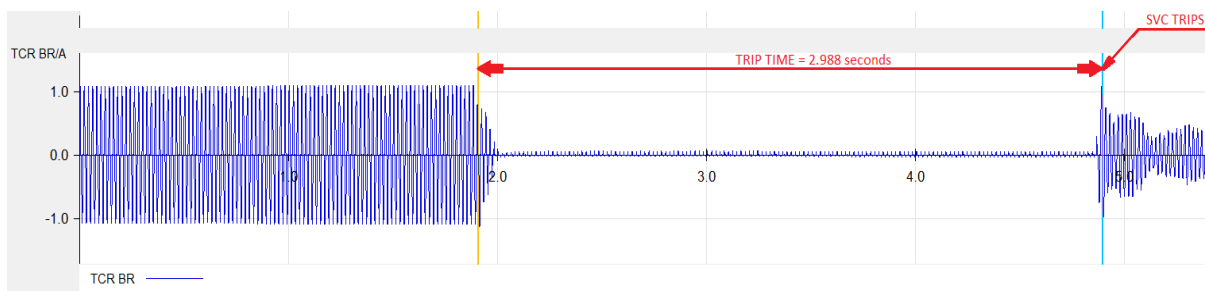


Figure 31: Case study 2 thyristor current during and after switching

Hence, we look closer at what particular protection function caused the SVC to trip and the reasoning behind the actual operation. Figure 32 indicates the LV current present during the three stages as indicated in Table 6.

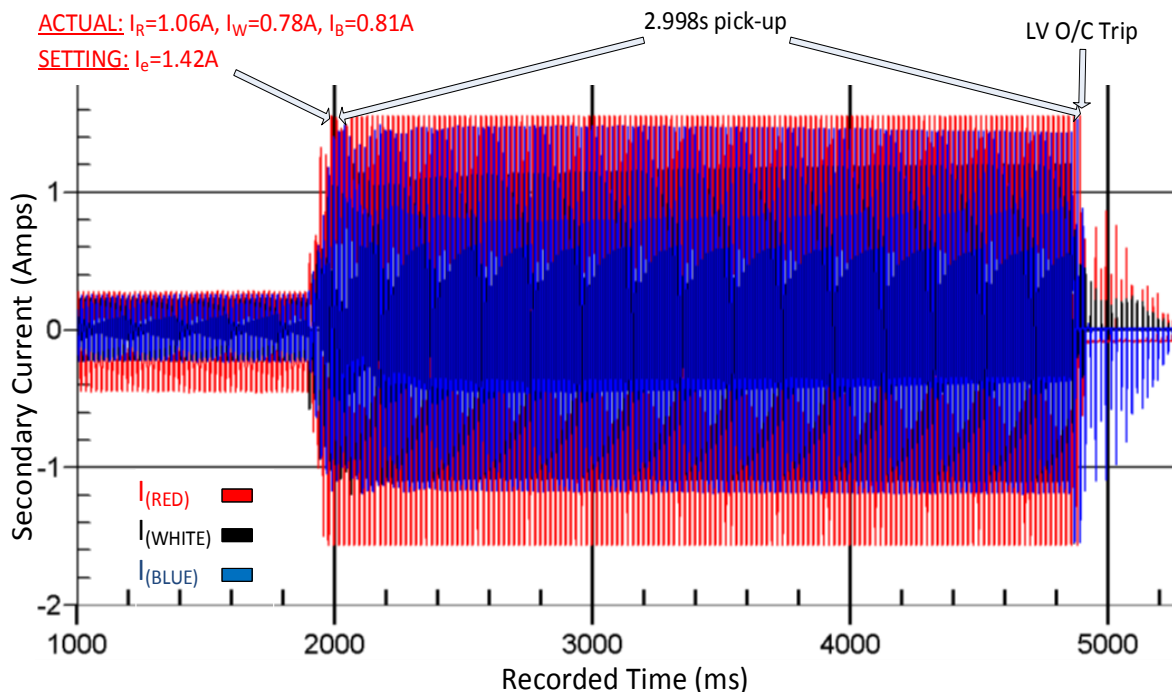


Figure 32: Case study 2 LV current before, during and after switching

Figure 32 clearly indicates that once the transformer is energised at Dedisa, the SVC reacts in such a manner that the phasor value of the relevant phase currents are boosted exponentially such that the threshold of the SVC is reached in a matter of milli-seconds. Therefore if we analyse this particular recording in depth we will find the following:

- The SIT 852 LV O/C is set with a pick up value $I_e = 1.42\text{A RMS}$ with a 0.1 time multiplier setting relative to a normal inverse curve.
- The O/C timed pick-up value according to the recording is below the setting of $I_e = 1.42\text{A RMS}$ secondary and is equal to 1.06A, 0.78A and 0.81A RMS for I_R , I_W or I_B respectively as seen in Figure 32.
- Therefore from equation (15) we find that the expected trip time is non-existent because the actual pick-up value has not been reached.
- Hence from the recordings a deviation exists such that the SIT 852 relay mal-operated and tripped for a RMS quantity well below the setting value.

A question then arises whether or not could the relay be able to deviate by a certain percentage over a period of time or does harmonics play a significant role in the mal-operation of the relay thus indicating that perhaps the filters in the relay are not operating correctly or perhaps there aren't any filters specified for the specific relay under test. Therefore further investigation will be done later in this chapter detailing the harmonic impact the relay undergoes.

4.2.3 Case Study 3 - Transformer 2 Energising, NO SVC Trip

Inrush conditions occur when transformer 2 is energised under no load conditions. The close command from the POW controller is issued via the close switch on the control panel. From Figure 33 it can be seen that the close command is executed from the controller however from the current waveforms it is clearly shown that the breaker does not close at that particular instant but rather 53.5ms later due to the operational mechanical characteristics of the breaker. Therefore, as seen from Figure 33 the POW controller effectively issued a close command at a peak white phase voltage as per the settings and is indicated with the orange vertical indicator, however the breaker poles made contact with the system voltage when the red phase voltage was at a peak, indicated with the blue vertical indicator, which effectively is an ideal situation to minimize inrush currents.

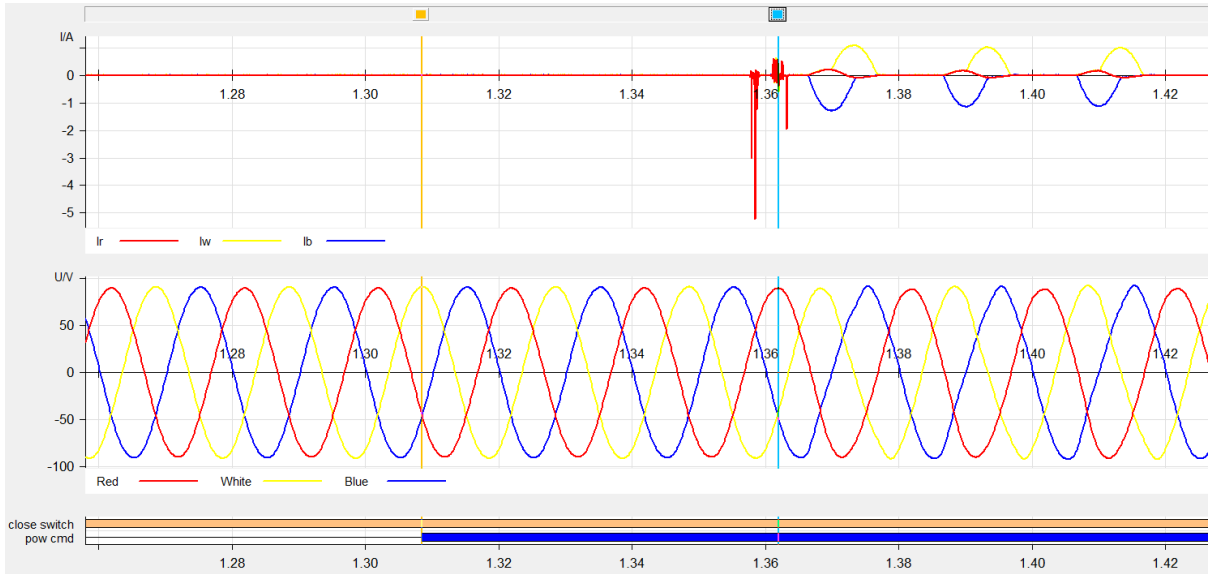


Figure 33: Case study 3 (inrush current and applied voltage)

Table 7 indicates the voltage magnitudes in a per unit value. Table 7 is divided into three sections (i.e. before, during and after the switching transient).

From Table 7 it is clearly shown that there is an average voltage dip of 2.5% across the relevant phases during the instant at which the transformer is connected to the 400kV busbar at Dedisa substation. This voltage dip is seen throughout the network, however it is not as severe as the previous case studies at the 132kV busbar at Grassridge substation. However after the system becomes stable the voltage recovers and the system is found to be in the steady state and thus stronger than before in terms of busbar voltage levels. It is therefore noted that the 132kV voltage at Grassridge substation is found to be much greater, after the switching transient, than the set-point value programmed into the control system of the SVC which is inherently set to 1.02pu.

Table 7: Case study 3 voltage magnitudes for the 400kV and 132kV busbar respectively

	Before switching	During the switching	After switching
Dedisa 400kV busbar			
Vr (pu)	1.001	0.995	1.006
Vw (pu)	1.012	0.976	0.992
Vb (pu)	1.009	0.973	0.989
Grassridge 132kV busbar			
Vr (pu)	1.102	1.128	1.137
Vw (pu)	1.091	1.054	1.148
Vb (pu)	1.094	1.057	1.146
DURATION OF THE TRANSIENT = +-180ms			

Figure 34 indicates the magnitude of the thyristors current for this particular case study. It indicates how the thyristors adjust accordingly with respect to the voltage depression detected and therefore begin to turn off

during this particular transient to allow the capacitor bank to boost the 132kV busbar. At the same instant whilst the capacitor bank is assisting with the voltage stability, gradually the thyristors begin to turn on as the busbar voltage strengthens once again, therefore allowing the reactors to attempt to control the 132kV busbar according to the set-point value. Thus, according to designs perspective the control system is operating correctly according to the recording captured.

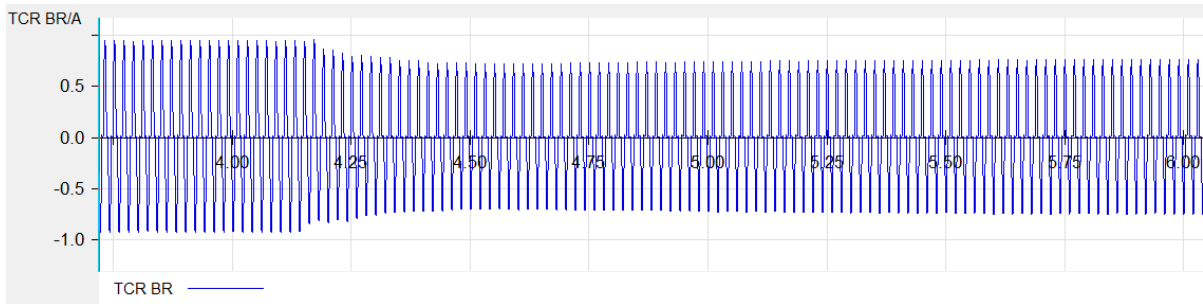


Figure 34: Case study 3 thyristor current during and after switching

4.2.4 Case Study 4 - Transformer 2 Energising, NO SVC Trip

Inrush conditions occur when transformer 2 is energised under no load conditions. The close command from the POW controller is issued via the close switch on the control panel. Figure 35 indicates the close command issued from the controller marked “pow cmd” however from the current waveforms it is clearly shown that the breaker does not close at that particular instant but rather 54.4ms later due to the operational mechanical characteristics of the breaker. Therefore, as seen from Figure 35 the POW controller effectively issued a close command at a peak blue phase voltage (negative peak) as per the settings and is indicated with the orange vertical indicator, however the relevant transformer HV winding made contact with the system voltage when the white phase voltage was at a negative peak, indicated with the blue vertical indicator.

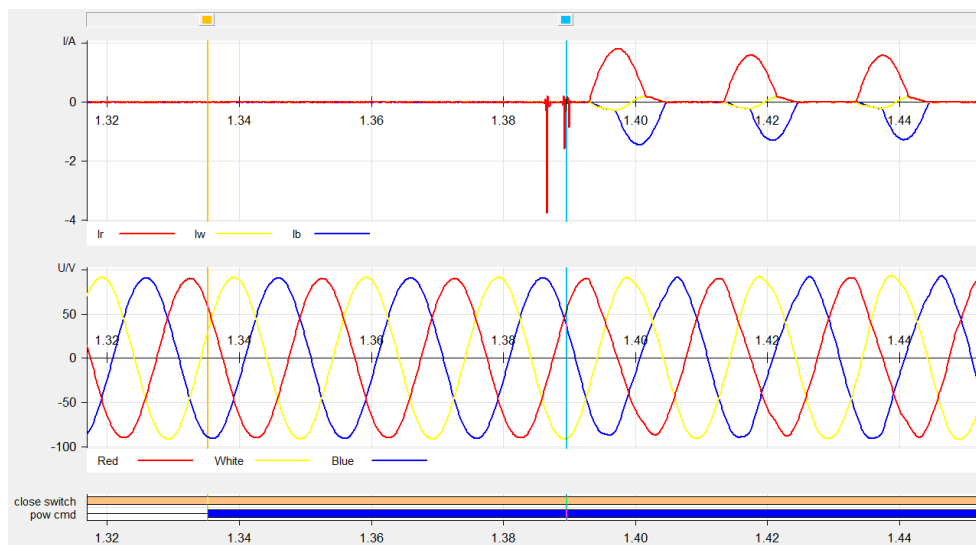


Figure 35: Case study 4 (inrush current and applied voltage)

Table 8 indicates the voltage magnitudes in a per unit value. Table 8 is divided into three sections (i.e. before, during and after the switching transient).

From Table 8 it is clearly shown that there is an average voltage dip of 3.6% across the relevant phases during the switching transient. This particular voltage dip is noticeable throughout the particular grid under investigation (i.e. the 400kV and the 132kV busbar). After the system becomes stable and found to be in the steady state, it is noticeable that the relevant busbar voltage level at Grassridge substation is substantially higher as compared to the scenario before the disturbance on the system. Therefore a question arises on whether or not the SVC at Grassridge substation is in fact operating correctly in order to effectively and correctly regulate and maintain the 132kV busbar magnitude in the order of the set-point value (i.e. 1.02pu).

Table 8: Case study 4 voltage magnitudes for the 400kV and 132kV busbar respectively

	Before switching	During the switching	After switching
Dedisa 400kV busbar			
Vr (pu)	1.005	0.943	0.967
Vw (pu)	1.014	1.006	1.019
Vb (pu)	1.012	0.973	0.983
Grassridge 132kV busbar			
Vr (pu)	1.085	1.054	1.133
Vw (pu)	1.074	1.057	1.141
Vb (pu)	1.078	1.028	1.126
DURATION OF THE TRANSIENT = +-190ms			

Figure 36 indicates the magnitude of the thyristors current for this particular case study. It is similar to case study 3 where the thyristor current is shown to adjust accordingly and effectively and work in harmony with the capacitor bank during the noticeable disturbance on the system relating to the transformer switching. Thus, according to designs perspective the control system is operating correctly according to the waveform captured.

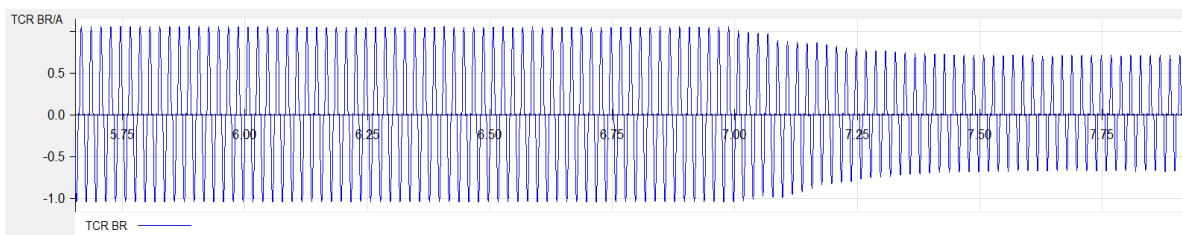


Figure 36: Case study 4 thyristor current during and after switching

4.2.5 Fast Fourier Transform Plots of the 4 Case Studies

To confirm whether or not harmonics, specifically 2nd harmonic inrush currents, play a significant role in the mal-operating of the AEG SIT 852 LV O/C relay, extensive Fast Fourier Transform (FFT) plots are generated in “TOP” software using the actual recorded comtrade values during the switching transient. The 2nd harmonic analysis, in particular, was performed in order to verify whether the SVC is operating normally under system

conditions or harmonic generating conditions. Therefore the 2nd harmonic order analysis was imperative in order to substantiate whether or not the filters at Grassridge substation, that are specifically tuned to filter out certain harmonics, inclusive is the 2nd harmonic order, is in fact operating correctly or not.

Now, Figure 37, 38, 39 is the FFT plots generated in “TOP” software and indicates a predominant 2nd harmonic current generation at Dedisa on the 400kV level when Transformer 1 and Transformer 2 are energised under no load conditions. The waveform plot for case study 2 is not shown due to the recorder not been able to capture a comtrade file due to an AC failure in the substation when transformer 2 was energised. Thus from the studies performed, the respective 2nd order harmonic content is found to be approximately 30% of the fundamental during the transformer energising stage. Therefore Figure 37, 38, 39 forms the basis and confirms previous studies that when a transformer is energised under no load conditions a predominant 2nd harmonic inrush is present and is affiliated by the switching conditions (i.e. the content of residual magnetism and the point on the voltage waveform at which the respective transformer is energised), the structure of the transformer (i.e. the type of core and limb arrangement within the transformer casing) [6].

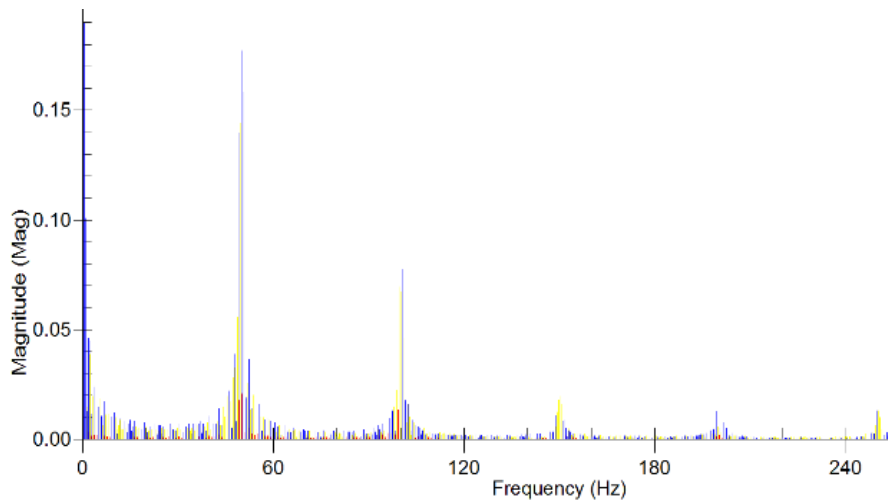


Figure 37: Case study 1 FFT plot representing the inrush current for transformer 1

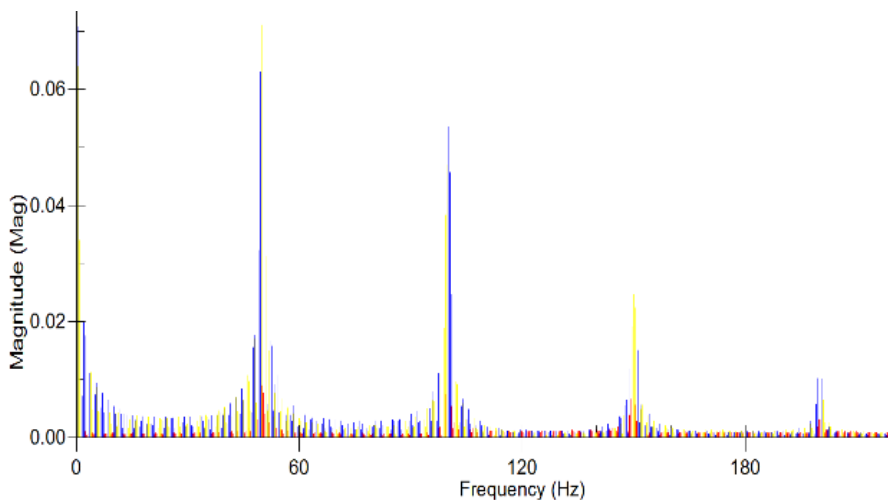


Figure 38: Case study 3 FFT plot representing the inrush current for transformer 2

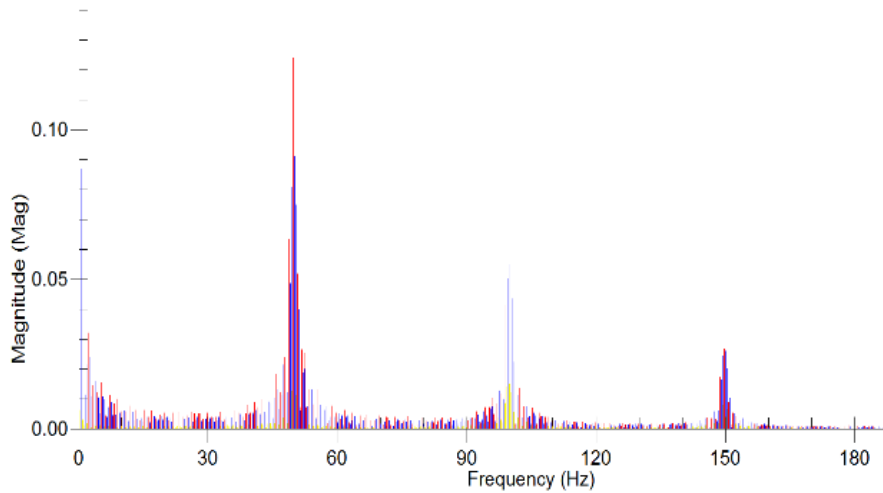


Figure 39: Case study 4 FFT plot representing the inrush current for transformer 2

Grassridge SVC has a capacitor bank that is specifically tuned to filter out specific harmonics produced by the TCR's (Thyristor Controlled Rectifiers). The nominal rating of the capacitor/filter bank in the 132kV SVC is 35 MVar. The filter is tuned to the 2nd, 3rd and 5th harmonic frequencies.

Now, Figure 40, 41, 42 and 43 are the FFT plots generated in "TOP" software and shows that there are no predominant harmonic orders present on the 132kV side of the SVC transformer, besides the fundamental, at Grassridge substation during the inrush transient stage during the switching at Dedisa substation. In addition, Figure 41 indicates case study 2 amongst the other three case studies and it is well established that it is the only case study that had a respective LV O/C trip. It is indicated clearly that there is a predominant fundamental component however only a minor 2nd and 3rd harmonic content is present on the 132kV busbar when transformer 1 is energised at Dedisa substation. Therefore from the detailed FFT plots generated and analysed, case study 2 does not pose a difference or trigger an indication that significant conditions occurred during this particular case as compared to any of the other three analytical conditions.

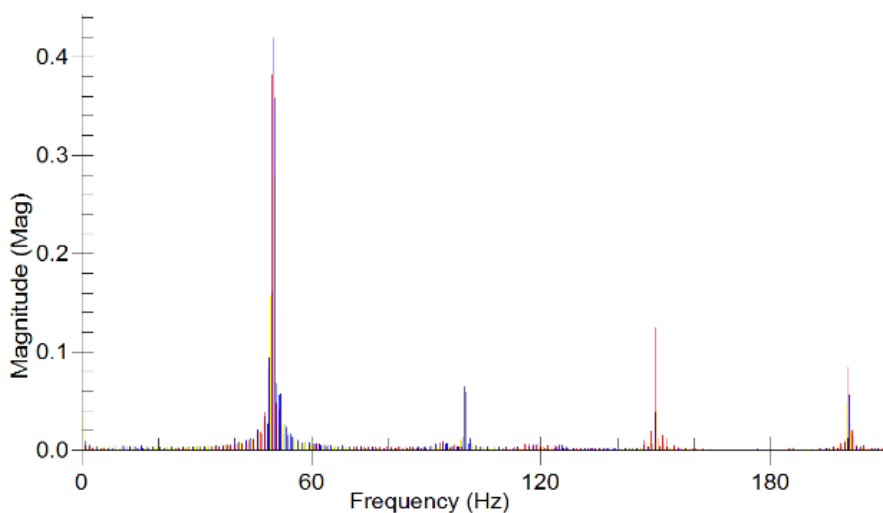


Figure 40: Case study 1 FFT plot representing the HV current on the SVC for transformer 1 switching

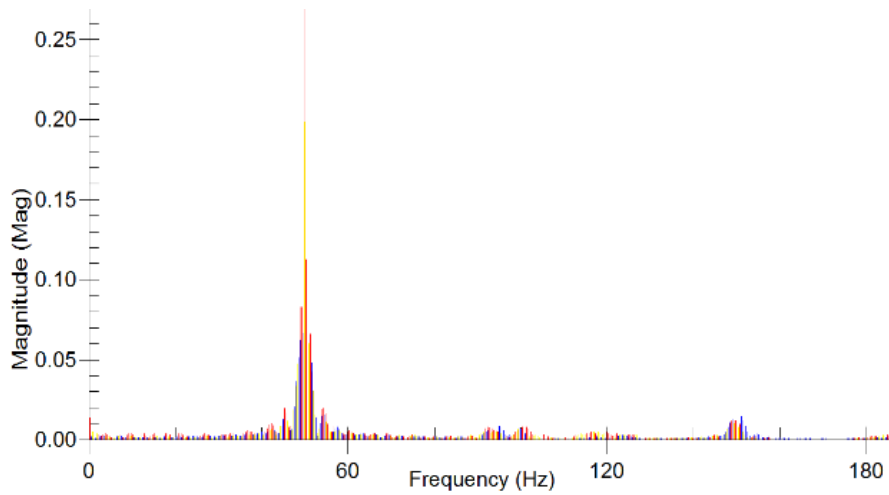


Figure 41: Case study 2 FFT plot representing the HV current on the SVC for transformer 1 switching

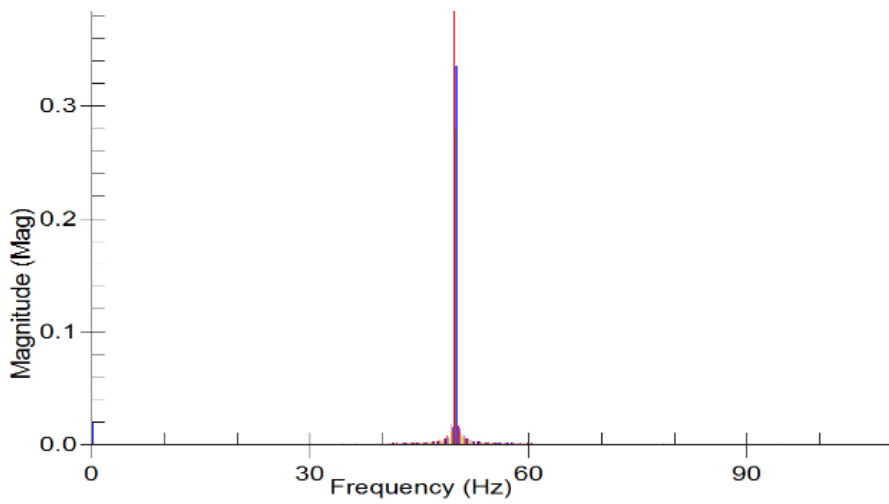


Figure 42: Case study 3 FFT plot representing the HV current on the SVC for transformer 2 switching

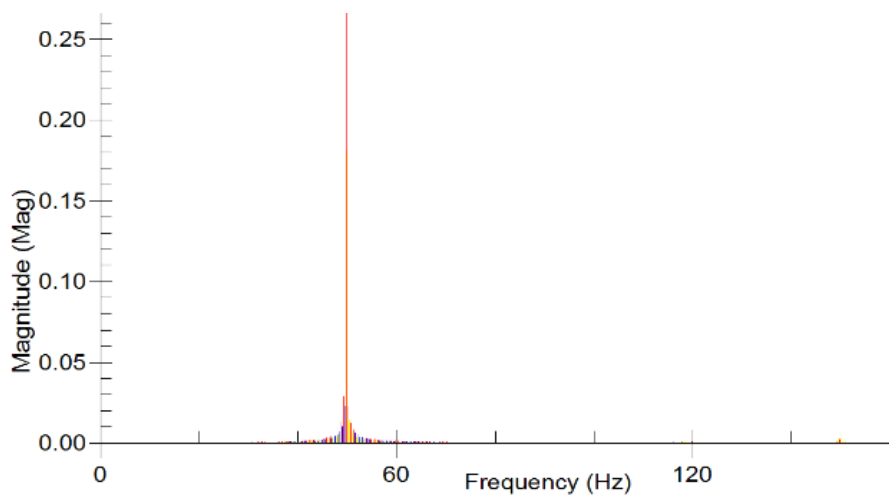


Figure 43: Case study 4 FFT plot representing the HV current on the SVC for transformer 2 switching

The harmonic blocking filters are shown to be effective on the SVC such that there are no predominant “stray” harmonics present during the energising transient at Dedisa. Figure 44, 45, 46 and 47 show the FFT plots on the 5.1kV side of the SVC and once again from the detailed FFT plots generated and analysed, case study 2 in Figure 45 does not pose any difference or trigger an indication that significant conditions occurred during this particular case as compared to any of the other three analytical conditions. If any concern should be considered then case study 1 in Figure 44 could pose a slight alarm as compared to the other three case studies due to the 3rd and 4th harmonic content “slipping” through the harmonic blocking filters. However case study 1 did not have a recorded trip therefore it is not significant to pursue the details outlined.

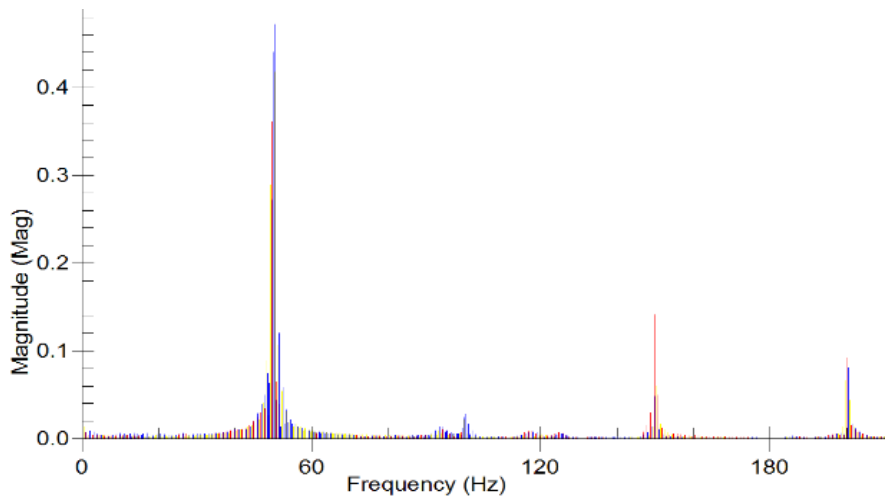


Figure 44: Case study 1 FFT plot representing the LV current on the SVC for transformer 1 switching

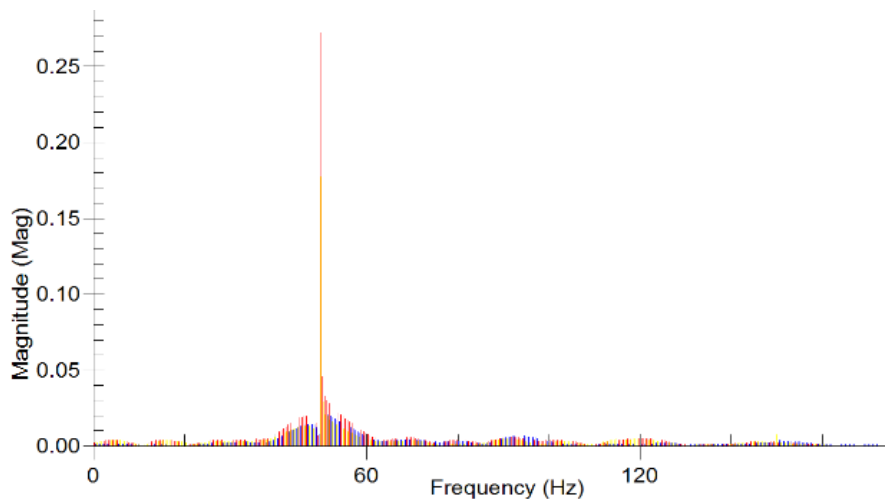


Figure 45: Case study 2 FFT plot representing the LV current on the SVC for transformer 1 switching

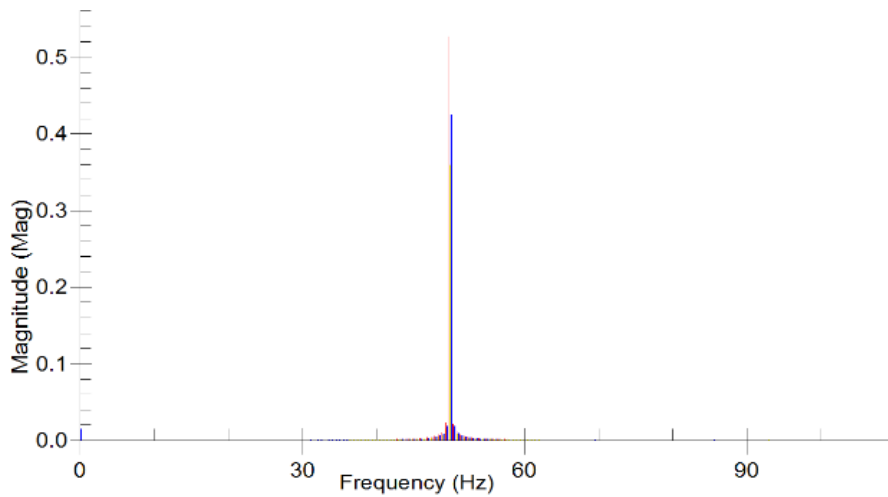


Figure 46: Case study 3 FFT plot representing the LV current on the SVC for transformer 2 switching

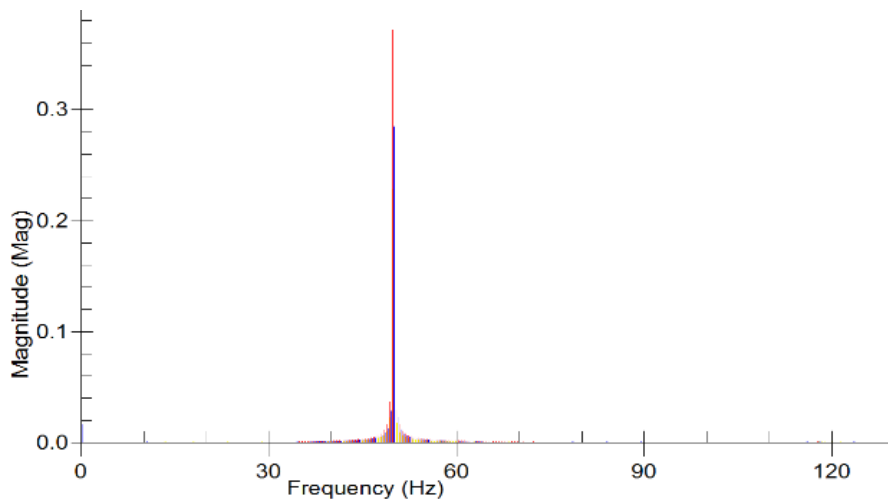


Figure 47: Case study 4 FFT plot representing the LV current on the SVC for transformer 2 switching

4.3 DIGSILENT RESULTS

Three scenarios are simulated within DlgSILENT PowerFactory in order to replicate the correct SVC operation in terms of how the thyristors respond to voltage variation on the 132kV busbar at Grassridge. The three scenarios in addition replicate the 2nd harmonic inrush current of the 500MVA transformer when it is energised. The three scenarios are imperative in order to verify actual system conditions and operations at both Dedisa and Grassridge substation. The three scenarios are as follows:

4.3.1 Poseidon as a weak source

This particular scenario depicts Poseidon as a weak source such that the external grid, which is modelled as a slack bus, relative to the 400kV busbar is set to $V = 0.83\text{pu}$. Therefore the expectation is such that the SVC will

have to compensate greatly on the 132kV busbar at Grassridge due to the low voltage level throughout the entire derived network model.

Hence, Figure 48 indicates the 400kV busbar voltage level at Dedisa together with the 2nd harmonic inrush current. From Figure 48 the busbar voltage level is $V = 0.808\text{pu}$ on all relevant phases before the transformer switching and directly during the switching transient the voltage dips to $V = 0.702\text{pu}$ on the blue phase and at the same instant the maximum peak inrush current on the blue phase is $I_{B(\text{max})} = 1.915\text{kA}$.

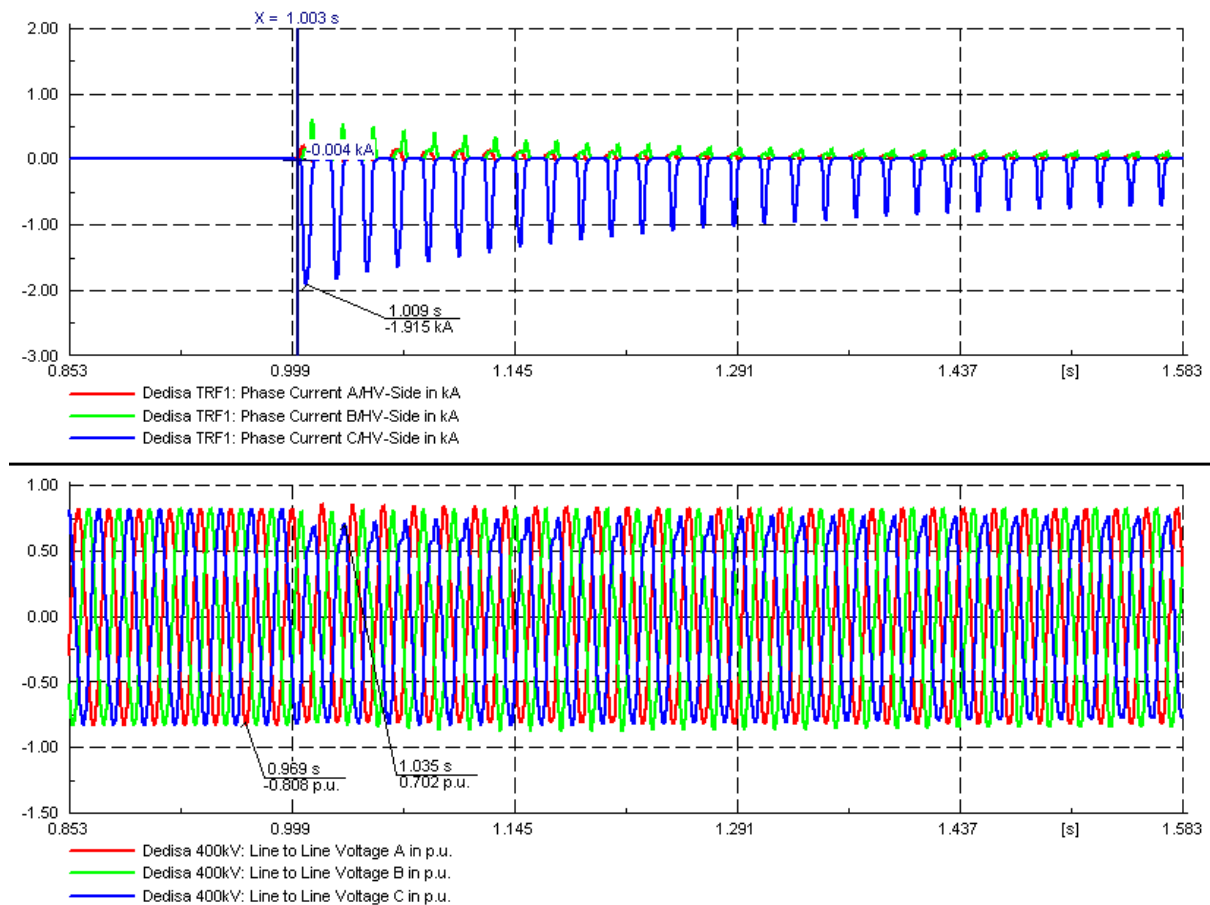


Figure 48: DIgSILENT (weak source) results for transformer inrush current and 400kV busbar voltage

Therefore as seen in Figure 49 the weak voltage is seen throughout the power system and the busbar voltage level on the 132kV busbar at Grassridge substation is $V = 0.915\text{pu}$ before the switching transient and dips to $V = 0.825\text{pu}$ during the transient and is corrected by the SVC and found to be $V = 0.869\text{pu}$ during the steady state. Now, taking into consideration the SVC is set with a set-point value of $V = 1.02\text{pu}$, the SVC “strives” to attain this particular value within the controller. Therefore, as expected, the Thyristors turn off completely during this scenario as the voltage is well below the set-point value on the 132kV busbar and only a spike of surge current is present during the first five cycles of the transient which can be ignored due to further analysis relative in Figure 50.

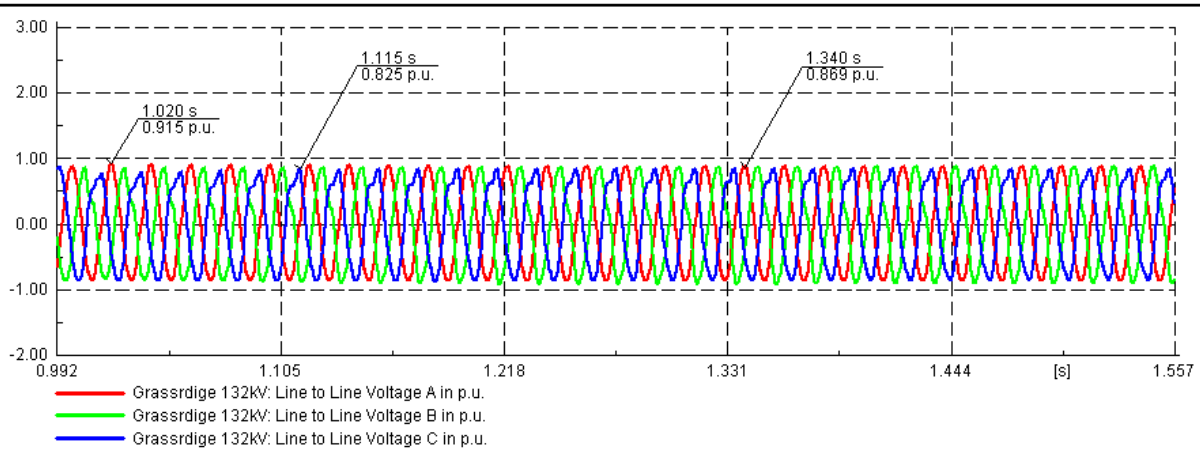
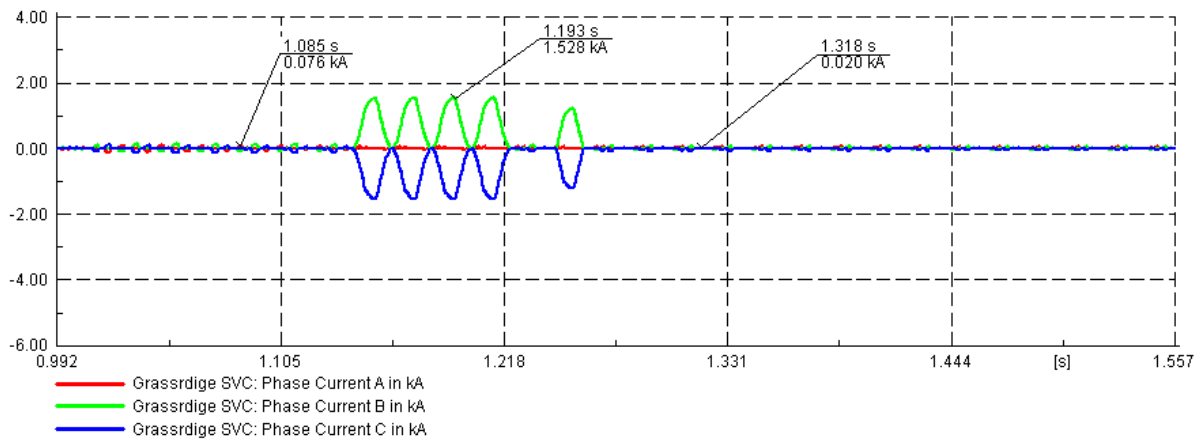


Figure 49: DIgSILENT (weak source) results for Grassridge 132kV voltage relative to the SVC LV current

Figure 50 verifies that the thyristors are not firing hard for the reactor to perform as the firing angle equals 163.4° . Thus the SVC is acting purely as a capacitor bank in order to “boost” the 132kV busbar as much as possible and within the rated characteristics of the SVC.

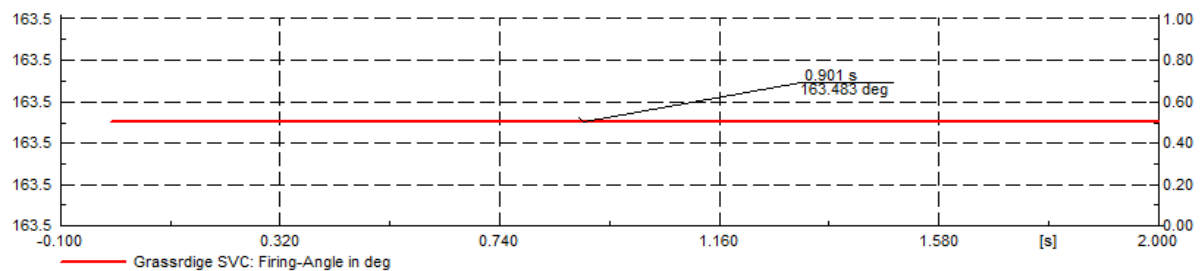


Figure 50: DIgSILENT (weak source) results for the thyristors firing angle during the switching transient

Figure 51 indicates the simulated FFT plots for this particular scenario for the indicated busbar depicted in the legend on the graph in Figure 51.

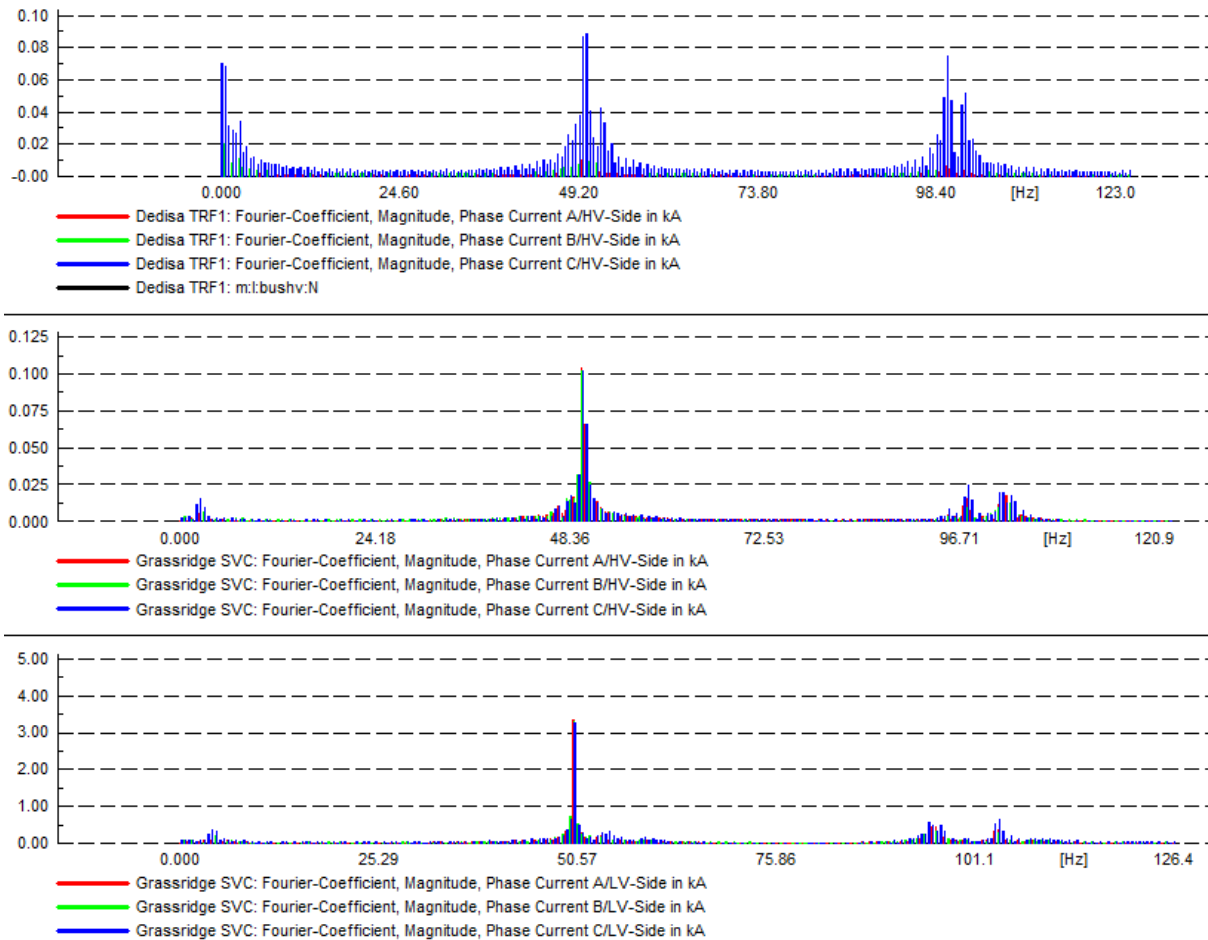


Figure 51: DIGSILENT (weak source) FFT plots for transformer 1 HV and the 132kV and 5.1kV side of the SVC

4.3.2 Poseidon as a strong source

This particular scenario depicts Poseidon as a strong source such that the external grid, which is modelled as a slack bus, relative to the 400kV busbar at Poseidon is set to $V = 1.1\text{pu}$. Therefore the expectation is such that the SVC will have to operate in such a manner in order to effectively attempt to reduce and regulate the 132kV voltage at Grassridge due to the high voltage level throughout the entire derived network model.

Hence, Figure 52 indicates the 400kV busbar voltage level at Dedisa together with the 2nd harmonic inrush current. From Figure 52 the busbar voltage level is $V = 1.078\text{pu}$ before the transformer switching and directly during the switching transient the voltage surges to $V = 1.172\text{pu}$ on the red phase at the same instant the maximum peak inrush current on the blue phase is $I_{B(\text{max})} = 3.839\text{kA}$.

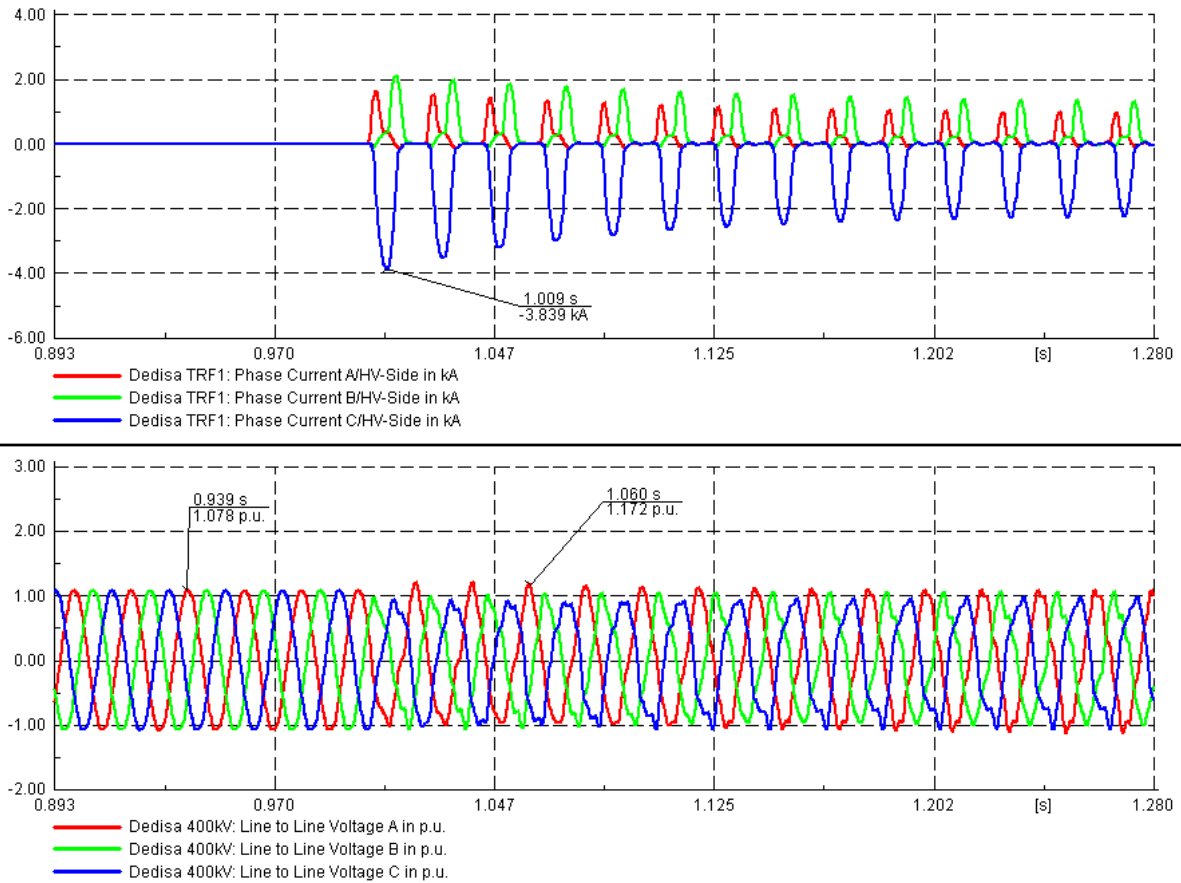


Figure 52: DIgSILENT (strong source) results for transformer inrush current and 400kV busbar voltage

Therefore as seen in Figure 53 the strong source voltage is seen throughout the power system and the busbar voltage level on the 132kV busbar at Grassridge substation is $V = 1.141\text{pu}$ before the switching transient and dips to $V = 1.059\text{pu}$ on the blue phase during the transient. Now, taking into consideration the SVC is set with a set-point value of $V = 1.02\text{pu}$, the SVC “strives” to attain this particular value within the controller. However a sudden change in voltage of **-7.2%** was detected and thus the thyristors turn off temporarily as shown by the indicator where $I_r = I_w = I_b = 0\text{kA}$. However during the first five cycles the SVC is in the process of making a decision relative to the voltage detected on the 132kV busbar, and therefore it can be seen that the voltage is continuing above the set-point value and is in fact $V=1.238\text{pu}$, therefore as expected the thyristors turn on completely during this scenario as the voltage is well above the set-point value on the 132kV busbar. Thus the relative peak current on the red phase and blue phase is found to be $I_{r(\text{max})} = 1.928\text{kA}$ and $I_{b(\text{max})} = 2.755\text{kA}$ respectively as seen in Figure 53.

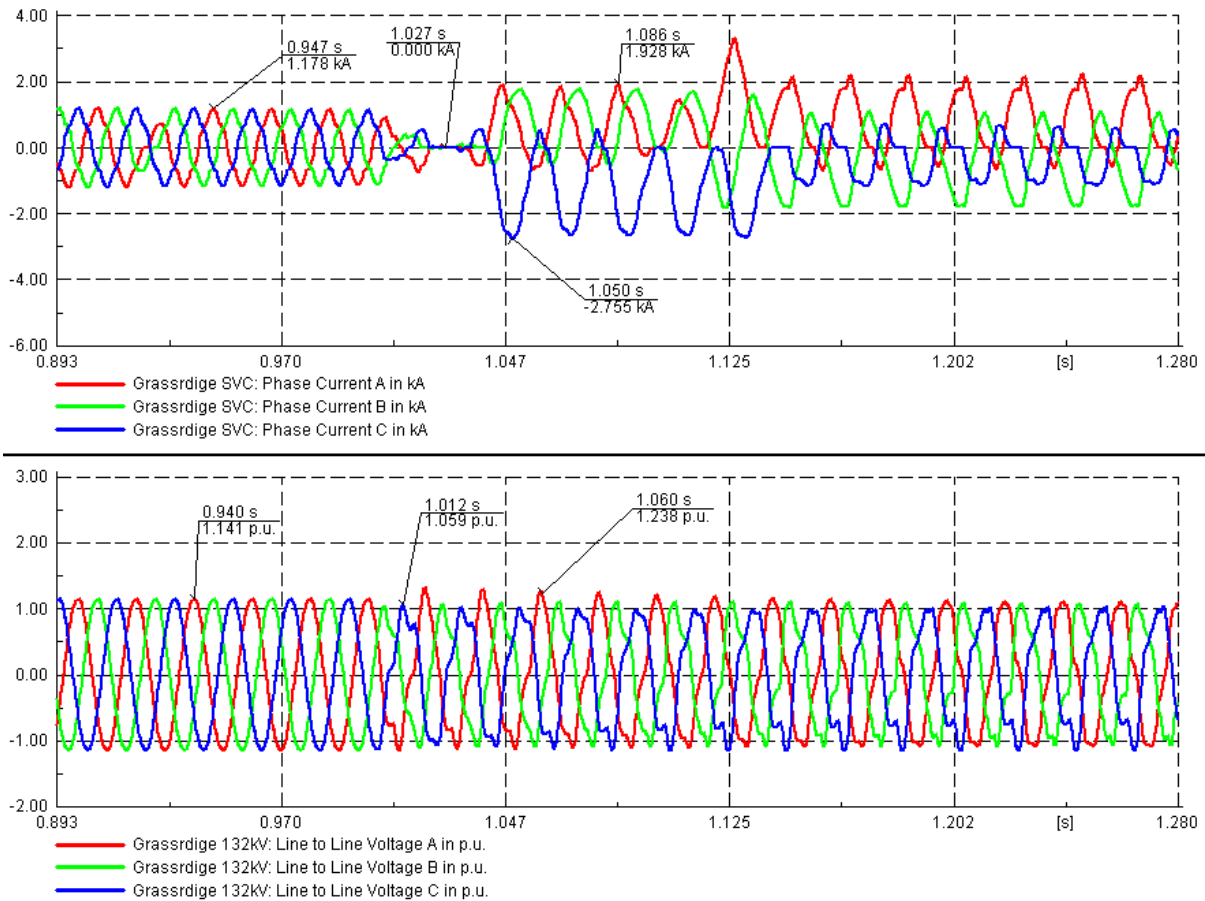


Figure 53: DIgSILENT (strong source) results for Grassridge 132kV voltage relative to the SVC LV current

Figure 54 is an indication from an input signal parameter within DIgSILENT and resembles only the state of change of the thyristors characteristic during the state of the switching transient. Therefore Figure 54 indicates that the thyristors were firing at an angle of 110° before the switching and then momentarily switched off at an angle of 163.4° during the transient response, thereafter the angle is ignored because it is only an input parameter within the controller. Emphasis is rather made on the currents indicated in Figure 53 for the time period after the transient where it is indicated that the SVC is acting purely as a reactor in order to compensate for the high voltage magnitude on the 132kV busbar.

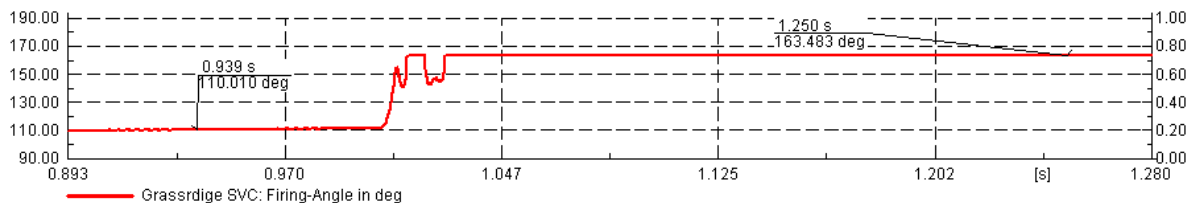


Figure 54: DIgSILENT (strong source) results for the thyristors firing angle during the switching transient

Figure 55 indicates the simulated FFT plots for this particular scenario for the indicated busbar depicted in the legend on the graph in Figure 55.

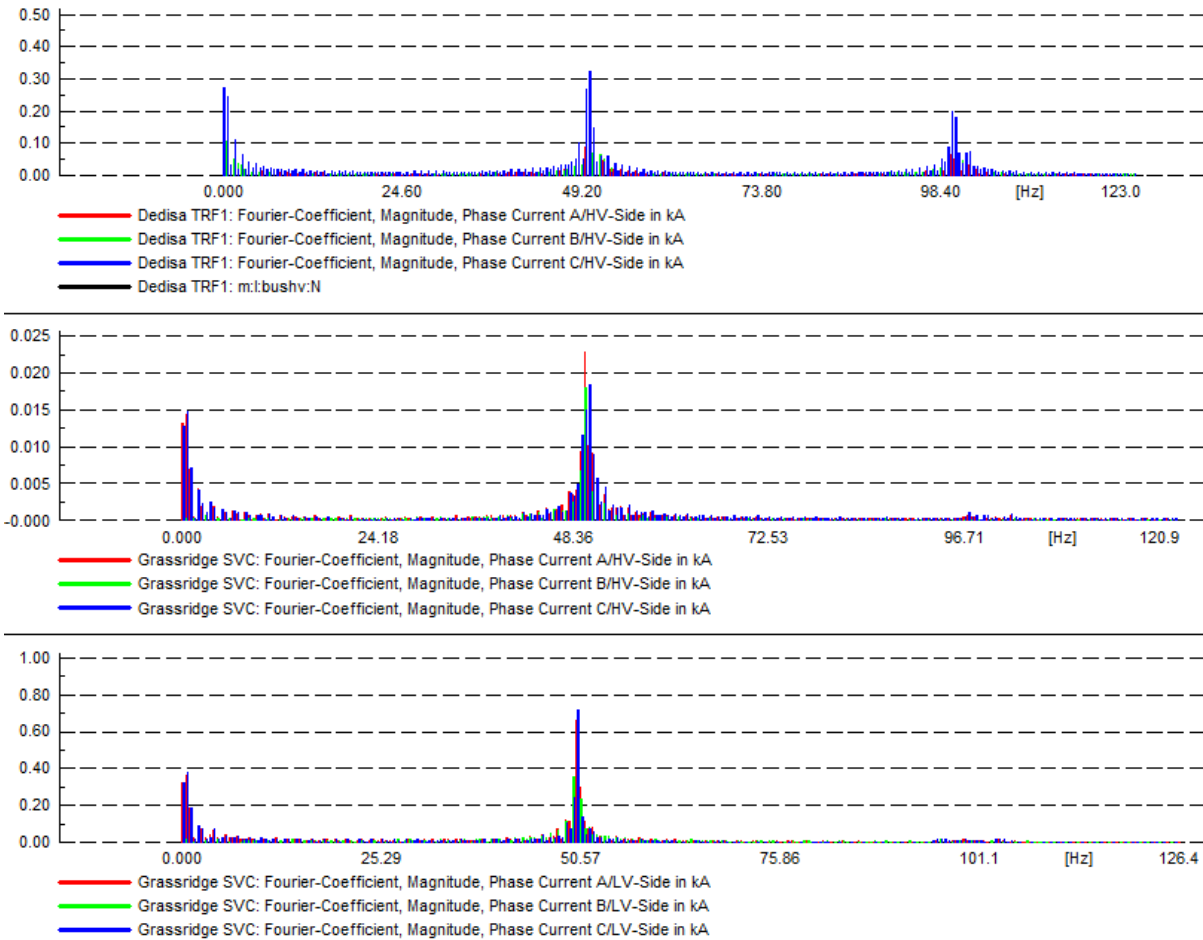


Figure 55: DIgSILENT (strong source) FFT plots for transformer 1 HV and the 132kV and 5.1kV side of the SVC

4.3.3 Poseidon replicating Case Study 2 - SVC Trip

This particular scenario replicates the actual busbar voltages extracted from the recordings, located in Table 6, when the SVC tripped due to an LV O/C operation. The external grid, which is modelled as a slack bus, relative to the 400kV busbar at Poseidon substation is set such that the magnitude of the 132kV busbar voltage at Grassridge substation is set to $V = 1.07pu$ as per the recording. Therefore the expectation is such that the SVC will have to react in such a manner in order to effectively compensate to reduce and regulate the 132kV voltage at Grassridge due to the high voltage level throughout the entire derived network model and effectively strive towards the set-point value of $V = 1.02pu$.

Therefore, Figure 56 indicates the 400kV busbar voltage level at Dedisa together with the 2nd harmonic inrush current. From Figure 56 the busbar voltage level is $V = 1.007pu$ before the transformer switching and directly during the switching transient the voltage dips to $V = 0.846pu$ on the blue phase at the same instant the maximum peak inrush current on the blue phase is $I_{B(max)} = 3.293kA$.

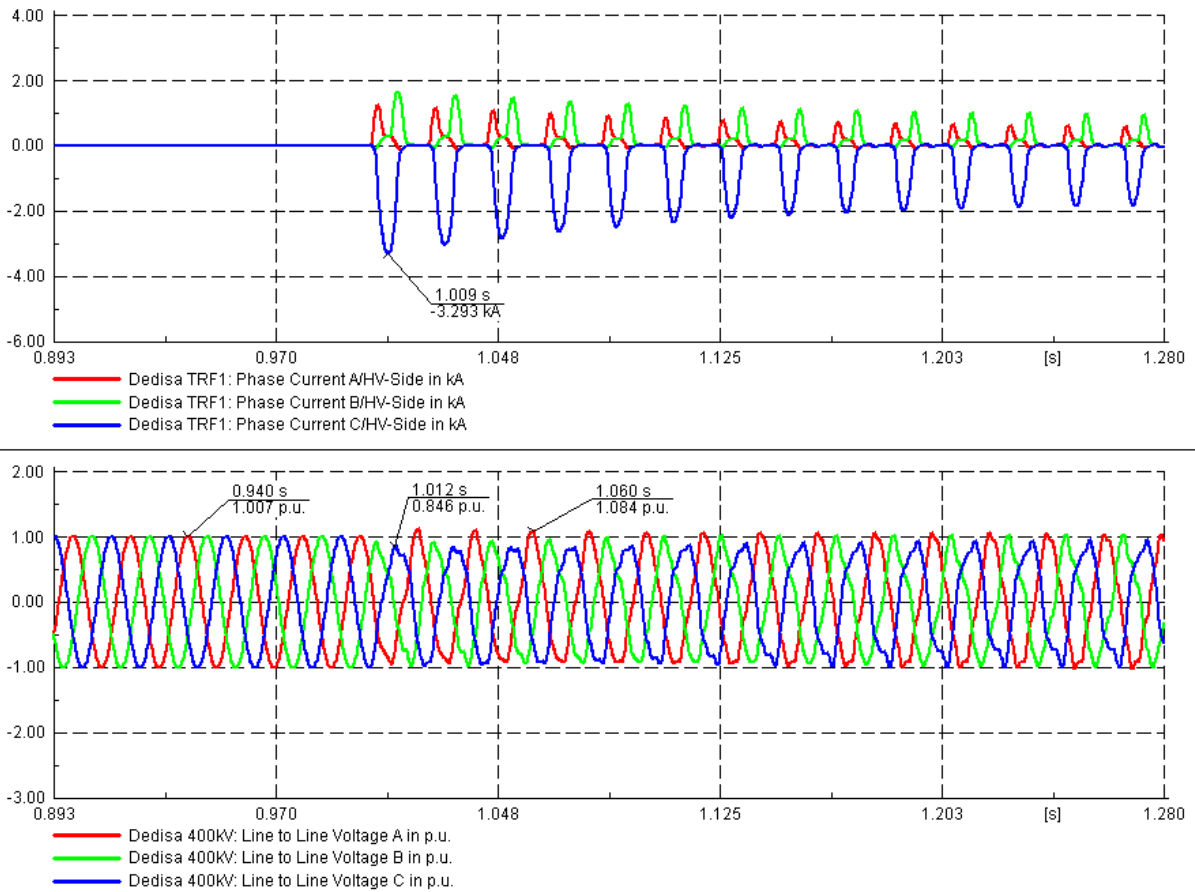


Figure 56: DIgSILENT (case study 2 replication) results for transformer inrush current and 400kV busbar voltage

As seen in Figure 57 the busbar voltage level on the 132kV busbar at Grassridge substation is $V = 1.07\text{pu}$ before the switching transient, thus replicating the actual OMICRON recording for case study 2, and dips to $V = 0.958\text{pu}$ on the blue phase during the transient. Now, taking into consideration the SVC is set with a set-point value of $V=1.02\text{pu}$, the SVC “strives” to maintain this particular value within the controller. Now analysing the reaction of the thyristors, it is seen that during the voltage dip the thyristors turn off momentarily however due to the 132kV voltage level maintaining $V = 1.176\text{pu}$, the thyristors allow full conduction and thus are on completely in order to reduce the voltage on the 132kV system towards the set-point value. Thus the relative peak current on the red phase and white phase is found to be $I_{r(\max)} = 1.762\text{kA}$ and $I_{w(\max)} = 2.858\text{kA}$ respectively as seen in Figure 57.

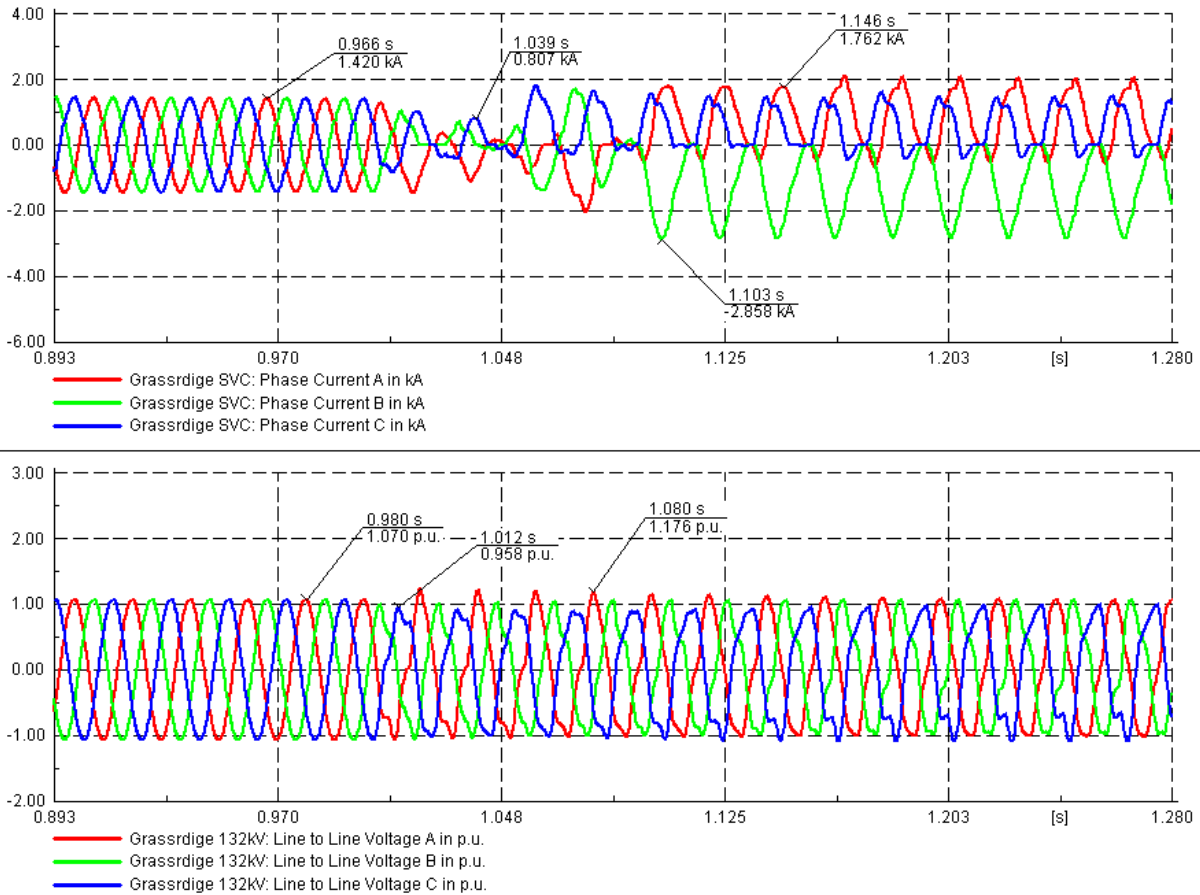


Figure 57: DIgSILENT (case study 2 replication) results for Grassridge 132kV voltage relative to the SVC LV current

Figure 58 is an indication from an input signal parameter within DIgSILENT and resembles only the state of change of the thyristors characteristic during the state of the switching transient. Therefore Figure 58 indicates that the thyristors were firing at an angle of 100° before the switching and then momentarily switched off at an angle of 163.5° during the transient response, thereafter the angle is ignored because it is only an input parameter within the controller. Emphasis is rather made on the currents indicated in Figure 57 for the time period after the transient where it is indicated that the SVC is acting purely as a reactor in order to compensate for the high voltage magnitude on the 132kV busbar.

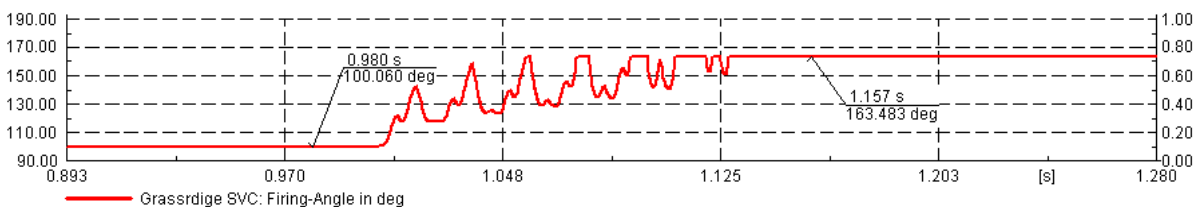


Figure 58: DIgSILENT (case study 2 replication) results for the thyristors firing angle during the switching transient

Figure 59 indicates the simulated FFT plots for this particular scenario for the indicated busbar depicted in the legend on the graph in Figure 59. No harmonic orders are present on the 132kV or 5.1kV system besides the 2nd order harmonic due to transformer inrush on the 400kV side of the applicable transformer.

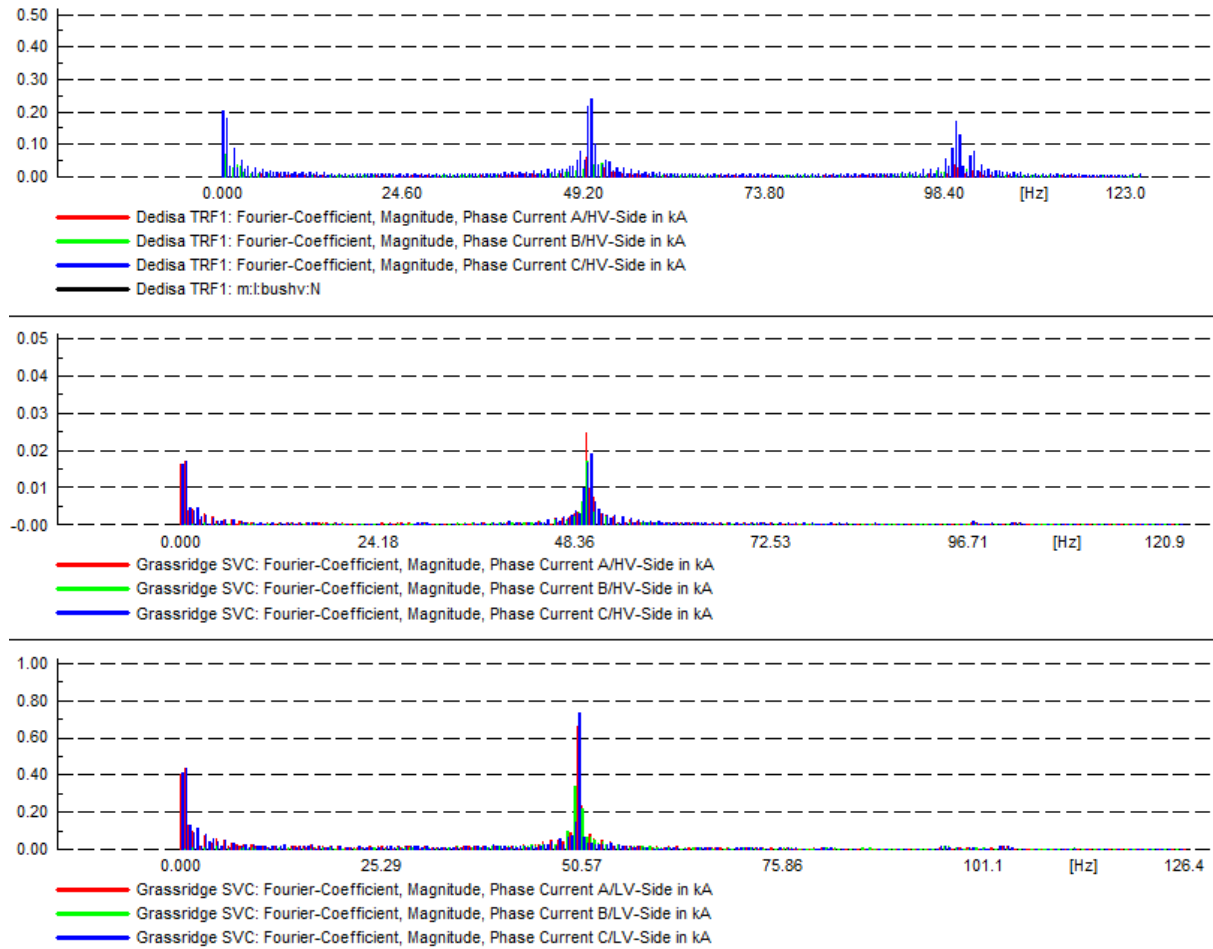


Figure 59: DIgSILENT (case study 2 replication) FFT plots for transformer 1 HV and the 132kV and 5.1kV side of the SVC

4.4 WORKED CALCULATIONS

4.4.1 Peak current calculation

In order to verify and supplement the simulated results obtained with DIgSILENT and the recorder results, verification in terms of the maximum expected value of the inrush current has been determined using (10) relating to an analytical approach.

Thus, an assumption has been made that the core of the 500MVA transformers saturate in 5 ms and a switching angle of $\theta=0^\circ$ and $\theta=90^\circ$ respectively have been selected for emphasis.

For $\theta=0^\circ$:

The source reactance of the system per phase $X_S = 11.88\Omega$

The source resistance of the system per phase $R_S = 4.95\Omega$

The transformer reactance per phase $X_T = 14.67\Omega$

Therefore $X_{TOTAL} = 26.55\Omega$, therefore $L = 0.085H$

$$i(t) = e^{-(R/L)t} \left\{ \frac{-E_{max}}{\sqrt{R^2 + \omega^2 L^2}} \sin \left[\theta - \tan^{-1} \left(\frac{\omega L}{R} \right) \right] \right\} + \frac{E_{max}}{\sqrt{R^2 + \omega^2 L^2}} \sin \left[\omega t + \theta - \tan^{-1} \left(\frac{\omega L}{R} \right) \right]$$

$$i(t) = e^{-(4.95/0.085)0.005} \left\{ \frac{-\sqrt{2} \times \frac{400kV}{\sqrt{3}}}{\sqrt{4.95^2 + (2\pi 50)^2 (0.085)^2}} \sin \left[0^\circ - \tan^{-1} \left(\frac{26.55}{4.95} \right) \right] \right\}$$

$$+ \frac{\sqrt{2} \times \frac{400kV}{\sqrt{3}}}{\sqrt{4.95^2 + (2\pi 50)^2 (0.085)^2}} \sin \left[(2\pi 50)(0.005) + 0^\circ - \tan^{-1} \left(\frac{26.55}{4.95} \right) \right]$$

$$i(t) = 0.7474(-12092.887)(-0.985) + (12092.887)(0.174)$$

$$i(t) = 11.007kA$$

Therefore the peak inrush current for worst case scenario (at the zero crossing on the voltage waveform where the switching angle $\theta=0^\circ$) is 11.007kA.

For $\theta=90^\circ$:

The source reactance of the system per phase $X_S = 11.88\Omega$

The source resistance of the system per phase $R_S = 4.95\Omega$

The transformer reactance per phase $X_T = 14.67\Omega$

Therefore $X_{TOTAL} = 26.55\Omega$, therefore $L = 0.085H$

$$i(t) = e^{-(R/L)t} \left\{ \frac{-E_{max}}{\sqrt{R^2 + \omega^2 L^2}} \sin \left[\theta - \tan^{-1} \left(\frac{\omega L}{R} \right) \right] \right\} + \frac{E_{max}}{\sqrt{R^2 + \omega^2 L^2}} \sin \left[\omega t + \theta - \tan^{-1} \left(\frac{\omega L}{R} \right) \right]$$

$$i(t) = e^{-(4.95/0.085)0.005} \left\{ \frac{-\sqrt{2} \times \frac{400kV}{\sqrt{3}}}{\sqrt{4.95^2 + (2\pi 50)^2 (0.085)^2}} \sin \left[90^\circ - \tan^{-1} \left(\frac{26.55}{4.95} \right) \right] \right\}$$

$$+ \frac{\sqrt{2} \times \frac{400kV}{\sqrt{3}}}{\sqrt{4.95^2 + (2\pi 50)^2 (0.085)^2}} \sin \left[(2\pi 50)(0.005) + 90^\circ - \tan^{-1} \left(\frac{26.55}{4.95} \right) \right]$$

$$i(t) = 0.7474(-12092.887)(0.174) + (12092.887)(0.985)$$

$$i(t) = 10.336kA$$

Therefore, the peak inrush current for a switching angle of $\theta=90^\circ$ (at the peak of the voltage waveform) is 10.336kA.

4.4.2 Total Harmonic Distortion Calculation for Case Study 2

Grassridge SVC “132kV” Currents:

From (20) one can calculate I_{THD} for each phase, hence

$$I_{THD(i)} = \frac{\sqrt{\sum_{\substack{h \neq 1 \\ i=R,Y,B,n}} I_{ih}^2}}{I_{i1}} \%$$

Therefore,

$$I_{THD(R)} = \frac{\sqrt{I_{R2}^2 + I_{R3}^2 + I_{R4}^2 + I_{R5}^2 + I_{R7}^2}}{I_{R1}} \times 100\%$$

$$I_{THD(R)} = \frac{\sqrt{13^2 + 23^2 + 18^2 + 5^2 + 2^2}}{169} \times 100\%$$

$$I_{THD(R)} = 19.18\%$$

$$I_{THD(W)} = \frac{\sqrt{I_{W2}^2 + I_{W3}^2 + I_{W4}^2 + I_{W5}^2 + I_{W7}^2}}{I_{W1}} \times 100\%$$

$$I_{THD(W)} = \frac{\sqrt{3.8^2 + 4.5^2 + 9.2^2 + 6.4^2 + 1.6^2}}{118} \times 100\%$$

$$I_{THD(W)} = 10.81\%$$

$$I_{THD(B)} = \frac{\sqrt{I_{B2}^2 + I_{B3}^2 + I_{B4}^2 + I_{B5}^2 + I_{B7}^2}}{I_{B1}} \times 100\%$$

$$I_{THD(B)} = \frac{\sqrt{7.6^2 + 32^2 + 19^2 + 9.2^2 + 0.4^2}}{122} \times 100\%$$

$$I_{THD(B)} = 32.04\%$$

From (18) one can calculate I_{RMS} for each phase, hence

$$I_{rms(i)} = \sqrt{\sum_{\substack{h=1 \\ i=R,Y,B,n}} I_{ih}^2}$$

Therefore,

$$I_{rms(R)} = \sqrt{I_{R1}^2 + I_{R2}^2 + I_{R3}^2 + I_{R4}^2 + I_{R5}^2 + I_{R7}^2}$$

$$I_{rms(R)} = \sqrt{169^2 + 13^2 + 23^2 + 18^2 + 5^2 + 2^2}$$

$$I_{rms(R)} = 172.1A$$

$$I_{rms(W)} = \sqrt{I_{W1}^2 + I_{W2}^2 + I_{W3}^2 + I_{W4}^2 + I_{W5}^2 + I_{W7}^2}$$

$$I_{rms(W)} = \sqrt{118^2 + 3.8^2 + 4.5^2 + 9.2^2 + 6.4^2 + 1.6^2}$$

$$I_{rms(W)} = 118.7A$$

$$I_{rms(B)} = \sqrt{I_{B1}^2 + I_{B2}^2 + I_{B3}^2 + I_{B4}^2 + I_{B5}^2 + I_{B7}^2}$$

$$I_{rms(B)} = \sqrt{122^2 + 7.6^2 + 32^2 + 19^2 + 9.2^2 + 0.4^2}$$

$$I_{rms(B)} = 128.1A$$

Grassridge SVC “5.1kV” Currents:

$$I_{THD(R)} = \frac{\sqrt{I_{R2}^2 + I_{R3}^2 + I_{R4}^2 + I_{R5}^2 + I_{R7}^2}}{I_{R1}} \times 100\%$$

$$I_{THD(R)} = \frac{\sqrt{300^2 + 500^2 + 400^2 + 60^2 + 200^2}}{4200} \times 100\%$$

$$I_{THD(R)} = 17.55\%$$

$$I_{THD(W)} = \frac{\sqrt{I_{W2}^2 + I_{W3}^2 + I_{W4}^2 + I_{W5}^2 + I_{W7}^2}}{I_{W1}} \times 100\%$$

$$I_{THD(W)} = \frac{\sqrt{90^2 + 100^2 + 200^2 + 200^2 + 50^2}}{3100} \times 100\%$$

$$I_{THD(W)} = 10.23\%$$

$$I_{THD(B)} = \frac{\sqrt{I_{B2}^2 + I_{B3}^2 + I_{B4}^2 + I_{B5}^2 + I_{B7}^2}}{I_{B1}} \times 100\%$$

$$I_{THD(B)} = \frac{\sqrt{100^2 + 80^2 + 400^2 + 300^2 + 30^2}}{3100} \times 100\%$$

$$I_{THD(B)} = 16.68\%$$

$$I_{rms(R)} = \sqrt{I_{R1}^2 + I_{R2}^2 + I_{R3}^2 + I_{R4}^2 + I_{R5}^2 + I_{R7}^2}$$

$$I_{rms(R)} = \sqrt{4200^2 + 300^2 + 500^2 + 400^2 + 60^2 + 200^2}$$

$$I_{rms(R)} = 4264.2A$$

$$I_{rms(W)} = \sqrt{I_{W1}^2 + I_{W2}^2 + I_{W3}^2 + I_{W4}^2 + I_{W5}^2 + I_{W7}^2}$$

$$I_{rms(W)} = \sqrt{3100^2 + 90^2 + 100^2 + 200^2 + 200^2 + 50^2}$$

$$I_{rms(W)} = 3155.6A$$

$$I_{rms(B)} = \sqrt{I_{B1}^2 + I_{B2}^2 + I_{B3}^2 + I_{B4}^2 + I_{B5}^2 + I_{B7}^2}$$

$$I_{rms(B)} = \sqrt{3100^2 + 100^2 + 80^2 + 400^2 + 300^2 + 30^2}$$

$$I_{rms(B)} = 3142.8A$$

4.5 DATA ANALYSIS AND INTERPRETATION

Validation in terms of the derived model in DIgSILENT is imperative in order to derive a conclusive result to substantiate claims whether or not the SVC operated correctly or not for the “suspected” mal-operating trips at Grassridge substation.

Firstly, Table 9 indicates the busbar results, during the switching transient, for the 400kV and 132kV busbar at Dedisa and Grassridge substation. Table 9 is the comparison between all four case studies respectively together with the relevant results obtained within the derived DIgSILENT model particular to case study 2 when the SVC issued an LV O/C trip.

Table 9: Voltage magnitudes and peak currents relevant to all four case studies during the switching transient together with DIgSILENT results

		Case Study 1	Case Study 2	Case Study 3	Case Study 4	Case Study 2	
	Index	Unit	OMICRON	OMICRON	OMICRON	OMICRON	DIgSILENT
400kV	$I_{peak(R)}$	A	334	-	155	1440	1245
	$I_{peak(W)}$	A	1271	-	872	215	1630
	$I_{peak(B)}$	A	1230	-	1032	1160	3292
	V_R	pu	1.003	-	0.995	0.943	1.084
	V_W	pu	0.946	-	0.976	1.006	1.009
	V_B	pu	0.935	-	0.973	0.973	0.846
132kV	V_R	pu	1.059	0.961	1.128	1.054	1.176
	V_W	pu	0.948	1.024	1.054	1.057	1.026
	V_B	pu	0.951	1.019	1.057	1.028	0.958

From Table 9, one notices that there is no abnormal activity on the 132kV busbar in terms of the relevant phases during the switching transient. More importantly case study 2 is the only scenario/switching where an LV O/C trip was issued to the SVC. From the results in Table 9 there is no difference in terms of busbar voltage magnitudes between the other three relevant case studies and the actual simulated results shown in DIgSILENT.

Therefore we move on and look at detailed analysis in terms of how the SVC reacted when a voltage dip was detected on the 132kV busbar. This is imperative for emphasis purposes relating to correct operation. Therefore, Table 10 indicates the recorded values for case study 2 for when the SVC issued a LV O/C trip. Case study 2 is now highlighted amongst the other cases and compared to a derived model within software. The 132kV busbar

is of particular importance as it is the relevant busbar that the SVC controls according to the set-point value on the PLC.

Table 10: Case Study 2 voltage magnitudes OMICRON vs. DIgSILENT

			Case Study 2		Case Study 2	
			OMICRON		DIgSILENT	
			BEFORE	TRANSIENT RESPONSE	BEFORE	TRANSIENT RESPONSE
132kV	V_R	pu	1.069	0.961	1.069	1.176
	V_W	pu	1.065	1.024	1.069	1.026
	V_B	pu	1.065	1.019	1.069	0.958

As seen from Table 10 the “before” scenario in DIgSILENT is correlated with exactly what was found with the recorded results for case study 2. The “transient response” scenario results indicate how the magnitude of the 132kV busbar changed when the transformer was energised at Dedisa substation. One can see that the results are evidently different specifically on the red and blue phase due to the actual controller’s reaction at site compared to a software based approach. However the more intriguing question is how the SVC effectively continued with normal operation after the “transient response”. Hence a way forward in terms of analysis is to verify the actual currents that evidently caused an LV O/C trip to the SVC.

Thus, the thyristors reaction according to a voltage dip or surge detection is of significant importance to validate the control system within the PLC program controlling the decision process of the SVC. Now, as discussed before in the earlier chapters, in short, a voltage surge on the 132kV busbar above the set-point value of $V = 1.02\text{pu}$ results in the thyristors switching on fully in order to reduce the 132kV busbar level. If a voltage dip is detected which is below the set-point value then the thyristors switch off accordingly until the capacitor bank has attempted to correct the 132kV voltage level once again.

Figure 60 indicates a plot waveform showing theoretically the LV O/C of the SVC and how it should have handled the voltage dip relevant to case study 2 and extracted from DIgSILENT, this is shown in plot 1. The reaction of the SVC which resulted in the actual LV O/C is shown in plot 2 (OMICRON recording). Plot 3, in Figure 60, is the voltage dip detected when the transformer is energised at Dedisa substation. The yellow indicator in Figure 60 indicates the beginning of the switching and the blue indicator represents the system stabilising once again. Thus, between the yellow and the blue indicator is of significant importance for emphasis purposes.

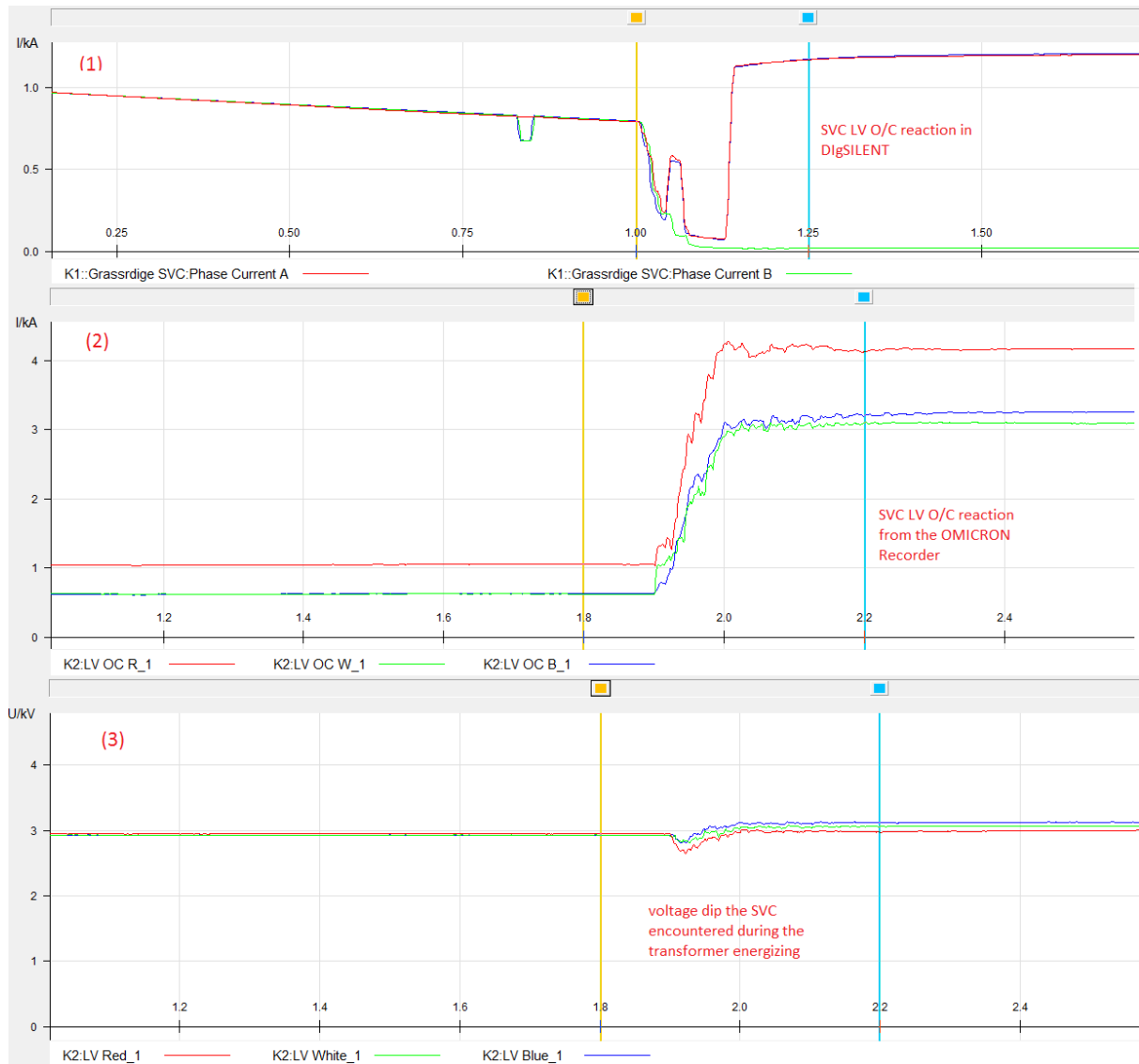


Figure 60: Case study 2 LV O/C current comparison relative to a voltage dip, OMICRON vs. DigSILENT

Hence, from Figure 60, the three plots indicate a clear view that the SVC did not operate correctly according to the voltage deviation detected on the busbar that it evidently controls. From earlier in the chapter this was clearly shown to be -6.1% voltage deviation, From the recordings, it is clear that when the SVC detects a deviation in the busbar voltage it reacts in such a manner that the current is boosted to 1.06A, 0.78A and 0.81A RMS for I_R , I_W or I_B respectively which equates to a primary value of 4197A, 3088A and 3207A respectively. These values are maintained even though the busbar voltage has been corrected. Plot 1 in Figure 60 indicates how the current should have returned back to its original position once voltage stability was achieved.

Reference is made to Figure 31 which showed the thyristor current for case study 2 during the switching transient, the thyristors switched off during the instant at which a voltage dip was detected on the 132kV busbar, which is correct, in order to allow the capacitive current to boost the busbar voltage. However when the busbar voltage was corrected and above the set-point value of $V = 1.02pu$, the thyristors remained off instead of

reacting accordingly as the simulation represents in Figure 57 for the replicated scenario. Therefore from conclusive evidence the controller is in a redundant loop mode instead of a real time analysing mode.

Therefore, the FFT plots are of significance due to their insight into whether or not harmonics caused the relay to operate prematurely due to the SIT 852 LV O/C settings that might have been breached. Thus, the FFT results generated within DIgSILENT are compared to the results obtained with the actual recordings for the particular case study that is of significance. Hence, Chart 1 highlights the comparison for case study 2 relevant to the HV side of the SVC.

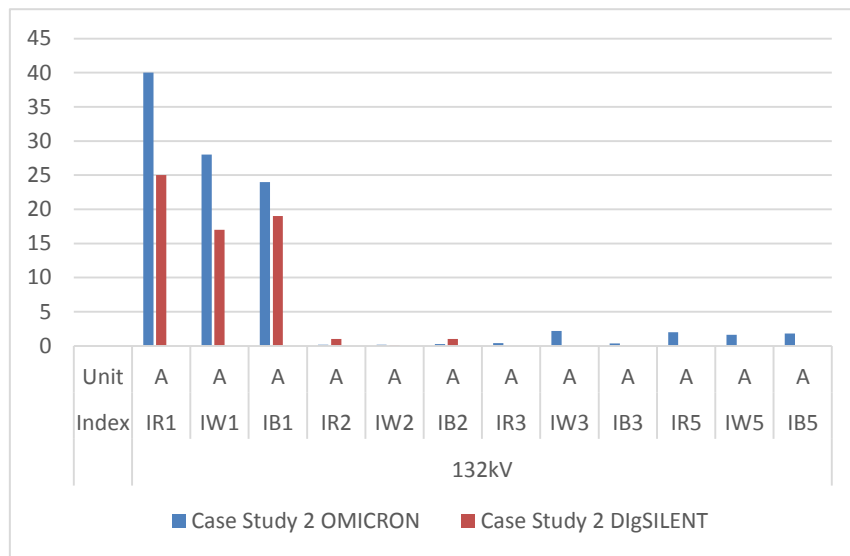


Chart 1: FFT Plot evaluation on the HV side of the SVC for case study 2, OMICRON vs. DIgSILENT

Chart 2 highlights the comparison for case study 2 relevant to the 5.1kV side of the SVC. The 5.1kV side is of significant importance as this is the origin of stray harmonics that may be generated due to the filtering technique of the filter bank not effectively tuning the correct harmonic orders out according to how and when the thyristors are firing or if the SVC is providing capacitive reactance to the system.

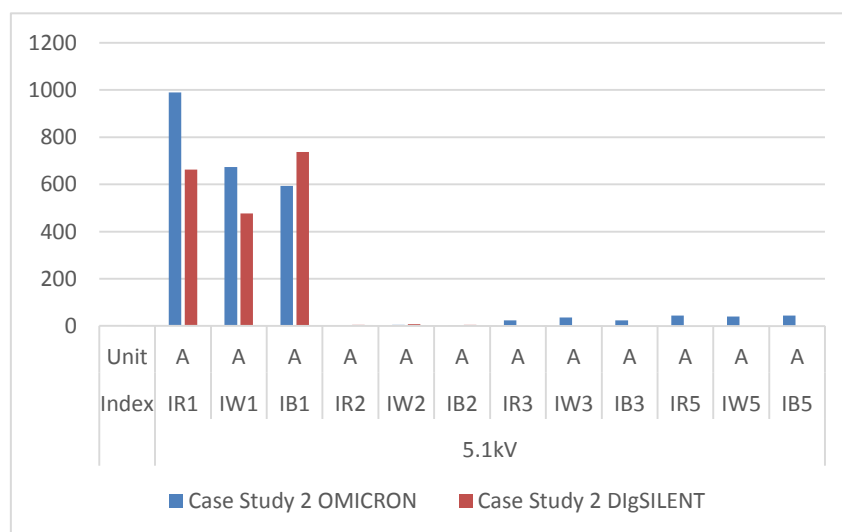


Chart 2: FFT Plot evaluation on the 5.1kV side of the SVC for case study 2, OMICRON vs. DIgSILENT

From Chart 1 and 2 it is clear that the predominant harmonic order on the 132kV and 5.1kV side of the SVC is the fundamental component. The results between the simulation and the actual recording are similar and made clear in Chart 1 and 2 respectively. There are no harmonic orders above the fundamental that influence the current on the LV side of the SVC in such a manner that the SIT 852 LV O/C relay is caused to mal-operate due to an obscure secondary reading during the transient.

A question arises whether the SIT 852 LV O/C relay is susceptible to harmonic impact? The answer is yes as seen from results obtained earlier in chapter 3 showing the laboratory secondary injections of a similar relay tested; results are shown in Table 4. The results clearly indicated how the relay trip times changed according to the amount of harmonic content that was superimposed on the fundamental component. This however does not impact the study as FFT plots indicate minimal harmonic influences, besides the fundamental component. Therefore, recommendations will be made on the protection type relays used currently in order to eliminate future potential system security issues. Relating to the problem at hand, a unique solution is required.

The IEEE Std.1459 was used to calculate the effective Total Harmonic Distortion (THD) and RMS current component for case study 2. This was calculated to evidently indicate the harmonic content on the system together with the induced harmonics from the SVC during the transformer switching transient. Table 11 indicates the results calculated using the IEEE Std.1459.

Table 11: IEEE Std.1459 calculation results for case study 2

			Case Study 2			Case Study 2			
		Index	Unit	IEEE Std.1459			Index	Unit	IEEE Std.1459
132kV		$I_{THD(R)}$	%	19.18	5.1kV		$I_{THD(R)}$	%	17.55
		$I_{THD(W)}$	%	10.81			$I_{THD(W)}$	%	10.23
		$I_{THD(B)}$	%	32.04			$I_{THD(B)}$	%	16.68
		$I_{RMS(R)}$	A	172.1			$I_{RMS(R)}$	A	4264.2
		$I_{RMS(W)}$	A	118.7			$I_{RMS(W)}$	A	3155.6
		$I_{RMS(B)}$	A	128.1			$I_{RMS(B)}$	A	3142.8

4.6 CONCLUSION

Detailed analysis was done on the four case studies detailed in this chapter. FFT results were extracted for the four case studies and compared to one another at various points on the network system under investigation. Three transient simulation scenarios within DIgSILENT PowerFactory were simulated in order to show how the SVC correctly regulates the 132kV busbar voltage at Grassridge substation. Detailed analysis was shown in terms of extracted thyristors switching currents and angles together with busbar variations during the applicable switching transient. Case study 2 was brought forward and compared to exact results found within the depicted simulation model. Hand calculations were conducted using the IEEE Std.1459 relative to case study 2 for emphasis on harmonic impact on the SVC. Detailed analysis was done in this particular chapter in order to derive conclusive evidence for the problem at hand.

CHAPTER 5 - CONCLUSIONS AND RECOMMENDATIONS

5.1 SUMMARY

Transient simulation studies were conducted in DIgSILENT PowerFactory. In light of the study results and real time results attained. It is shown that the POW controller, such as the ABB F236 used in the case studies, has no real effect on the total effective current magnitude on the 5.1kV busbar and effectively the 132kV busbar at Grassridge substation. The results show that the magnitude of the inrush current is reduced when switching a transformer at a peak on the voltage waveform. Therefore there is no necessity for the device to be implemented in order to eradicate the nuisance tripping on the SVC.

From Table 4 the results indicate the actual pick up level set on an AEG specific relay, such as the SIT 852 LV O/C implemented at Grassridge SVC, varies in relation to the amount of harmonic content superimposed on the fundamental component. Thus, mal-operations may occur if large non-linear waveforms are secondary fed into the AEG specific relay concerned. Thus the entire AEG protection installation at Grassridge SVC is at jeopardy if the particular filters fail at each voltage level or if stray harmonics filter through on the SVC system level.

Furthermore from all the case studies put forward in chapter 4, case study 2 is the only one that represents the SVC issuing a LV O/C trip to the SVC. However closer analysis shows that all the case studies indicate that the effective LV O/C RMS quantity been fed into the SIT 852 LV O/C relay is well below the pick-up level of $I_c = 1.42A$ and therefore it was by mere coincidence that a mal-operated trip occurred for case study 2, therefore indicating that a relay mal-operation is related to the problem statement. From the derived model in software replicating this exact event, it is clear how the SVC correctly responds to a voltage depression on the 132kV busbar as shown in Figure 57. Figure 60 also indicated how the SVC incorrectly boosted the current continuously and evidently turned off the thyristors indefinitely during the detection of the voltage dip. Conclusions are drawn from the results found.

5.2 CONCLUSIONS

DIgSILENT PowerFactory proved to be a suitable simulation tool to effectively analyse and simulate the network under scrutiny. It was also found that the derived EMT model created justifies and substantiates the correct operation of the SVC. Hence *hypothesis A* is shown to be true such that the equivalent source at Poseidon replicating the rest of Eskom's entire grid is adequate in order to verify correct SVC VAR compensation on the 132kV busbar at Grassridge substation. The DIgSILENT model was shown to be effective and that the TCR and TSC part of the model together with the user defined controller is the way forward when analysing EMT disturbances consisting of an SVC within the defined network model.

Hypothesis B relating to the problem statement is proven such that the statement that the SIT 852 LV O/C relay is mal-operating is true. The relay is operating for a RMS quantity well below the setting of $I_e = 1.42A$. From all the case studies it is clearly shown that similar RMS components across all three phases are achieved however only one LV O/C trip occurred during all the switching scenarios. Therefore a discrepancy exists within the internal measuring circuit of the SIT 852 LV O/C relay as it proves to be unreliable.

The POW controller was shown to effectively reduce the magnitude of the 2nd harmonic inrush current when energising a transformer under no load conditions. From **hypothesis C**, the statement is proven incorrect that the POW controller will solve the problem statement. This is shown clearly in the case studies where the device was implemented in the control circuits when energising the relevant transformers and from case study 2 a trip occurred even though the device was implemented for test purposes.

It is concluded from the FFT's performed that there is no predominant 2nd, 3rd or 5th harmonic current present at the SVC during the switching transient, thus confirming that the SIT 852 LV O/C relay is not mal-operating due to an obscure secondary reading during the switching transient, therefore disproving **hypothesis D**. This however does not eliminate the fact that the SIT relay range is susceptible to harmonics as shown in the test results, thus recommendations are required to ensure further system security.

It is therefore deduced that the nuisance sporadic tripping's occur firstly because there is a discrepancy within the internal measuring circuit of the SIT 852 relay and secondly the 35MVAR SVC operates at its maximum Inductive capabilities when the 400kV system is strong. This is due to the balance controller essentially ramping into a redundant loop when it detects a voltage depression on the 132kV busbar and not ramping back once the voltage stabilizes and is above the set-point value once again. Therefore essentially the controller is not ramping back after the transient response. Thus it is purely useful only as a capacitor bank for an "n-2" or "n-3" scenario because of the method of incorrect control that has been inherently accepted.

5.3 RECOMMENDATIONS

Therefore it is recommended that an overall protection relay upgrade is effectively carried out on the SVC at Grassridge substation purely due to the fact that the existing AEG installation is susceptible to harmonics. Due to the age of the AEG protection installation, Eskom should consider a revised installation using micro-processor based technology relays such as the GE T60 and F35 which are the same relays used at other SVC installation within Eskom's power system. Alternatively the 132kV/5.1kV SVC could be relocated within Eskom's power system where it could strengthen a weaker 132kV part of the grid.

It is suggested that Eskom can implement the ABB F236 POW controller on the HV breaker of the applicable transformers at Dedisa substation. This will have an effect such that the magnitude of the inrush current can be reduced when all poles close at a peak on the voltage waveform.

Furthermore the model derivative that Eskom use within the standard “pfd” file that they continuously update should be altered in such a manner in order to accommodate for the SVC in all the regions to be modelled as per a SVS model. The SVS model should be modelled such that it accommodates for the amount of reactance and capacitance required to make up the SVC model thereof. Thus the overall composite model including the controller will relate to the TCR amount for the reactance and TSC amount for the capacitance respectively. By implementing this approach within DIGSILENT will therefore do away with the generic model of a fixed capacitor and a switched thyristor composition. This will be helpful for future models that might and will have switched capacitor banks that can produce a variable amount of capacitance dependant on the voltage deviations detected. The advantages is such that it will allow the user to have more flexibility to control the thyristor switching with a preferable controller together with a controlled capacitor switching setup within the SVC model.

CHAPTER 6 - LIST OF REFERENCES

- [1] DIgSILENT PowerFactory “Technical Reference”, DIgSILENT PowerFactory version 13.1, DIgSILENT GmbH Gormaringen, Germany, 2004, Chapter 6, pp. 45-48
- [2] A.E. Emanuel, “Summary of IEEE Standard 1459: Definitions for Measurement of Electric Power Quantities under Sinusoidal, Non-sinusoidal, Balanced or Unbalanced Conditions”, IEEE Trans. on Industry Applications, Vol.40, No.3, May/June 2004, pp.869-876.
- [3] W.C. Stemmet, G. Atkinson-Hope, “A Software Based Methodology for Calculating Powers in Three Phase Networks”, presented at the 11th Int. Conf. on Harmonics and Quality of Power, Lake Placid, New York, 2004, ICHQP Paper no.028.
- [4] P.C. Sen, “Principles of Electric Machines and Power Electronics 2nd Edition, ISBN: 0471022950.
- [5] AREVA, “Network Protection and Automation Guide 1st Edition July”, 2002.
- [6] DIgSILENT Power Factory, “Basic Software Features and Calculation Functions, Advanced Functions and Features”, DIgSILENT PowerFactory Version 14, Rev1. 14/04/2010.
- [7] IEEE Trial-Use Standard, “Definitions for the measurements of electric power quantities under sinusoidal, non-sinusoidal, balanced or unbalanced conditions”, IEEE Std.1459-2000, published June 2000, ISBN: 0-7381-1962-8.
- [8] Y.Baghzouz, X.D Gong, “Analysis of Three-Phase Transformers No-Load Characteristics”, IEEE Transactions on Power Systems, Vol-10, No.1, February 1995.
- [9] Z.Yunhai, W.Z Tanlicun, “Analysis of Magnetizing Surge in a No-Load Transformer during Black-start”, College of Electrical Engineering and Information Technology, China Three Gorges University, IEEE.
- [10] Working Group of the Substation Protection Subcommittee of the IEEE Power System Relaying Committee, S.R Chano, A. Elneweihi, L.H Alesi, H. Bilodeau, D.C Blackburn Jr. L.L Dvorak, G.E Fenner, T.F Gallen, J.D Huddleston III, K.A Stephan, T.E Wiedman, P.B Winston, “Static VAR Compensator Protection”, IEEE Transactions on Power Delivery, Vol-10, No.3, July 1995.
- [11] D.J.J Conradie, J. Du Preez, “Training Manual for SVC by AEG – Telefunken (1983-1985)”, Eskom South Africa.

- [12] Yi-Kuan Ke, Pei-Hwa Huang, Ta-Hsiu Tseng, "Performance Measurements of Static VAR Compensators in Distribution System", IEEE, SICE Annual Conference 2010, August 18-21, 2010, The Grand Hotel, Taipei, Taiwan.
- [13] A. Janke, J. Mouatt, R. Sharp, H. Bilodeau, B. Nilsson, M. Halonen, A. Bostrom, "SVC Operation and Reliability Experiences", ©2010 IEEE.
- [14] Lou Van Der Sluis, "Transient in Power Systems", John Wiley and Sons Ltd, Published 2001, ISBN: 0-471-48639-6/0-470-84618-6.
- [15] ABB, "Instruction Manuel for Controller SWITCHSYNC Model F236 for Controlled Switching of Circuit Breakers", REV 3, 31 December 2005.

APPENDICES

Appendix A – IEEE Conference ICIT 2013

Transient Analysis of Erroneous Tripping at Grassridge SVC

M.W. Taberer

Eskom – Power and Energy Provider for South Africa
East London, South Africa
taberemw@eskom.co.za

A.G. Roberts, R.T. Harris, W. Phipps

NMMU – Nelson Mandela Metropolitan University
Port Elizabeth, South Africa
Alan.Roberts@nmmu.ac.za, Raymond.Harris@nmmu.ac.za
William.Phipps@nmmu.ac.za

Abstract—The research work conducted in this paper is the evaluation of real time values obtained using two OMICRON 356's at two independent locations and implementing them as recorder devices in Eskom's power system. A derived model within DIGSILENT is created and EMT studies are performed and compared to the real time values obtained. Transformers are normally closed via an auxiliary contact. Thus by applying system voltage at a random instant in time on the transformer windings result in a high transient magnetizing inrush current which causes high orders of 2nd harmonic currents to flow under no load conditions. A philosophy to mitigating these currents is to energize the transformer by controlling the circuit breaker closing times such that the magnetic flux produced in the windings corresponds to the prospective flux in the core. Transients produced can cause nuisance tripping's at the particular location where the respective transformers are energized. OMICRON EnerLyzer is the software tool used for the Comtrade recordings at both locations. Two "real time" case studies are evaluated using OMICRON EnerLyzer and TOP software. Results are formulated and then evaluated against a derived Electromagnetic transient model using DIGSILENT software.

Index Terms—Inrush current, Inrush transient, RMS current, Peak current, Harmonics, Electromagnetic transient, Static Var Compensator.

I. INTRODUCTION

The Static Var Compensator (SVC) located at Grassridge substation within Eskom's power grid plays a vital role in ensuring the improvement of power system stability by providing voltage support. The application of an SVC in particular is to maintain voltage at a set level by compensating for varying loads and to correct fluctuating voltages caused by load rejections and outages [1]. In practical situations, it is impossible to find perfectly balanced and sinusoidal voltages. A certain degree of imbalance and waveform distortion (with mainly odd harmonics) is always present due to the nature of distribution systems and electrical loads. Even harmonics are also found in supply voltages due to half-wave rectifier loads, arc furnaces, electrical discharge devices and lack of isotropy

in core materials, but are often much smaller than adjacent odd harmonics [2].

The SVC located at Grassridge has been operating effectively since 1987 with AEG numerical protection relays being more than adequate to accommodate for overcurrent (O/C) and earth fault (E/F) conditions [3]. However since a recent network upgrade has occurred where two 500MVA transformers were commissioned in close proximity to Grassridge substation, sporadic low voltage (LV) O/C tripping has occurred on the 132/5.1kV SVC. Figure 1 shows the created model within DIGSILENT Power Factory software replicating the network arrangement of the two affected transmission stations [4].

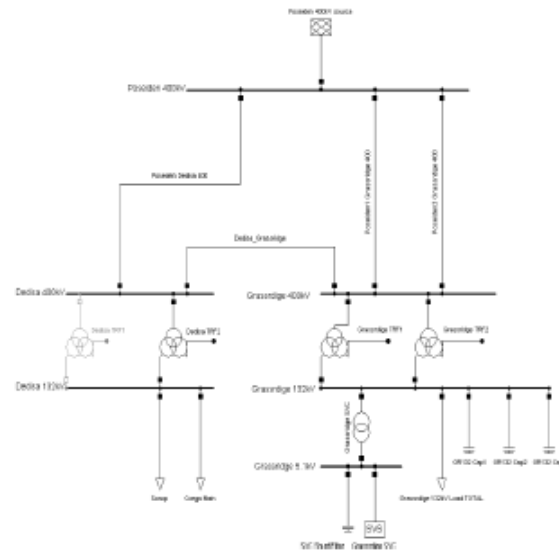


Fig. 1. Dedisa and Grassridge network arrangement

It is a well-established phenomenon that a transformer will experience magnetizing inrush currents during energization. Inrush current occurs in a transformer whenever the residual flux does not match the instantaneous value of the steady-state flux which would normally be required for the particular point on the voltage waveform at which the circuit is closed [5].

The general equation that gives the amplitude of inrush current as a function of time can be expressed as in (1).

$$i(t) = \frac{\sqrt{2}V_m}{Z_t} \cdot K_w \cdot K_s \cdot (\sin(\alpha t - \varphi) - e^{-\frac{t-t_0}{\tau}} \cdot \sin \alpha) \quad (1)$$

where V_m is defined as the maximum applied voltage, Z_t is defined as the total impedance under inrush, including the system, φ is defined as the energization angle, t is defined as the time, t_0 is defined as the point at which the core saturates, τ is defined as the time constant of the particular transformer winding under inrush conditions, α is defined as the function of t_0 , K_w accounts for the 3 phase winding connection and K_s accounts for short-circuit power of the network [5].

The peak value of transient inrush currents is an important factor when designing protection systems for a transformer and imperative for the verification of surrounding protection philosophies relating to network upgrades as in the case studies that will be exposed. A simplified equation can be used to calculate the peak value of the first cycle of the inrush current as in (2).

$$i_{peak} = \frac{\sqrt{2}V_m}{\sqrt{(\omega \cdot L)^2 + R^2}} \cdot \left(\frac{2 \cdot B_N + B_R + B_S}{B_N} \right) \quad (2)$$

where V_m is defined as the maximum applied voltage, L is defined as the air core inductance of the transformer, R is defined as the total dc resistance of the transformer, B_N is defined as the normal rated flux density of the transformer core, B_R is defined as the remnant flux density of the transformer core, B_S is defined as the saturation flux density of the core material. As seen from the equations (1) and (2), the value of inrush current is dependent on the parameters of the transformer in addition to the operating conditions of the power system.

There is thus a need to investigate the implications involved, regarding protection, when a power system is altered in such a manner that the transients of a large 500MVA transformer could cause protection grading issues on specific overcurrent relays (i.e. LV O/C relay on the 5.1kV side of the SVC at Grassridge substation) [6]. OMICRON software such as EnerLyzer, in addition to "TOP" software, are well known tools for investigating and analyzing RMS and peak currents and voltages that contain harmonics. DIGSILENT software is a powerful package for Electromagnetic transient (EMT) studies [7]. A derived model within DIGSILENT will be produced to replicate the Dedisa/Grassridge network scenario. Instantaneous EMT scenarios of the derived model are simulated in order to emphasize the harmonic impact and Var compensation the SVC has during the transformer switching transient.

II. RESEARCH STATEMENT

To evaluate the LV O/C tripping at Grassridge SVC when one of the 500MVA transformers at Dedisa Substation is energized under no load conditions.

III. METHODOLOGY

Sophisticated recording devices are setup at both Dedisa and Grassridge substations. OMICRON test equipment and software is the primary tool to investigate real time data obtained at both substations. Real time analysis is extremely sensitive to the type of measurement tool used for the interconnection between the test set and the protection relay. OMICRON EnerLyzer is a recording medium specific for real time analysis. Sensitivity settings on the current and voltage probes are imperative when evaluating distorted waveforms. An OMICRON 356 test set allows for 10 channels to be configured as analogue or digital recording inputs. Figure 2 shows the test set used for recording purposes.



Fig. 2. OMICRON 356 Test Equipment

Secondary transient current and voltage waveforms are recorded for various switching scenarios according to a POW controller issuing switching commands to the relevant transformer HV breaker. These recordings are then analyzed to determine whether a POW controller is significant at Dedisa for the sporadic tripping of the SVC at Grassridge. DIGSILENT results formulated from a derived model, mimicking the switching scenario causing the sporadic tripping of the SVC, will be compared, in terms of busbar voltage variations and current magnitudes, to the actual real time results obtained using the OMICRON 356's. Analysis will confirm whether further recommendations are required for the entire protection setup at Grassridge SVC due to harmonic sensitive relays.

IV. RECORDED CASE STUDIES

The LV overcurrent relay located at Grassridge SVC was analyzed when the 500MVA transformer at Dedisa was energized under NO-LOAD conditions. The arrangement of the OMICRON recorders together with the network configuration is detailed in Figure 3.

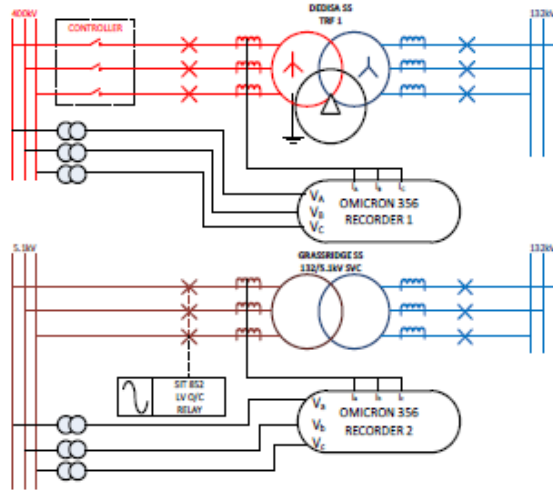


Fig. 3. OMICRON 356 Recorder Setup

Table I indicates the relevant overcurrent ($I_{c>}$) and time (t) operating characteristic for the SIT 852 relay that protects the SVC. $I_{c>}$ and t are defined as the relevant secondary curve parameters relating to a LV O/C condition. These particular quantities were determined according to the test set maintenance results and thus deviates slightly from the actual potentiometer dial values found on the actual relay, indicated in Table I. K is defined as the time dial setting for the relay and is in accordance to a normal inverse curve.

TABLE I
AEG SIT 852 LV O/C RELAY SETTINGS

Element	Setting on Relay	Actual Operating Characteristic of Relay
$I_{c>}$	1.43A	1.57A
K	0.1 (inverse)	N/A
Time Multiplier	N/A	3.1s

A. Transformer 1 Energized AND SVC Remains Closed

The Point onto Wave (POW) controller was set such that a close pulse was sent to the breakers poles after a pre-defined time. The waveforms in Figure 4 show the initial secondary transient inrush current of the transformer upon closing. Due to the breakers operating time of +52milli seconds, attained from accredited speed test results of the breaker, the actual

poles of the breaker closed when the red phase voltage of the busbar was at peak.

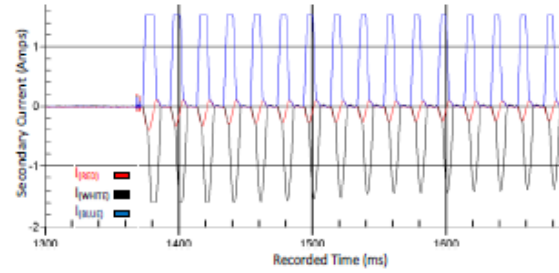


Fig. 4. TRF1 Inrush Current Relative to a Peak Red Phase Voltage Closing

Table II shows the OMICRON results of the secondary values of the peak and RMS transient inrush currents, in Amps (A), at the initial point when the transformer was energized. Table III shows the OMICRON results of the secondary values, in Amps (A), of the peak and RMS currents present on the 5.1kV side of the SVC at Grassridge during transformer inrush conditions at Dedisa.

TABLE II
DEDISA'S TRANSIENT RMS AND PEAK CURRENTS

Element	Magnitude (A)	Element	Magnitude (A)
$I_{R(peak)}$	0.42	$I_{R(RMS)}$	0.19
$I_{W(peak)}$	1.59	$I_{W(RMS)}$	0.89
$I_{B(peak)}$	1.54	$I_{B(RMS)}$	0.95

TABLE III
GRASSRIDGE 5.1kV RMS AND PEAK CURRENTS

Element	Magnitude (A)	Element	Magnitude (A)
$I_{R(peak)}$	1.57	$I_{R(RMS)}$	1.07
$I_{W(peak)}$	1.55	$I_{W(RMS)}$	0.96
$I_{B(peak)}$	1.55	$I_{B(RMS)}$	1.07

B. Transformer 1 Energized AND SVC Trips

Now, as compared to Case A there was a recorded trip at Grassridge SVC due to the SVC's LV O/C relay operating. Figure 5 shows the instantaneous value of the secondary currents relative to the 5.1kV side of the SVC. Figure 5 also shows the time from when the relay picked up an O/C condition to when the Breaker poles were opened and the current diminished to zero. As seen previously from Table I the operating characteristic of the relay is 3.1s and from the recorded results in Figure 5 it can be seen that the current waveforms relate to the maintenance test results.

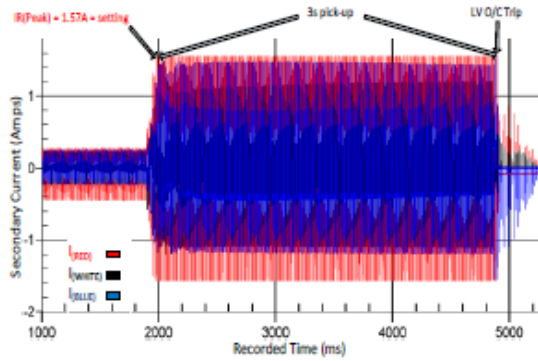


Fig. 5. Instantaneous value of the SVC's LV Current for a Trip Condition

Table IV shows the results of the secondary peak and RMS currents, in secondary Amp (A), present on the 5.1kV side of the SVC at Grassridge during transformer inrush conditions.

TABLE IV
GRASSRIDGE 5.1kV RMS AND PEAK CURRENTS

Element	Magnitude (A)	Element	Magnitude (A)
$I_{R(peak)}$	1.57	$I_{R(RMS)}$	1.05
$I_{W(peak)}$	1.55	$I_{W(RMS)}$	0.78
$I_{B(peak)}$	1.55	$I_{B(RMS)}$	0.82

V. ANALYSIS OF RESULTS

From the results obtained for "Case A" and "Case B" it is clear that the threshold at which the relay operates is 1.57A secondary, thus confirming that the relay operates correctly according to the attained test results. This is confirmed with the recorded SVC trip as indicated in "Case B".

The point at which the transformer was effectively energized in terms of a peak voltage value or a zero crossing had no real significance of how hard the SVC had to work at Grassridge. The emphasis on Harmonics within the case studies will always pose questions; however it is proven from the relevant Comtrade files recorded during the switching transients, that harmonics are not the direct cause of the mal-operation of the LV O/C relay.

Therefore a derived model using DIGSILENT software was constructed in order to supplement the OMICRON real time results attained. All vector groups of the relevant transformers in the simulation model were represented as per the relevant nameplates. The model is simulated according to the exact setup at both Dedisa and Grassridge however current loads vary due to the instant at which the real time values were obtained with the OMICRON recorders. The EMT simulation was such that the total simulation ran for 5 seconds and the energizing of transformer 1 occurred 3 seconds into the simulation. Results indicate that the transient simulations within DIGSILENT correlate with the OMICRON recorded values during the switching transient which result in the SVC

operating at its maximum Inductive capabilities. Due to this phenomenon an LV O/C trip is predominant at every switching but is dependent on the 400kV and 132kV bus bar voltages.

Figure 6 shows how the SVC attempts to correct system voltage at Grassridge during transformer inrush conditions at Dedisa. However it can be seen from figure 6 that the SVC is working at its threshold and is therefore at its limit of maximum Var capacity and the LV O/C setting, if calculated with a CT Ratio of 3960:1, shows that the secondary value within software is 1.53A or 6.064kA primary.

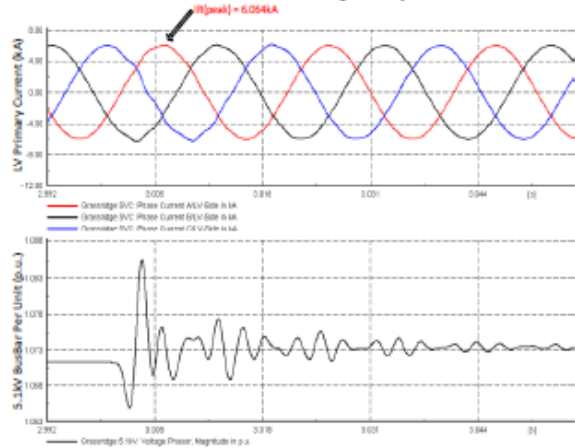


Fig. 6. DIGSILENT's EMT Results for the 5.1kV Busbar Voltage and the SVC's LV Current

Figure 7 indicates how the 132kV busbar at Grassridge tries to adjust in such a short time span to accommodate for the system network change at Dedisa when Transformer 1 is placed into operation.

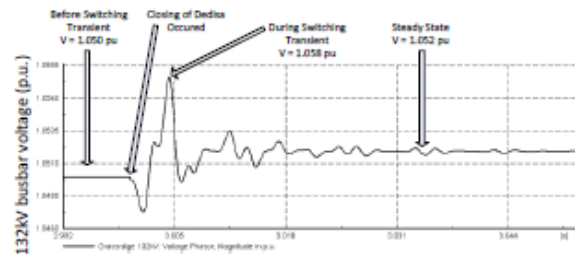


Fig. 7. DIGSILENT's EMT Results for the 132kV Busbar at Grassridge

Therefore from Figure 6 and 7 it is clear that the sudden change in network operation at Dedisa causes busbar voltage variations in magnitudes such that the LV current on the SVC operates at threshold values very close to the setting value of the LV O/C relay.

Table V shows a comparison, at the SVC's 5.1kV busbar, between the results obtained with the OMICRON Recorders and DIGSILENT software in order to validate the results and

operation of the SVC. Results are shown for particular points "BEFORE" the switching of the transformer at Dedisa which therefore indicates normal load characteristics. The "AFTER" results of the switching transient recorded with the OMICRON's are then indicated to show how the secondary currents increase drastically due to the transformer switching at Dedisa. However the "AFTER" results of the switching transient simulated in DIGSILENT software show that there is no rapid change in the currents due to the SVC operating at its threshold before the switching occurred. The cause of variation for the "BEFORE" affect recorded with the OMICRON's is due to the loading at the time when the recording was taken.

TABLE V
REAL TIME RESULTS COMPARED TO EMT STUDY IN
DIGSILENT

Index	Unit	OMICRON		DIGSILENT	
		BEFORE	AFTER	BEFORE	AFTER
$I_{I(\text{peak})}$	A	0.439	1.56	1.53	1.53
$I_{W(\text{peak})}$	A	0.227	1.38	1.53	1.54
$I_{B(\text{peak})}$	A	0.261	1.41	1.53	1.57
$V_{(5.1kV)}$	pu	1	1.05	1.07	1.073

Therefore it can be deduced that the operational currents of the SVC during transient conditions are unfortunately in regions extremely close to the suspected "mal-operating" relay pick-up levels.

VI. HARMONIC ANALYSIS

To confirm whether or not harmonics, specifically 2nd harmonic inrush currents, play a significant role in the mal-operating of the LV O/C relay, extensive Fast Fourier Transform (FFT) plots are generated in "TOP" software using the actual recorded values during the switching transient. The 2nd harmonic analysis, in particular, was performed in order to verify whether the SVC is operating normally under system conditions or harmonic generating conditions. Therefore the 2nd harmonic order analysis was imperative in order to substantiate whether or not the filters at Grassridge substation, that are specifically tuned to filter out certain harmonics, inclusive is the 2nd harmonic order, is in fact operating correctly or not.

Figure 8 is the FFT plot generated in "TOP" software and indicates a predominant 2nd harmonic current generation at Dedisa on the 400kV level when Transformer 1 is energized under no load conditions. Therefore figure 8 is basis and confirms previous studies that when a transformer is energized under no load conditions a predominant 2nd harmonic inrush is present and is affiliated by the switching conditions, the structure of the transformer and the position of the transformer in the power system [8].

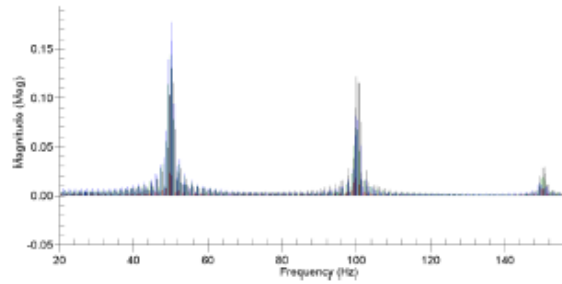


Fig. 8. Dedisa Transformer 1 2nd Harmonic Inrush Transient FFT Plot

Grassridge SVC has a capacitor bank that is specifically tuned to filter out specific harmonics produced by the TCR's (Thyristor Controlled Rectifiers). The nominal rating of the capacitor/filter bank in the 132kV SVC is 35 MVar. The filter is tuned to the 2nd, 3rd and 5th harmonic frequencies.

Figure 9 is the FFT plot generated in "TOP" software and shows that there are no harmonic orders present on the 132kV side of the SVC transformer, besides the fundamental, at Grassridge substation during the inrush transient stage at Dedisa.

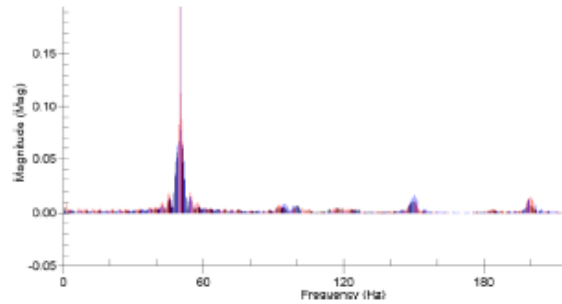


Fig. 9. Grassridge HV current FFT Plot

The harmonic blocking filters are shown to be effective on the SVC such that there are no predominant "stray" harmonics present during the energizing transient at Dedisa. Figure 10 shows the FFT plot on the 5.1kV side of the SVC.

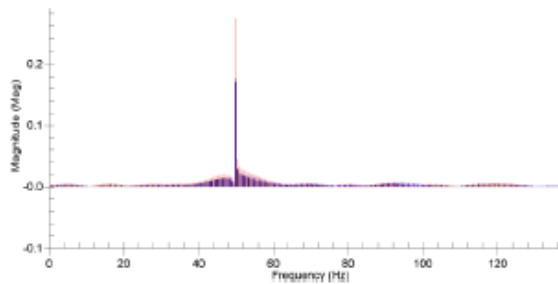


Fig. 10. Grassridge 5.1kV SVC Current FFT Plot

VII. CONCLUSIONS

Transient simulation studies were conducted. In light of the study results and “real time” results attained. It is shown that the POW controller, such as the ABB F236 used in the case studies, has no real effect on the total effective current magnitude on the 5.1kV busbar at Grassridge. Therefore there is no necessity for it to be implemented in order to eradicate the nuisance tripping on the SVC.

It can also be concluded from the FFT's performed that there is no predominant 2nd or 3rd harmonic current present at the SVC during the switching transient, thus confirming that the SVC's Filters operate correctly.

It is therefore deduced that the nuisance sporadic tripping's occur purely due to the fact that the 35Mvar SVC operates at its maximum Inductive capabilities when the 400kV system is strong. Thus it is purely useful only as a capacitor bank for an “n-2” or “n-3” scenario.

Therefore it is recommended that protection settings be effectively revised so that when the SVC operates at maximum Inductive mode then an LV O/C scenario does not occur. Alternatively the 132kV/5.1kV SVC could be relocated within Eskom's power system where it could strengthen a weaker 132kV part of the network.

VIII. REFERENCES

- [1] Alwyn Janke, John Mouatt, Ron Sharp, Hubert Bilodeau, Bo Nilsson, Mikael Halonen and Anders Bostrom, “SVC Operation & Reliability Experiences”, IEEE Power and Energy Society General Meeting, March 2010.
- [2] Y.Baghzouz, X.D Gong, “Analysis of Three-Phase Transformers No-Load Characteristics”, IEEE Transactions on Power Systems, Vol-10, No.1, February 1995.
- [3] D.J.J Conradie, J. Du Preez, “Training Manual for SVC by AEG – Telefunken (1983-1985)”.
- [4] Nicola Chiesa, Bruce A. Mork, Senior Member, IEEE, and Hans Kristian Hoidalen, Member, IEEE, “Transformer Model for Inrush Current Calculations: Simulations, Measurements and Sensitivity Analysis”, IEEE transactions on power delivery, vol. 25, no.4, Oct 2010.
- [5] M. Jamali, M. Mirzaie, S. Asghar Gholamian, “Calculation and Analysis of Transformer Inrush Current Based on Parameters of Transformer and Operating Conditions”, ISSN 1392-1215, 2011. No3 (109).
- [6] C. Russell Mason, “The Art and Science of Protective Relaying”, Wiley Publishers, 1956.
- [7] DlgSILENT Power Factory, “Basic Software Features and Calculation Functions, Advanced Functions and Features”, DlgSILENT PowerFactory Version 14, Rev1. 14/04/2010.
- [8] Y. Najafi Sarem, E. Hashemzadeh, M.A. Layegh, “Transformers Fault Detection using Wavelet Transform”, International Journal on “Technical and Physical Problems of Engineering” (ITPE), vol. 4, issue. 10, no. 1, March 2012.

Appendix B – OMICRON CMC 356 Calibration Certification



OMICRON
electronics GmbH

Oberes Ried 1
A-6833 Klaus, Austria
Tel. +43 5523 507 0
Fax +43 5523 507 999
E-Mail: info@omicron.at

Certificate of Calibration and Conformance

Conformance

OMICRON electronics GmbH certifies that the product detailed below (Device Type, Serial No) has been designed, manufactured, tested, adjusted and calibrated to the highest quality standards of workmanship and materials in compliance with a quality system registered to ISO 9001:2000 (SGS Austria Control-Co GmbH, certificate number AT08/0046).



The product conforms to all specifications published in the manual and has

passed all tests successfully.

More detailed test data can be found on the enclosed CD/DVD in the directory Report.
Warranty (one year) and calibration are valid from Date of Issue.

Traceability Information

Traceability is to national standards administered by EURAMET and ILAC members (e.g. ÖKD, DKD, NIST, NATA, NPL, PTB, BNM etc.) or other recognized standard laboratories. Some measurements are traceable to natural physical constants, consensus standards or ratio type measurements.

Device Type **CMC356**
SNo **DF038F**
Option **NET-1, ELT-1**
Calibration Date **2010-08-20**

Test Equipment

Model	Type	Company	Trace No	Serial No	Due date
175-H2	Climate	Testo	09-115	38225835/811	2012-05-10
CNT-90	Counter	Pendulum	09-139	SN993452	2011-04-28
3458A	DMM	Agilent	06-176	MY45041841	2010-11-24
OPM 100	Phase Meter	Omicron	04-101	04-101	2011-04-30
1659	Shunt	Tinsley	04-113	29/01	2011-12-04
3111	Shunt	Tinsley	07-157	11862/01	2010-11-18

Date of Issue
2010-08-27

Manager Operations

Dietmar Gehrman

Testengineer

Markus Märk